



**USE OF SOLAR ENERGY TO CONTROL THE ENVIRONMENT FOR
AQUAPONICS IN LOW INCOME COMMUNITIES**

by

FAREED ISMAIL

Dissertation submitted in fulfilment of the requirements for the degree

Doctor of Engineering in Mechanical Engineering

in the Faculty of Engineering and the Built Environment

at the Cape Peninsula University of Technology

Supervisor: Prof J. Gryzagoridis

Bellville
November 2020

CPUT copyright information

This dissertation may not be published either in part (in scholarly, scientific or technical journals), or as a whole (as a monograph), unless permission has been obtained from the University.

DECLARATION

I, Fareed Ismail, declare that the contents of this dissertation represent my own unaided work, and that the dissertation has not previously been submitted for academic examination towards any qualification. Furthermore, it represents my own opinions and not necessarily those of the Cape Peninsula University of Technology.



04/11/2020

Signed

Date

ABSTRACT

South Africa has one of the rising economies on the African continent, but faces great challenges as to how to reduce its dependency on a coal powered industry, improve outdated agricultural methods, reduce poverty and create awareness of the use of renewable energy amongst low income communities.

The research led to the design and development of a prototype Modular Solar Powered Aquaponics System. The system makes use of solar energy such as photovoltaics (PVs) to generate electricity and solar thermal energy to heat the aqueous medium. The use of this renewable energy improves the prototype's environment, encouraging fauna and flora to flourish for human consumption. The prototype combines an intense vegetable and fish farming production system which has the ability to reduce water and land usage as compared to traditional farming methods.

The system successfully yielded a healthy growth of leafy vegetables. Experiments showed that in four weeks' time, lettuce grew 130 mm, ruby chard 170 mm, spinach 180 mm, rocket 300 mm and cherry tomatoes 515 mm. Lettuce grew particularly quick in this system, where it took 35 days to mature to harvest compared to 50 days when grown by conventional farming methods.

The fish growth was carefully monitored and compared to the Von Bertalanffy growth model with results indicating that the growth rate reduced to almost zero after about 400 days, with the fish reaching a mass and a length of about 470 g and 27 cm, respectively, which conforms to the model's predicted values of mass = 426 g and length = 27 cm.

The PV system proved reliable and could sustain the load of 1352 Wh/day for the operation of the aquaponics pump and the four hours of night lights. The energy output from the stand-alone PV system was monitored over an eight-day period during the winter, whereby clear, cloudy and worst-case stormy weather was experienced. An average energy of 1167 Wh/day was recorded for this period. This average slightly underperformed the design criteria of 1352 Wh/day; however, the shortfall was carried by the two days' autonomy built in the batteries' storage capacity.

The design of the SWH system proved to be adequate during clear sunny days, but lacked capacity during adverse weather conditions (prominent in winter months). It was possible to maintain a temperature close to the required 29° C at the outlet of the collector during ideal weather conditions. Maintaining an average flow rate of 1.78 l/min proved adequate to allow most of the water (~750 l) to pass through the solar collector

in one day (~7 hours of sunlight). During winter months, the model predicted a smaller increase in temperature, where the temperature of the water could be raised from 15° C to an average of 19.1° C, with a maximum of 23.4° C just after midday.

A pilot system (of which the design is not covered in this thesis) was erected at a low-income community near CPUT: The Africa Community Project (ACP), a non-profit organisation, runs an early childhood development program (ECP) which caters for 125 toddlers, youth and community members. The pilot system currently consists of 4 x 1000 litres capacity fish tanks and a total grow-bed area of 18 m². In spite of minor difficulties, it has yielded good crop growth and has been accepted as a significant activity by the community. The community supplies crops harvested from the pilot system, such as green and red leaf lettuce, spinach, mint and basil, to a company called Pure Good Food on a monthly basis.

This research endeavoured to address the possibility of combining existing with new technologies to empower low-income communities. The research has led to the filing of an SA patent (PA161202P, filed on 17 August 2015).

ACKNOWLEDGEMENTS

I wish to thank the following:

- Supervisor: Prof J. Gryzagoridis for continuous support, mentorship and motivation.
- Lecturing staff: Dr O. Nemraoui, Vicky Cain, S. Pietrangeli, M. Ludick and all lecturing staff for continuous support and motivation.
- Workshop staff: V. Moni, G. Janodien and other technicians who assisted in building the prototype.
- CPUT students: M.W. Schouw, B. Jantjies, C. Matejoa and all students who assisted on the project.
- NESDAF: Dr S. Khamlich for continuous support and assistance.
- Delft University of Technology students: Douwe Schoemaker, Nina van Savooijen and Stijn Burmanje for their positive contribution to the Pilot Project in the low-income community and starting an NGO in The Netherlands to ensure continuous support.
- Ernst Abbe University of Technology students: Johannes Meidl, Jonas Waldhäusl, Sarah Mahlerwein and Selina Meiser for their passion and commitment in helping the low-income community overcome adversities by securing the Pilot Project and bringing hope to the 125 toddlers with their fun learning activities.
- Community leader: Mr. C. Hartzenberg for his patience, continuous support and accommodation of the Pilot Project at the community centre.
- CPUT URF: This work is supported in part by the Cape Peninsula University Research Fund (URF) Grant received 2013 and 2014.

DEDICATION

I dedicate this dissertation to my lovely wife, Firoza, and my wonderful children,
Aatiqah, Amirah and Uwais

TABLE OF CONTENTS

DECLARATION	iii
ABSTRACT	iv
ACKNOWLEDGEMENTS	vi
DEDICATION	vii
LIST OF FIGURES	xi
LIST OF TABLES	xv
GLOSSARY	xvi
CHAPTER ONE: INTRODUCTION	1
1.1 Agriculture, energy and sustainable livelihoods in South Africa.....	1
1.2 Aquaponics.....	2
1.3 Food security	2
1.4 Renewable energy.....	9
1.4.1 Solar energy: SA’s major renewable energy source.....	9
1.4.2 Historical and modern harvesting methods of solar energy.....	11
1.4.3 Orientation of solar energy collector panels	13
1.5 Research questions	14
1.6 Statement of research problem.....	14
1.7 Research aim and objectives.....	14
1.8 Significance and justification of this work.....	15
1.9 Delineation of the research.....	16
1.10 Ethical considerations.....	16
1.10 Thesis outline	17
CHAPTER TWO: DESCRIPTION OF THE MODULAR SOLAR POWERED AQUAPONICS PROTOTYPE AND THE DESIGN OF ITS COMPONENTS	18
2.1 Aquaponics prototype section’s design.....	18
2.2 Renewable energy section’s design: optimisation and sizing	21
2.2.1 Optimising the solar energy collectors’ orientation for Cape Town	22

2.2.2	PV system design.....	28
2.2.3	SWH design	36
CHAPTER THREE: THE MSPAS EXPERIMENTS		44
3.1	Aquaponics experimental set-up.....	44
3.1.1	Experimental set-up of the aquaponics section	44
3.2	Sun path orientation for experiments of solar collector alignment.....	49
3.1.1	The basic operation of the tracker	50
3.1.2	Experimental procedure for tracking vs stationary PV	50
3.2	Solar photovoltaic electricity supply experiment: introduction.....	52
3.2.1	Experimental set-up and equipment used	52
3.2.2	Instrumentation for the PV experiment	55
3.2.3	Battery bank autonomy experiment.....	57
3.2.4	PV system experimental procedure.....	57
3.3	Solar water heating experiment: introduction.....	58
3.3.1	Experimental set-up.....	58
3.3.2	Instrumentation for the SWH experiment.....	60
3.3.3	Solar water heating experimental procedure	65
CHAPTER FOUR: DISCUSSION OF RESULTS		67
4.1	Overview.....	67
4.2	Growth rate of leafy greens	67
4.3	Growth rate of fish	68
4.4	Orientation experiments of solar collector.....	70
4.5	PV experimental results	71
4.5.1	Battery autonomy experiment.....	71
4.5.2	MSPAS PV system experiment	72
4.6	SWH experimental results	74
CHAPTER FIVE: COMMUNITY ENGAGEMENTS		76
5.1	The low-income community Pilot Project	76

5.2	Scholarly and general community outputs	78
	CHAPTER SIX: CONCLUSIONS AND RECOMMENDATIONS	80
6.1	Conclusions	80
6.2	Recommendations.....	82
	REFERENCES	83
	APPENDIX A: Ethical Clearance: University	92
	APPENDIX B: Ethical Clearance: Faculty.....	93
	APPENDIX C: Weighted average for solar collector inclination.....	94
	APPENDIX D: Tracking code for Arduino	95
	APPENDIX E: Battery specifications	97
	APPENDIX F: SWH “KOLEKTOR” software application.....	99
	APPENDIX G: SWH flat plate collector design summer and winter day	101
	APPENDIX H: Method of transporting fish.....	106
	APPENDIX I: PV specifications	116
	APPENDIX J: Charge controller specifications	118
	APPENDIX K: Inverter specification	119
	APPENDIX L: Anemometer	120
	APPENDIX M: Community report	122

LIST OF FIGURES

Figure 1.1: Ancient practice of aquaponics farming methods	3
Figure 1.2: Backyard aquaponics	3
Figure 1.3: Commercial aquaponics	3
Figure 1.4: Flood and drain	5
Figure 1.5: Bell siphon	6
Figure 1.6: Nutrient cycle	6
Figure 1.7: Cherry tomato bush and leafy vegetables in aquaponics environment.....	7
Figure 1.8: Nile tilapia	8
Figure 1.9: Mozambican tilapia	8
Figure 1.10: Global horizontal irradiation for SA	10
Figure 1.11: Direct normal irradiation for SA	10
Figure 1.12: De Saussure's hot box 1760's	11
Figure 1.13: Schematic of modern flat plate solar collector	11
Figure 1.14: Solar glass tube with vacuum envelope	12
Figure 1.15: Rooftop PV array	12
Figure 1.16: Sun's rays at summer and winter solstice	13
Figure 2.1: Aquaponics system schematic.....	19
Figure 2.2: Aquaponics Isometric lay-out.....	20
Figure 2.3: Optimum seasonal angles for Cape Town	22
Figure 2.4: Schematic illustration of the sun's tracker control system	23
Figure 2.5: Tracking frame.....	23
Figure 2.6: Motor drive.....	24
Figure 2.7: Relay board	25
Figure 2.8: Arduino uno board	25
Figure 2.9: Light sensor and its positioning on the PV panel.....	26

Figure 2.10: Internal wiring of the light sensor	26
Figure 2.11: Showing the connection on the Limit switches	27
Figure 2.12: Typical battery connections for 24 V 200 Ah output	33
Figure 2.13: Expected output temperature for summer and winter days ...	39
Figure 2.14: Effects of ambient conditions on the performance of the SWH.....	40
Figure 3.1: Aquaponics schematic.....	44
Figure 3.2: Hydroponics grow-bed.....	45
Figure 3.3: The siphon.....	45
Figure 3.4: Method of measuring plant growth.....	46
Figure 3.5: Fish photographed swimming over the 'background' grid in the control tank.....	46
Figure 3.6: Fish and feed weight.....	47
Figure 3.7: Sun's path at CPUT's Bellville campus for winter	49
Figure 3.8: Sun's path at CPUT's Bellville campus for summer	49
Figure 3.9: Operation of PV panel solar tracker	50
Figure 3.10: Solar tracking set-up at CPUT Bellville campus	51
Figure 3.11: Schematic illustration of the PV system	52
Figure 3.12: Prototype battery bank.....	53
Figure 3.13: Steca PR 3030 12/24 V	53
Figure 3.14: KS-1500P 1500 W 24 V inverter	54
Figure 3.15: Submersible pump.....	54
Figure 3.16: 4 W LED light bulb.....	55
Figure 3.17: Programmable timer	55
Figure 3.18: Agilent data logger model 34972A	55
Figure 3.19: 50 A 50 mV shunt	56
Figure 3.20: Battery analyzer.....	56
Figure 3. 21: Clamp meter	56
Figure 3.22: Battery autonomy set-up.....	57

Figure 3.23: Schematic illustration of the SWH set-up	58
Figure 3.24: SWH experimental set-up	59
Figure 3.25: Thermocouple set-up	59
Figure 3.26: T Type thermocouple	60
Figure 3.27: Agilent data logger circuit board (24 channel multiplexer)...	60
Figure 3.28: Thermocouples inserted in boiling water in the kettle	61
Figure 3.29: Thermocouple calibration in water and ice mixture in a bucket.....	61
Figure 3.30: Flow meter	62
Figure 3.31: Beaker collecting water flowing through a device.....	62
Figure 3.32: Flow rate test calibration set-up	63
Figure 3.33: Flow rate measurement using beaker, stop watch and variable area flow meter.....	63
Figure 3.34: Anemometer	64
Figure 3.35: Solar radiation meter	64
Figure 3.36: Throttling valve	65
Figure 3.37: Pyrometer reading	66
Figure 3.38: Anemometer reading	66
Figure 4.1: Plant growth rate total number of weeks: five weeks, total number of days: 35 days to harvest.....	67
Figure 4.2: Comparative power output for stationary vs tracking collectors	70
Figure 4.3: Battery capacity	71
Figure 4.4: PV system power performance	72
Figure 4.5: Energy system power performance	73
Figure 4.6: Typical system power performance	73
Figure 4.7: Comparison of experimental and analytical results (clear day)	74
Figure 5.1: Pilot schematic lay-out.....	76
Figure 5.2: Grow-beds.....	76

Figure 5.3: Fish tanks 77

Figure 5.4: Teaching activities at the community centre..... 77

LIST OF TABLES

Table 2.1: Cape Town optimum tilt of solar panels by month.....	22
Table 2.2: Losses due to external factors	30
Table 2.3: PV panel specifications.....	31
Table 2.4: PV panel specifications.....	35
Table 2.5: Flat plate solar collector specifications.....	36
Table 2.6: Summer day with high irradiation and low-moderate wind.....	37
Table 2.7: Winter day with low irradiation and high wind.....	37
Table 2.8: Design flow rate for summer	43
Table 3.1: Tilapia growth and feeding rate	47
Table 3.2: Fish growth rate	48
Table 3.3: Sun position	50
Table 3.4: Sun position day tracking	51
Table 3.5: Typical results using beaker and stop watch and variable flow meter	63
Table 4.1: Data collected on a clear sunny day	75

GLOSSARY

Terms/Acronyms/Abbreviations	Definition/Explanation
SA	South Africa
CPUT	Cape Peninsula University of Technology
MSPAS	Modular Solar Powered Aquaponics System
RE	Renewable energy
PV	Photovoltaics
SWH	Solar water heating
HYE	Highest yearly energy
HMDE	Highest minimum daily energy
CSP	Concentrated solar power
GHI	Global horizontal irradiation
DNI	Direct normal irradiance
CPV	Concentrator solar photovoltaic
MPPT	Multi point power tracker
PWM	Pulse width modulation
AC	Alternating current
DC	Direct current
STC	Standard test conditions
NOCT	Nominal operating cell temperature
SOC	State of charge
Ah	Amp-hour
DOD	Depth of discharge
VRLA	Valve regulated lead-acid batteries
AGM	Absorptive glass matt
RAFT	Root floating technique
DRFT	Dynamic root floating technique
LED	Light emitting diodes
P	Power
V	Volt
I	Current
VBGF	von Bertalanffy growth function

L_R	Load required in Watt Hours (Wh)
V_{oc}	Volt open circuit (V)
I_{cs}	Current closed circuit (A)
PV_{gf}	PV generator factor
S_l	System's loss factor
P_a	Total PV array power (W)
P_n	Number of PV panels
W_p	PV panel's rated power (W)
I_B	Battery capacity (Ah)
L_B	Battery loss factor
C_D	Battery depth of discharge
V_{nB}	Battery nominal voltage (V)
n_{ad}	Battery number of days of autonomy
I_{cc}	Charge controller's rating (A)
I_{scPV}	Total circuit current of the PV array/panel (A)
P_i	Inverter's power (W)
P_T	Total Watt-hours used per day (W)
Q_u	Useful energy gain of the SWH (W)
G	Solar radiation absorbed by solar collector (W/m ²)
A_a	Aperture area of the collector (m ²)
A_g	Gross area (m ²)
τ	Solar radiation transmittance of collector cover glazing
α	Solar radiation absorptance of collector absorber
U_t, U_b	Top and bottom collector heat transfer loss coefficient due to conduction, convection and radiation (W/m ² K)
T_{abs}	Mean absorber plate temperature (K)
T_a	Ambient temperature (K)
h_{pg}	Natural and forced convection at exterior surface of cover glazing (W/m ² K)

h_v	Heat conduction through cover glazing (W/m ² K)
h_{sg}	Radiation between exterior surface of cover glazing and sky (W/m ² K)
h_{pa}	Radiation between absorber and interior surface of glazing cover (W/m ² K)
h_{sa}	Natural convection between absorber and interior surface of cover glazing (W/m ² K)
T_g	Glass temperature (K)
u_w	Wind speed (m/s)
$\tau\alpha$	Glass transmittance-absorptivity product
ε	Emissivity
C_p	Specific heat capacity (J/kg K)
\dot{Q}_w	Heat gain in the water (W)
\dot{Q}_{col}	Heat gain in the collector (W)
\dot{Q}_{conv}	Heat loss by convection (W)
\dot{Q}_{rad}	Heat loss by radiation units (W)
T_{sky}	Sky temperature units (K)
\dot{m}_{water}	Mass flow rate (kg/min)
\dot{V}	Volumetric flow rate (l/min)
m	Mass (g with respect to fish growth)
t	Time (days with respect to fish growth)
m_∞	Mass of full-grown fish (g)
k	Energy loss constant (with respect to fish growth)

CHAPTER ONE: INTRODUCTION

1.1 Agriculture, energy and sustainable livelihoods in South Africa

The South African Western Cape Finance Minister, in his budget speech, mentioned that economic growth and development is critical to improve living standards and socio-economic conditions in South Africa (SA) (Meyer, 2018). The continuously growing SA population desperately *needs* a sustainable means of food production.

In the agricultural sector, outdated farming methods are heavily dependent on synthetic fertilisers which reduce soil fertility (Mulvaney *et al.*, 2009). The abuse of fertilisers can cause major damage to the environment. Fertilisers run off into rivers and pollute groundwater. Large doses of nitrogen are released into the atmosphere as nitrous oxide, a greenhouse gas 300 times more powerful than carbon dioxide. SA's outdated farming methods are now heavily dependent on these synthetic fertilisers (Goldblatt, 2011).

In addition, SA's agriculture is reliant on the scarce water resource which amounts to about 50% of the country's capacity (SA Yearbook, 2008). As the recent drought in the Western Cape further exacerbated water scarcity, a more conservative approach to water usage for agricultural purposes needs to be addressed (Rawlins, 2019).

New farming methods could require more energy input. SA's energy producer Eskom is battling to supply the needs of the country with recent blackouts being a common occurrence (Fin24, 2019a). The power utility, reliant on burning fossil fuel, is struggling to keep abreast financially (Fin24, 2019b). It is imperative that focus be directed to the use of clean energy and educating people on the use of it.

The bulk of SA citizens live under the breadline with few opportunities for education on producing sustainable livelihoods. Nako (2010) explains that there is an ever-increasing need to encourage low-income communities to educate themselves in science and technology as well as about developing an industry and welfare without dramatically increasing the traditionally based fossil fuel energy consumption (Bah & Azam, 2017).

It is therefore necessary to source alternate methods of farming that are more sustainable and environmentally friendly. The vision of the Cape Peninsula University of Technology (CPUT), which has been espoused by the author, is at the heart of technology education and innovation in Africa. The author wishes to create awareness in low-income communities about the effectiveness of renewable energy (RE) and the self-sustainability of alternate farming methods. The Modular Solar Powered

Aquaponics System (MSPAS) has the potential to harness RE in the form of solar thermal energy using photovoltaics (PV) panels. The MSPAS, the system under investigation, is enhanced by the usage of sustainable energy.

1.2 Aquaponics

Aquaponics can briefly be explained as a combination of hydroponics and aquaculture. The hydroponics unit is used to grow vegetables or plant life and the aquaculture unit is used for the breeding of aquatic organisms such as fish or shellfish (Goddek & Keesman, 2018). The fish and plants live together with symbiotic benefits that maximise the use of nutrients and minimize the waste of valuable resources such as water (Kyaw & Ng, 2017). According to Belton *et al.* (2014), fish cultivation through aquaculture has expanded rapidly in recent years. Aquaculture helps the smoothing out of seasonal variabilities in consumption. The hydroponics unit filters the water which contains the building blocks for the nutrients required by the plants, and in so doing, cleans and oxygenates the water for the aquaculture unit (Love *et al.*, 2015). Aquaponics has the potential to alleviate the problem of poor food security.

1.3 Food security

Food pricing is vastly dependent on water, energy and food production cycles (Gulati *et al.*, 2013). The value chain of food production, processing, packaging and distribution requires the input of energy and water. Environmental changes and constant increase in population growth impose heavy strains on these three resources (food, energy, water). Developing countries account for 95% of the world's population growth. As SA is regarded as a developing country, the rise in food prices in the country is on par with the global trend (Merwe, 2011). SA is food self-sufficient, or near food self-sufficient, with the ability to import when shortcomings occur, but with the growth in population and rapid urbanization, food security is a growing concern (du Toit, 2011).

Implementing MSPAS into rural or sub-economic communities in SA could alleviate the strain on energy, water and food resources. Teaching such communities about RE and new optimized farming methods such as aquaponics could usher in sustainable livelihoods. This would be beneficial in reducing poverty and the need for urbanization.

Aquaponics has been around for many centuries: combining fish and vegetable production into an integrated system is far from new. Ancient precedents for integrated aquaculture include the Chinampas of Mexico and the integrated rice paddy systems across parts of Asia (Figure 1.1).



Figure 1.1: Ancient practice of aquaponics farming methods (Milkwood, 2014)

The cycle of nutrients in aquaponics systems differs from traditional soil farming due to the presence of the fish. In aquaponics, fish supply the nutrients through their waste (faeces and urine). In a functioning aquaponics system, new supplemental nutrients do not need to be added as in traditional soil farming. More can be read on aquaponics from Graber and Junge (2009) regarding the nutrient recycling from fish waste water treatment by vegetable production. In recent times, aquaponics has grown in popularity as 'backyard farming' but more and more farmers are looking to upscale this to a sustainable financially viable option (Figures 1.2 & 1.3).



Figure 1.2: Backyard aquaponics (Aquaponichowto, 2009)



Figure 1.3: Commercial aquaponics (Aquaponichowto, 2009)

There are various types of aquaponics farming methods: root floating technique (RAFT); Nutrient Film Technique (NFT); and the ebb and flow media-filled grow-bed system.

The RAFT employs floating Styrofoam wherein the plants are accommodated. This tank is normally separate from the fish tank. Water continuously circulates from the fish tanks, through filtration components, to the raft tanks. The beneficial bacteria live in the raft tank and throughout the system. The extra volume of water in the raft tank provides a buffer for the fish, reducing stress and potential water quality problems – one of the significant benefits of the raft system.

The NFT grows plants in long narrow channels. A thin film of water continuously flows down each channel, providing the plant roots with water, nutrients and oxygen. As with the raft system, water flows continuously from the fish tank, through filtration components, through the NFT channels where the plants are grown and then back to the fish tank. A separate bio filter is required as the quantity of circulating water is minimal and not beneficial for bacteria to live in. In addition, the plumbing used in a hydroponic NFT system is usually not large enough to be used in aquaponics as clogging of pipes due to organic waste poses a problem. While NFT aquaponics shows potential, presently it is used less than the other two methods.

A media-filled bed system uses gravel, perlite or another media for the plant bed. This bed is periodically flooded (also known as the ebb and flow technique) with water from the fish tank. The water is then siphoned back to the fish tank. All waste generated, such as fish excretion, uneaten food and other solids, is broken down within the plant bed. This method uses the fewest components and no additional filtration, rendering it simple to operate (Nelson & Pade, n.d.).

The media-filled bed system was employed in the prototype (Figure 1.4). Water is allowed to fill in the grow-bed until it touches the plant's roots, then automatically siphons away. These cycles are continuously repeated, thus enticing the plant's root to grow faster.

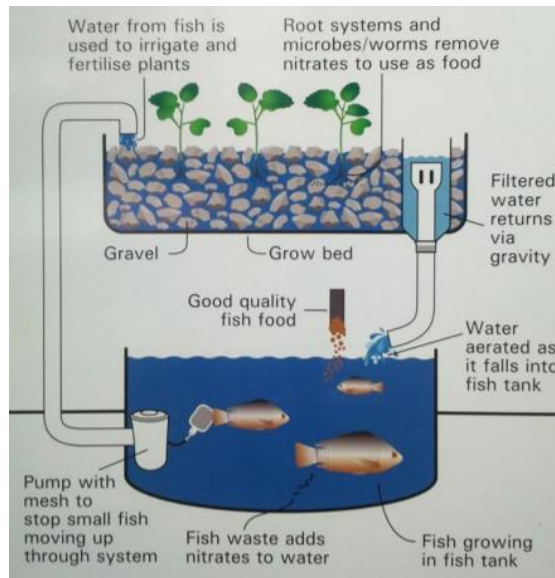


Figure 1.4: Flood and drain (Hambrey, 2013)

The flood and drain process is facilitated by a bell siphon which regulates water levels in the grow-bed.

Bell siphoning uses principles of physics and atmospheric pressure; it does not need any external energy input (Japanaquaponics, 2019). Fox *et al.* (2010) describe how to make a bell siphon; these principles were applied to the one placed in the prototype grow-bed. The siphon action and water cascading across the grow-bed promote the oxygenation of the water which is required for the fish or aquatic species.

The bell siphon fitted in the prototype's grow-bed consists of a both ends open vertical standpipe for the water to drain into (Figure 1.5). Around it is the bell pipe with slits for water flow at the bottom and an air tight cap on top. This outer pipe, called the siphon pipe, sits over the standpipe. Bell siphoning in aquaponics regulates the water height in the grow-bed. The standpipe determines the highest level the water can reach before it siphons.

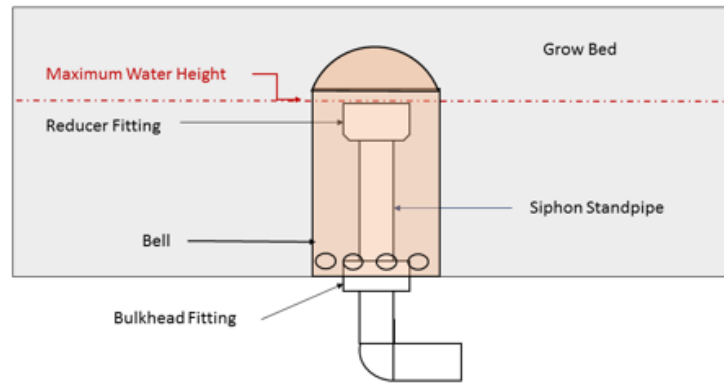


Figure 1.5: Bell siphon (Pattillo, 2017)

Bacteria (Nitrosomonas and Nitrobacter) play an important role in aquaponics systems, as they are responsible for nitrifying ammonia (toxic to fish) into nitrate which is safe to consume by plants. The Nitrosomonas create nitrites from their consumption of the ammonia. However, Nitrites are still toxic to fish so Nitrobacter is needed, which consume the nitrites to create the nitrates, the nutrients required for plant growth to excel (Figure 1.6).

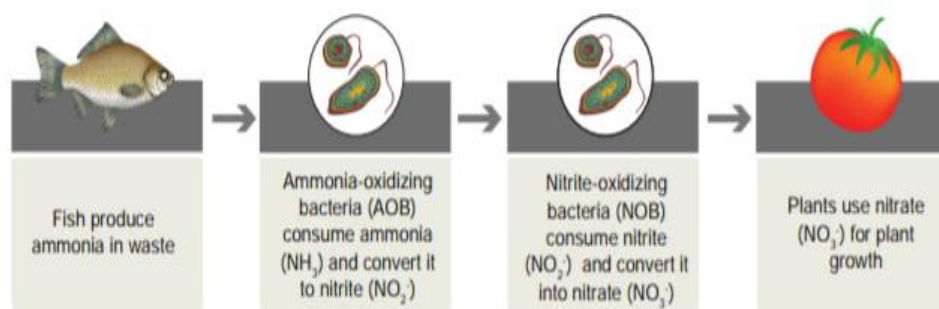


Figure 1.6: Nutrient cycle (Somerville *et al.*, 2014)

Many of the nutrients may take some time before they accumulate to significant levels in the system. When starting up an aquaponics system, it is important to choose plants or vegetables that are not high nutrient users. Leafy plants such as spinach, lettuce and spring onions have quick growth in aquaponics (Figure 1.7). The RSA and Department of Agriculture Forestry and Fisheries (2012) insist that tomatoes are the second most essential planted vegetable in South Africa after potatoes. Tomatoes contribute up to 24% of the total vegetables in the country, showing great potential for specialised aquaponics farming.



Figure 1.7: Cherry tomato bush and leafy vegetables in aquaponics environment

The aquaculture reservoirs of the prototype will house the fish. Rakocy *et al.* (2012) identify types of tilapia, koi, catfish, carp, shrimp and crayfish as suitable inhabitants in an aquaponics system.

Tilapias are the most widely cultivated fish species reared in aquaponics systems (Rakocy *et al.*, 2012; Love *et al.*, 2015; Mchunu, Lagerwall & Senzanje, 2018b). Two species are available in SA, namely Nile tilapia (*Oreochromis niloticus*) and Mozambican tilapia (*Oreochromis mossambicus*).

Nile tilapia (*Oreochromis niloticus*), with a weight of approximately 79 g, are known as fingerlings. An adult tilapia will weigh approximately 813 g, taking about 28 weeks to reach this weight. The Nile tilapia species, intended for breeding, need the water to be in the range of 27-30° C for proper growth (Somerville *et al.*, 2014).

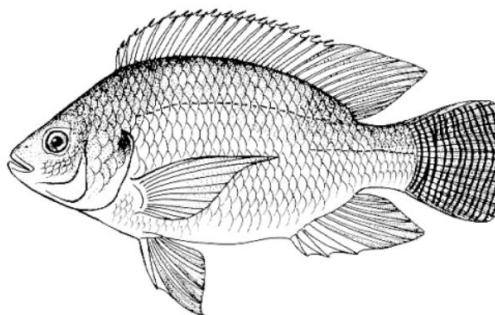


Figure 1.8: Nile tilapia (Somerville *et al.*, 2014)

Mozambican tilapia (*Oreochromis mossambicus*) can be found in all but fast-flowing waters as they grow well in standing waters. They are tolerant of fresh, brackish or marine waters and even higher salinity concentrations. They are a resilient species and can tolerate a wide range of temperate fluctuations from 15°C to 42°C (Skelton, 2001).

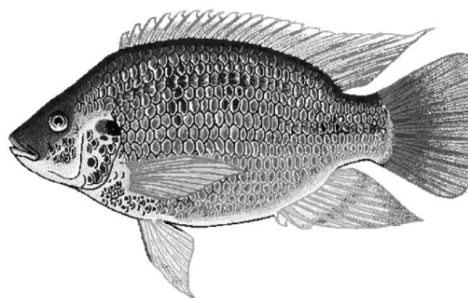


Figure 1.9: Mozambican tilapia (Somerville *et al.*, 2014)

Water quality for these fish is important. The recommended practice is to keep the pH between 7.0 and 7.5, ammonia (<0.6 mg/l), Nitrite (<1 mg/l), temperature (24-29° C) and oxygen (4-6 mg/l) as described by Rakocy (1989) and Somerville *et al.* (2014).

1.4 Renewable energy

The sun is one of the most predictable and reliable sources of RE available to Earth. According to Prasad and Snow (2005), it is estimated that one hour of solar energy received by the earth is equal to the total amount of energy consumed by humans in one year. This energy is eco-friendly and inexhaustible (Buker & Riffat, 2015). Ironically, though, sub-Saharan Africa has an abundance of RE resource yet only 30% of the population have electricity (Brew-Hammond & Kemausuor, 2009). Solar energy released by the sun is in the form of radiant light that can be harnessed using a wide range of technologies such as photovoltaics for electrical generation and solar thermal energy for heating.

Energy radiated from the sun is split into visible light, infrared light and ultraviolet light. Irradiation, the measure of energy flow (energy density) of sunlight per unit of area, is measured in kilowatt hours per square meter. Location, season, weather conditions, and the amount of sunlight are all factors which affect solar irradiation (Liang & Xia, 2005). One of the most promising renewable energy technologies is PV power. PV power is a means of producing on-site electricity from the sun without any concern for environmental harm. The focus on solar water heating and PV collectors will be discussed in more detail in the following sections.

1.4.1 Solar energy: SA's major renewable energy source

SA is situated in one of the best sunspots on the earth, ideal for PV and concentrated solar powered (CSP) plants (Pan & Dinter, 2017). In fact, SA has one of the highest potential of solar energy at its disposal (Aliyu *et al.*, 2018). SA receives eight to 10 hours of sunshine per day. The DoE (2014) published that a nationwide average of 2500 hours of sunshine per year yields 4.5 to 6.6 kWh/m² of radiation. Global horizontal irradiation (GHI) is vital for energy yield calculations and performance for PV technologies. The GHI (kWh/m²/a or W/m²) is the total amount of irradiation, consisting of a direct (beam) and a diffuse (scattered) portion that reaches a horizontal area. The inclined GHI (global tilted irradiance – GTI) is used primarily for power approximation determinations related to a solar PV or a solar water heater (SWH) with a fixed inclined angle. The solar irradiance is represented by the GHI and/or the direct normal irradiance (DNI). The GHI for SA is in the region of 2 300 kWh/m²/a (Solargis, 2019), demonstrating the promising potential for high-yield use of PV and SWH systems (Figure 1.10). DNI is an important parameter for energy yield calculation and performance assessment of concentrating solar power (CSP) and concentrator solar photovoltaic (CPV) technologies. The DNI for SA is in the region of 2 900 kWh/m²/a.

This is important for global irradiation received by tilted or sun-tracking PV modules (Figure 1.11) (Solargis, 2019).

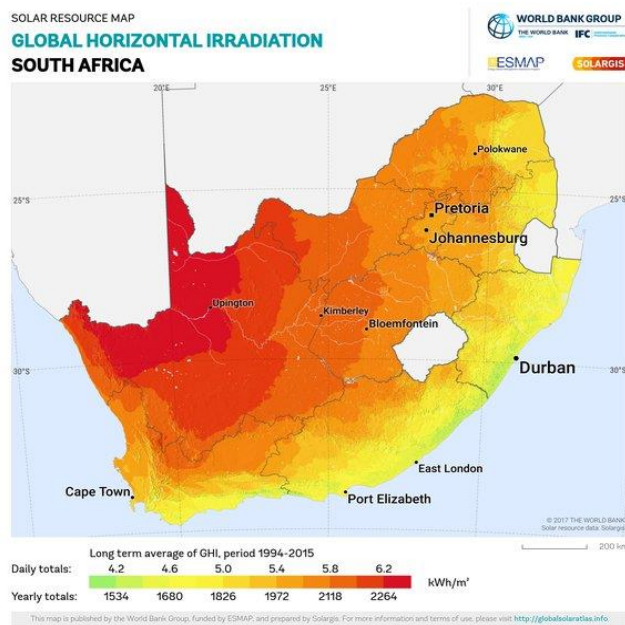


Figure 1.10: Global horizontal irradiation for SA (Solargis, 2019)

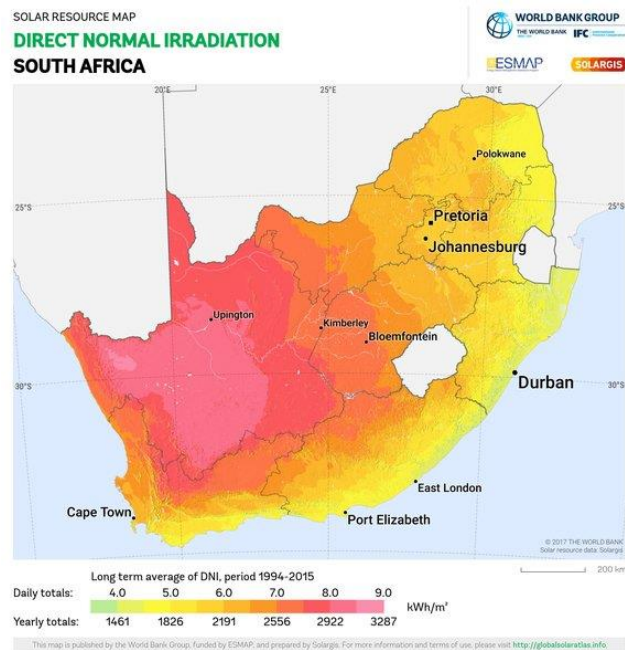


Figure 1.11: Direct normal irradiation for SA (Solargis, 2019)

1.4.2 Historical and modern harvesting methods of solar energy

Solar Heating: Long before PV was introduced, solar thermal energy was harvested by the Greeks in the 5th century B.C. They designed their homes to capture the heat of the sun's rays during winter. In the 1760s, the Swiss scientist Horace de Saussure built a prototype insulated box with a glass cover which became the baseline for modern solar collectors used to heat water (Figure 1.12) (Butti & Perlin, 1980). The glass cover easily allows the radiation from the sun's rays to pass through and a black body inside the box absorbs and transforms this radiation into heat energy which gets trapped in the insulated box. Some heat is lost by conduction through the glass cover.

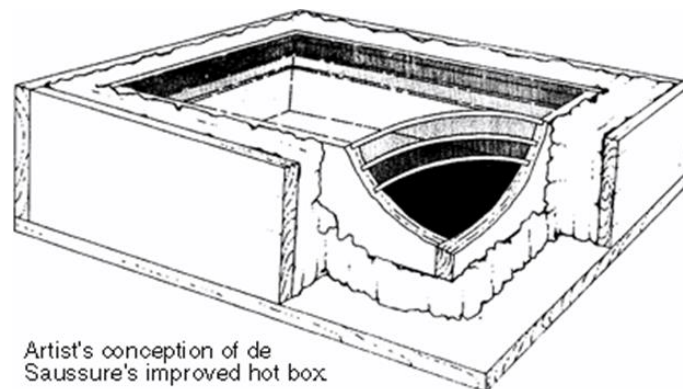


Figure 1.12: De Saussure's hot box 1760's (Butti & Perlin, 1980)

Solar water heating, one of the most popular solar thermal systems, accounts for 80% of the solar thermal market worldwide (Wang *et al.*, 2015). Modern solar flat plate collectors can operate at low to medium temperatures less than 100° C and can therefore be used for a wide variety of domestic hot water applications (Figure 1.13) (Kalogirou, 2004). The main component of the solar thermal system is the solar collector, also known as the solar water heater/collector (SWH).

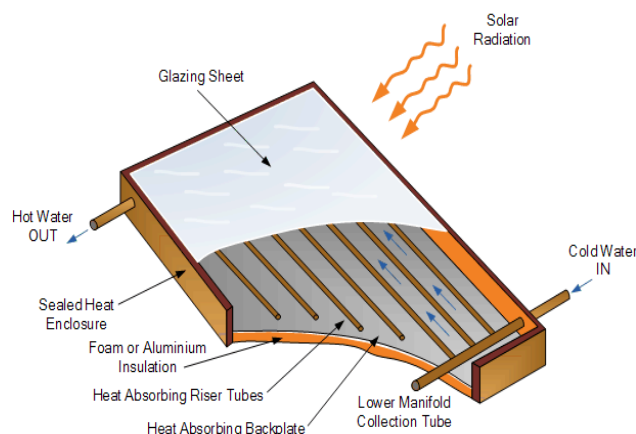


Figure 1.13: Schematic of modern flat plate solar collector (Alternative energy, 2019b)

During the 20th century, the development of evacuated solar tube collectors proved to be a more efficient method for harvesting solar energy. This was achieved by minimising the heat losses caused by conduction and convection (Figure 1.14) (Sabiha *et al.*, 2015). The evacuated tube collector is generally more expensive due to a more complex manufacturing process than the flat plate collector. The evacuated tube collector, however, is more effective per unit area than the flat plate collector and requires a smaller installation area.

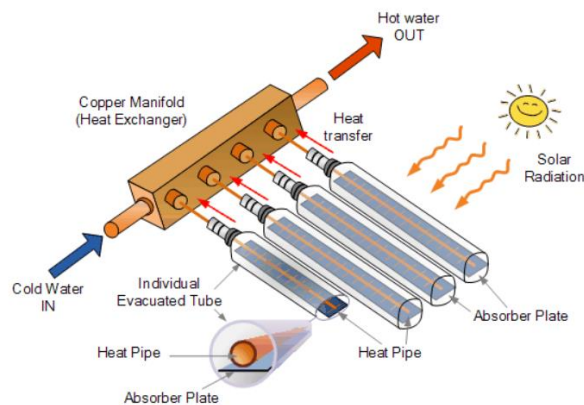


Figure 1.14: Solar glass tube with vacuum envelope (Alternative energy, 2019a)

Photovoltaics: PV is the conversion of light energy into electrical energy (Yilmaz *et al.*, 2015; Sampaio & González, 2017). A typical PV system consists of solar panels comprised of a number of solar cells. PV, when operating, does not generate any pollution and creates no greenhouse gas emissions. The cells are largely manufactured from silicon which is in abundance in the Earth's crust.

Stand-alone and grid-connected PV systems have been in use since the 1990s. They were first mass-produced in 2000, when German environmentalists and the Eurosolar organisation received governmental funding for a 'ten thousand roof' programme (Palz, 2014). Typical rooftop PV arrays are shown in Figure 1.15. Advances in technology and an increased manufacturing have reduced the cost while increasing the reliability and efficiency of PV installations (Swanson, 2006; Bazilian *et al.*, 2013).



Figure 1.15: Rooftop PV array (Yang *et al.*, 2019)

The most common type of PV collectors available are mono-crystalline silicon, polycrystalline silicon and thin film amorphous silicon. Crystalline (mono- or poly-) PV panels are readily available for home and business use. These types of solar panels account for 90% of PV market share as opposed to the 10% market share for the thin film solar panels. While crystalline panels come in a variety of shapes and sizes, the rectangular shape is the most common (El Chaar *et al.*, 2011).

1.4.3 Orientation of solar energy collector panels

The solar constant (energy from the sun per unit time received on a unit area) outside the atmosphere of the earth has been determined to be 1367 W/m^2 with an uncertainty of about 1% (Duffie & Beckman, 2013).

To get the maximum productivity out of solar energy, collectors must be angled towards the sun. The optimum angle varies throughout the year, depending on the seasons and location (Figure 1.16).

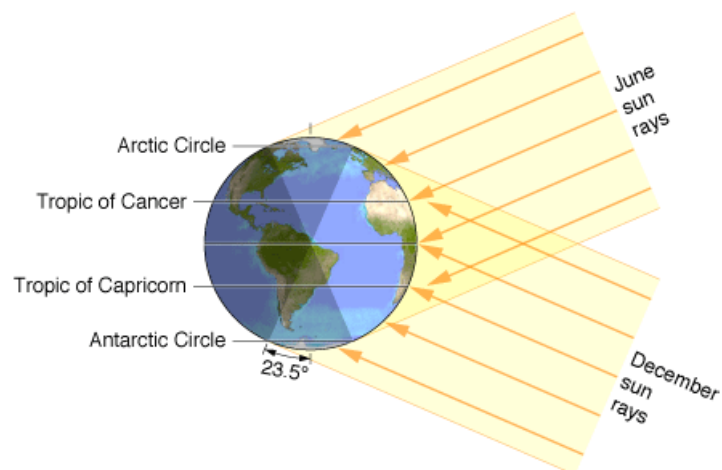


Figure 1.16: Sun's rays at summer and winter solstice (Schroeder, 2011)

As the sun is continually moving throughout the day, to optimise the energy received it would be ideal to track the sun minute by minute. However, sun tracking devices are expensive and consume additional energy. If space is not a problem, the purchase and installation of more fixed panels would be a more cost-effective solution than tracking (Vermaak, 2014).

1.5 Research questions

This research aims at answering the following questions:

- Is the integration of renewable energy to power an aquaponics system possible?
- Will the system be able to run sustainably off-grid?
- Compared to conventional aquaponics, will the integration of renewable energy technology produce similar harvesting outputs?
- Can this system be implemented in a low-income community and will it be possible to transfer technical aspects of the system's operation so that the community can operate it autonomously?

1.6 Statement of research problem

Tessema *et al.* (2014) recognise the importance of access to sustainable energy in rural, sub-Saharan poverty-stricken populations. Globally, the traditional fishing industry is experiencing a downward trend, while aquaculture has increased over the recent past and is demanding more energy. Belton *et al.* (2014) contend that the growth of aquaculture activity reduces the pressure on fisheries and eases the problems associated with vegetable seasonal variety.

This study will attempt to develop a modular solar powered aquaponics system (MSPAS) prototype, assembled using commercially available aquaponics and renewable energy equipment.

1.7 Research aim and objectives

The aim of the research was to demonstrate the amalgamation of solar energy and aquaponics systems for potential application in low income and remote communities in South Africa.

The objectives in support of the research were as follows:

Aquaponics: The concept of the aquaponics system was demonstrated.

Photovoltaic electricity generation: Experimentally it was demonstrated that solar energy can provide sufficient electricity to supply the pump (water re-circulation system) and for night-time illumination with light emitting diodes (LEDs).

Solar water heating: It was demonstrated that solar energy can provide thermal energy to improve the water temperature conducive to and beneficial for fish breeding.

Social: A pilot plant, placed in a low-income community, proved an adequate method of technology transfer and was accepted as an improvement in food security.

1.8 Significance and justification of this work

The research seeks to address the development of a sustainable and secure future for low-income communities in the Western Cape region of SA, which can then be expanded to other regions and nations. Considering the complex relationship between water, energy and food, it is imperative to find sustainable and affordable food production methods for SA (Gulati *et al.*, 2013). Aquaponics powered with RE is one farming method that encompasses all of the attributes of the combination and could alleviate some of the problems associated with poverty and food security.

Aquaponics is an evolving closed-system food production technology that integrates recirculating aquaculture with hydroponics. Rizal *et al.* (2018) refers to the benefits of aquaponics by discussing its social, environmental and economic impacts in different potential settings. He concludes that there are limited reliable empirical data available on energy use, accidents, repairs and social change pertaining to the technology. Mchunu, Lagerwall and Senzanje (2018a) suggest that aquaponics in SA is still at its infancy in terms of popularity and size of the productions systems. Lapere (2010) indicates that while aquaculture is the fastest-growing type of food production in the world, SA is lagging behind in efforts to boost the industry. It is accepted, however, that aquaponics has the potential to address food security challenges. According to Badiola *et al.* (2018), the main issues of recirculating aquaculture systems are poor designs and absence of skilled people taking responsibility for water quality and mechanical problems. The author sees this as an opportunity to work with a low-income community where such systems can be built and growth in expertise mutually developed.

Fuller (2007) indicates that there has been a continued interest in using passive and active solar technologies to reduce the conventional energy required to maintain water temperatures in small recirculation aquaculture systems, but with little available information to guide the designers of such systems. One of the requirements in the aquaponics system is to maintain a good water temperature for the fish to grow; exploring solar heating technologies for this purpose would be valuable.

RE systems, including electricity generation by using PV and solar water/environment heating, using various collector types in combination with aquaponics will be investigated. The optimisation of these collectors and integration of RE into aquaponics farming methods is novel and unique to low-income communities.

1.9 Delineation of the research

The following delineations pertain to this research:

- The research was exclusively focused on the technical aspects of the development of a prototype MSPAS and did not digress into the social study impacts of impoverished communities. The pilot system implemented in the community was with the assistance of the author; however, its design is not covered in this research, but a brief description of the performance and impact in the community appears in Chapter Five.
- The quality of the produce, such as plants and fish, was not analysed and does not form part of this research. However, rudimentary experiments were conducted to showcase proof of concept.
- The results of this research are only viable for the Cape Town region in South Africa; however, the methodology could apply to other regions.

1.10 Ethical considerations

The research encompassed the use of live fish and therefore animal ethical clearance was obtained at faculty and university levels (Appendices A & B).

The concept requires fish to be added to the MSPAS. The transportation and environment of the fish need to be comfortable and conducive to minimise stress build-up in the fish.

Berka (1986) highlights a few conditions to be adhered to when dealing with the environment and transportation of live fish:

- The fish required for transportation are to be healthy and in good condition.
- The fish must be starved for at least a day prior to transporting. Fish with a full digestive track require more oxygen and produce excrement which consumes the dissolved oxygen in the water.
- Water temperature differences should not be greater than 12-15° C with respect to species and size of fish.
- Adequate levels of dissolved oxygen are critical for stress-free transport.
- Good quality water is required when transporting fish. The stock density and time anticipated for transport both play a role in maintaining good quality water. Toxic ammonia and CO₂ produced by the fish affect the pH level. Consequently, the water's

pH levels should be monitored prior to and during the transport of fish, especially if long distances are involved. A pH level of about seven (7) to eight (8) must be maintained.

The Belhar Community Centre is, currently farming with tilapia, has agreed to assist with the growth experiments of fish to be added to the MSPAS prototype at CPUT BV campus. This document will serve as a guideline for the transportation and welfare monitoring of the fish.

1.10 Thesis outline

The thesis comprises six chapters as outlined below:

Chapter One: Consists of a general introduction and background information about RE resources on Earth and more specifically in SA. There are also introductions into the historical background of the two technologies, RE and aquaponics. Various components are identified and explained. It also describes the motivation for the work and objectives of this thesis. Literature reviewed are intertwined throughout the thesis when pertinent to the research conducted.

Chapter Two: Contains the description of the MSPAS and the design of the components for the prototype.

Chapter Three: Consists of the experiments conducted when testing some of the components of the prototype, the overall performance of the MSPAS and the results obtained thereof.

Chapter Four: Consists of the discussion of experimental results.

Chapter Five: Describes the engagement of the low-income community during the implementation of the pilot MSPAS and contributions made to scholarly and general communities.

Chapter Six: Consists of the conclusion and recommendations.

CHAPTER TWO: DESCRIPTION OF THE MODULAR SOLAR POWERED AQUAPONICS PROTOTYPE AND THE DESIGN OF ITS COMPONENTS

2.1 Aquaponics prototype section's design

The MSPAS consists of aquaponics (aquaculture and hydroponics) and renewable energy (RE) modules.

The following section presents a brief understanding as to what is required to design an aquaponics system, building on the development of the prototype. This study does not cover an in-depth analysis of nutritional development of the plants and fish. Instead, the emphasis is on the enhancement of the system's sustainable energy usage applied to aquaponics.

A brief description of the prototype aquaponics design follows. Aquaponics farming methods can be complex as fish have different nutrient requirement to that of plants. It is important to balance the amount of fish and fish feed with the hydroponics area (Lennard, 2012). Rakocy *et al.* (2012) and Lennard (2012) address the nutrient flow in aquaponics solutions. The conversion of fish waste generated by bio fluid excretion to nutritional base for the plants is described by the microbial component responsible for the nitrogen transformation process. This process allows the cleansing of the water by transforming ammonia into a nitrate form suitable for plant uptake (Mchunu, Odindo & Muchaonyerwa, 2018).

- Aquaculture section:

As illustrated in the schematic and the isometric view, the components numbered (in brackets) comprise the aquaculture section (Figures 2.1 & 2.2).

The design embodies an aquaculture section consisting of two 500 litre reservoirs which are used for breeding fish. The top reservoir (1) also known as the *grow-out tank* can hold 500 litres of water with an overflow that leads to the grow-bed. This reservoir is used as a grow-out tank for larger fish. The bottom reservoir (2) also known as the *sump tank* contains a minimum of 250 litres of water, which increases after the siphon effect takes place in the grow-bed (6). The water, which increases to about 400 litres in the sump tank after every siphon, is continuously pumped from the sump tank to the grow-out tank via the submersible pump (5). The sump tank is used to grow fingerlings to a large enough size before placing them into the grow-out tank.

The two reservoirs are connected by means of pipes. Reservoir (1) is fitted with a float valve (3) which is used to provide make-up water to the system when required. The

water to the system is provided via the municipality's mains. Once the system is filled to capacity, it operates as a closed looped system whereby the submersible pump (5) located in the sump tank (2) pumps water continuously to the grow-out tank (1). The flow rate is controlled by a valve (7) located at its exit. The stand-pipe (4) in reservoir (1) allows for the overflow of the water, carrying the dissolved waste of the fish to the hydroponics grow-bed filtration unit (6). In other words, this overflow water carries the relevant building blocks for developing nutrients to support and stimulate plant growth. Solid waste generated by the fish, together with the unconsumed excess food which concentrates at the bottom of the reservoirs, can also be removed by drain valves located at their base. This excess waste can be manually redistributed to the grow-bed (6). The reservoirs (1 & 2) can be insulated with any suitable insulation material (not shown on the schematic, Figure 2.1). The insulation limits the energy expended to heat the water in maintaining temperatures that facilitate fish growth. The open tops allow for oxygen absorption through the water surface and access to the aquatic species for their feeding and growth monitoring. Reservoir (1) requires temperature control whereby heating is provided by a flat plate solar water heater (SWH) (10). The water circulates directly through the SWH. The temperature is controlled by a valve (11) located at its exit which can regulate the flow rate and thus control the water's temperature. Thermocouples are attached to measure and monitor temperature variations within the system.

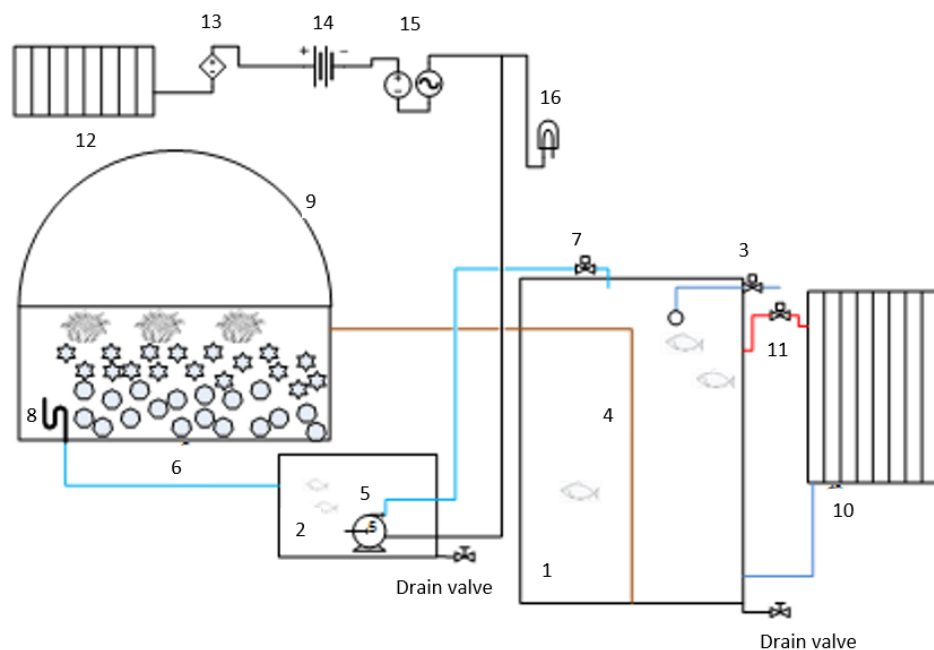


Figure 2.1: Aquaponics system schematic

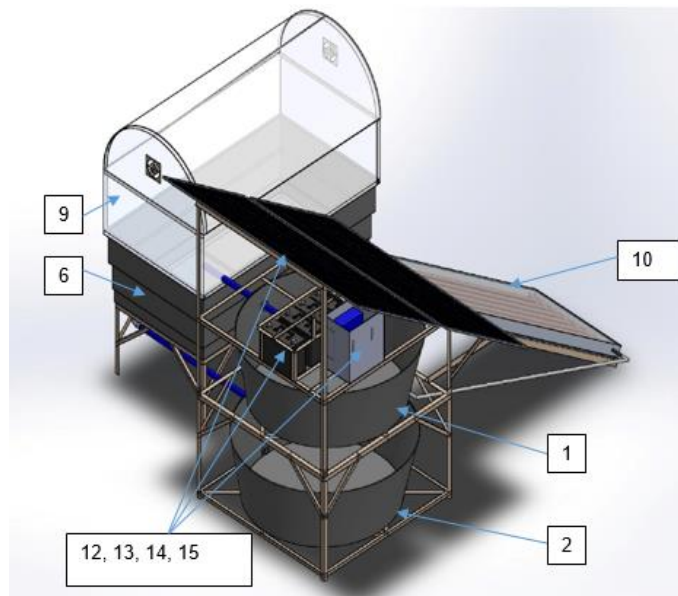


Figure 2.2: Aquaponics Isometric view (some components omitted for clarity)

- Hydroponics section

The grow-bed (Hydroponics filtration unit) (6) consists of a reservoir 1.2 m x 1.8 m x 0.5 m deep (standard cattle trough) which is filled with lightweight expanded clay aggregate (LECA) to an approximate height of 300 mm. The LECA has a low bulk density between 300 to 600 kg/m³ and tends to float when flooded with water. A 50 mm layer of building stone (19 mm) covers the LECA to weigh it down.

The grow-bed (6) filters the water that is re-circulated by gravity back to the sump tank (2). A covering (9) made of metal straps supporting a transparent material over the grow-bed creates the greenhouse effect suitable for stimulating plant growth. The cleansed water is siphoned from the hydroponics grow-bed (6) via the bell siphon (8) into the sump tank (2).

This conditioning and recycling of water minimises the loss of the valuable (water) resource. The pump required to circulate the water is powered by electricity generated by harvesting solar energy.

2.2 Renewable energy section's design: optimisation and sizing

While developing the prototype, the focus was on how to optimise and size the renewable energy section (RE), which consisted of PV panels, the SWH and associated equipment.

The concept of the prototype integrates the use of solar energy and employs technology such as photovoltaics (PV) to generate electricity, and a flat plate collector to heat the water as illustrated above in the schematic diagram and the isometric drawing (Figures 2.1 & 2.2).

The flat plate SWH (10) is connected to the grow-out reservoir (1) to supply heat for the water. Two PV modules (12) are coupled to a battery bank consisting of deep cycle 12 V batteries (14). The controller (13) regulated the charge to the deep cycle batteries (14). An inverter (15) delivers the necessary power to the pump (5) and during the night for lights (16) suspended over the fish reservoirs to attract insects, the natural food for the fish when caught on the water's surface.

By powering the system with RE, it could be located where grid power is not available; however, if necessary, it would operate when connected to the conventional grid.

In accordance with recommendations, the following factors were considered when designing the stand-alone PV system. However, some of these factors apply to the SWH and its associated equipment, i.e. the entire RE module (Wang & Lu, 2015).

- The location and conditions of the environment where the system is located, regarding, for example, sufficient exposure to solar radiation.
- The number of hours per day for the system's operation.
- Whether the output voltage required from the PV should be AC or DC.
- The power demand (including losses) to size the system accordingly.
- A decision on the amount of energy that should be stored (in batteries) to allow for conditions of un-available solar radiation.
- The selection of a charge controller to protect the batteries.
- The selection of the inverter to convert DC to AC.
- The electrical cable size requirement.

2.2.1 Optimising the solar energy collectors' orientation for Cape Town

It would be ideal to continuously adjust the orientation of the solar collectors, tracking or facing the sun throughout the year, to optimise the collection or harnessing of the available solar energy.

The governing equations to obtain optimum angles for the PV panels and the SWH to face the sun have been dealt by a number of researchers (for example, Duffie & Beckman, 2013). The author chose a more direct and user-friendly method.

Using an online solar calculator, the following optimal solar noon conditions were determined for the Cape Town area, showing the sun's height on a monthly basis (Table 2.1 & Figure 2.3) (solarelectricityhandbook, 2019).

Table 2.1: Tilts for solar panels Cape Town, north facing (in degrees from the vertical)

Jan	Feb	Mar	Apr	May	Jun	Jul	Aug	Sep	Oct	Nov	Dec
72°	64°	56°	48°	40°	32°	40°	48°	56°	64°	72°	80°



Figure 2.3: Optimum seasonal angles for Cape Town (solarelectricityhandbook, 2019)

To determine the annual optimum tilt angle for Cape Town, a weighted average of the seasonal angles was taken with the conservative approach to favour winter. The calculation resulted in an angle of inclination with respect to the vertical of 52.7° (Appendix C). The angle is very close to 50° (with respect vertical) obtained by Bekker (2007) for achieving the highest minimum daily energy (HMDE) through the year for Cape Town. Based on the calculation and Bekker (2007), the solar energy collectors of the MSPAS prototype were positioned at 50° (relative to the vertical). This angle also favoured the design of the prototype, keeping it compact and modular.

Tracking would require considerable expense which could be a burden to low-income communities during the start-up phase. Instead, it was decided orientate the solar collectors at a fixed angle (Figure 2.2).

A basic tracking mechanism was developed for testing the prototype that could bolt onto the existing MSPAS frame should it be required at a later stage. At the time of testing, it was decided to place the experimental apparatus at an angle of 30° to the horizontal which was in line with harnessing the highest yearly energy (HYE) for this tilt angle in Cape Town (Bekker, 2007). This angle would be more favourable should tracking be applied.

- Components of the tracking mechanism

The tracking mechanism consists of the frame, motor drive (adapted 12 V car jack components), channel relay board, an Arduino programmable microprocessor, light sensor, two limit switches and a 12 V DC power supply. Figure 2.4 illustrates how the control components are connected for the tracking mechanism.

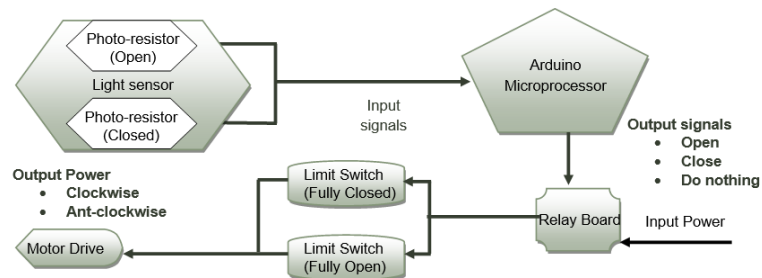


Figure 2.4: Schematic illustration of the tracker control system

- The frame of the tracking mechanism

The frame can be mounted on the existing structure (Figure 2.5). It consists of a metal structure that allows for unilateral solar tracking. The lifting/top frame is for mounting the PV module which is hinged to the base frame. The tracking motion is powered through the adapted 12 V car's jack, driving the threaded screw which is controlled by Arduino equipment.

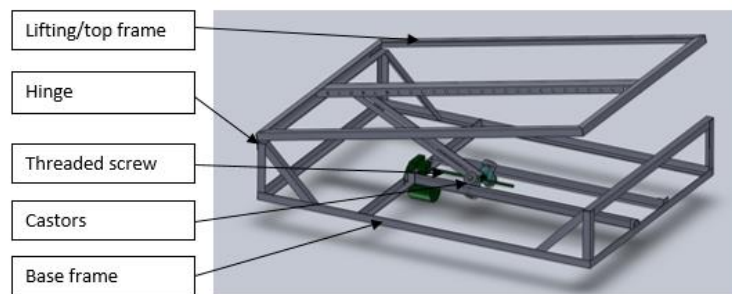


Figure 2.5: Tracking frame

- Powering the motion of the tracking mechanism

The 12 V DC car jack was dismantled and its electric motor was incorporated in the tracking mechanism. The car jack comes standard with a 1:52 reduction gearbox capable of moving the top frame when tracking the sun (Figure 2.6). The motor's maximum working current is 10 A which is supplied from the battery bank via the relay board. The motor's rotational direction is controlled through this relay board by switching the polarity of the power supplied to the motor terminals when the tracker's top frame must move up or down. The drive screw push and pulls the caster and link; its action swings the top frame around the pivotal hinge point (Figure 2.5). The manual crank handle is supplied as standard equipment in case of prolonged power failure or equipment malfunctioning.

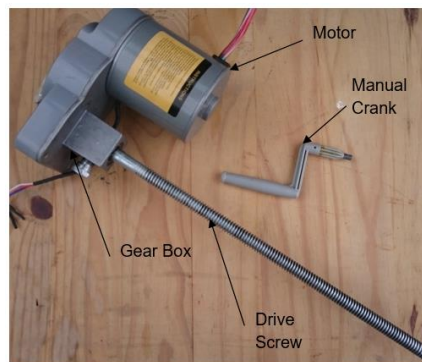


Figure 2.6: Motor drive

- The relay board

The relay board consists of four relays (Figure 2.7). The relays require a small five V signal at 30 mA to activate the contacts, which are rated at 12 V and 10 A. The signal voltage is sent directly from the Arduino microprocessor. The four relays are used to switch the high voltage, high current electrical supply from the battery bank to the electric motor. Two of the relays switch the negative power supply and two relays switch the positive power supply.

By cross wiring the relay outputs to the motor driver's terminals, it was possible to activate one pair of relays to drive the motor clockwise and the other pair of relays to drive the motor anti-clockwise.

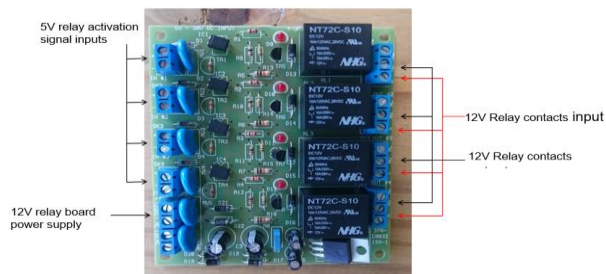


Figure 2. 7: Relay board

- The Arduino microprocessor

The Arduino microprocessor was programmed to read the signals from light sensors and limit switches, and based on a logic sequence, send output signals to the relay board to move the motor clockwise, anti-clockwise or not at all (Appendix D, open source code).

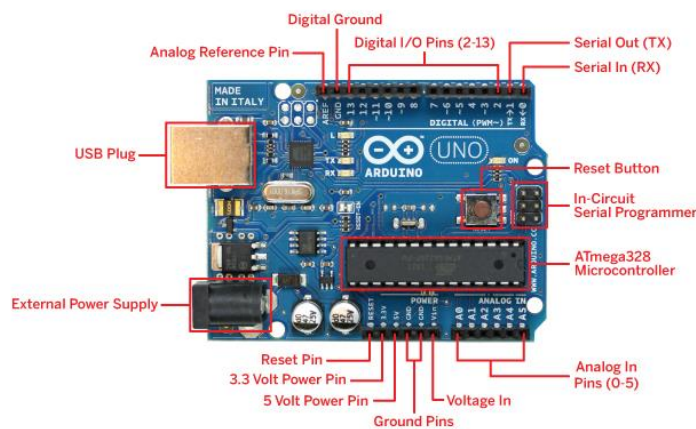


Figure 2.8: Arduino uno board (Badamasi, 2014)

- The light sensors

The light sensor is a set of two photo resistors separated by a partition that will cast a shadow on one of the photo resistors if the sensor is not perfectly aligned with the sun (Figure 2.9). If one photo resistor sees more sunlight than the other, the signal from the sensor to the Arduino microprocessor will be unbalanced and therefore the Arduino microprocessor will know which direction to move the motor until the light sensor signal is balanced again.

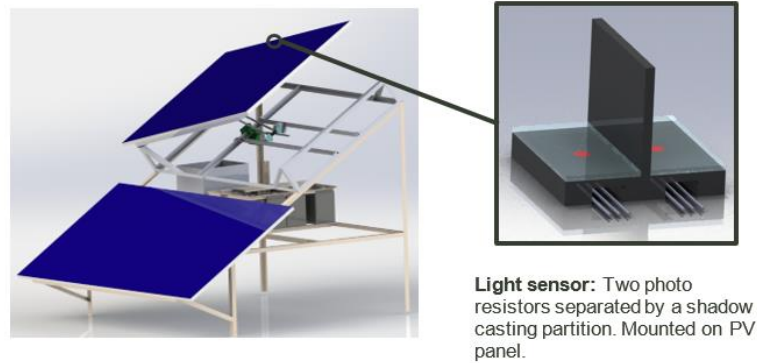


Figure 2.9: Light sensor and its positioning on the PV panel

The two photo resistors are connected to the Arduino's five V power supply in parallel (Figure 2.10). Directly after each photo resistor, a 'signal' wire branches off to two of the Arduino's analogue inputs. This signal allows the Arduino to read and compare the voltages after each photo-resistor. A standard 10K resistor is connected after each photo resistor to protect the Arduino from short circuit in the case of the photo resistor's resistance being low when exposed to intense sunlight.

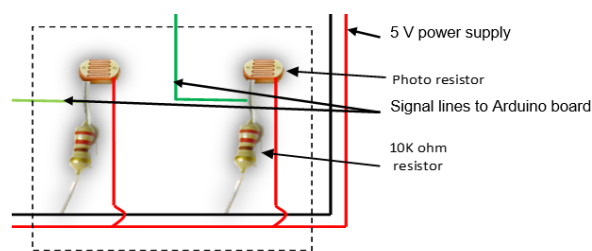


Figure 2.10: Internal wiring of the light sensor

- The limit switches

Two limit switches are used in the system to send signals to the Arduino. This indicates to the Arduino when the tracker is fully open or fully closed (Figure 2.11). The limit switch has a set of normally closed contacts and a set of normally open contacts. The positive power cables that supply the motor with power from the relays run through the normal close contacts of the limit switches; therefore, when the limit switch is activated it breaks the circuit feeding power to the motor drive. The motor stops closing or opening when it reaches the limit. The normally open contacts send a low voltage signal to the Arduino microprocessor when the limit switch is activated. This signal is used in the programme code to stop sending opening or closing signals to the relay board.

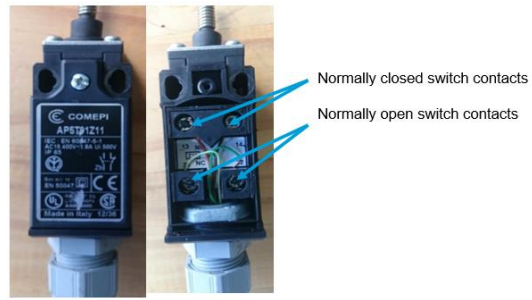


Figure 2.11: Showing the connection on the limit switches

- The power supply

The MSPAS battery bank consists of a 24 V bank made up of four 12 V batteries, two pairs connected in series and then connected in parallel. To power the motor, a supply from the battery bank connections between the two batteries in series produce 12 V.

2.2.2 PV system design

In order to maintain a symbiotic relationship between the plants and fish, the requirement of constant circulation of water in the aquaponics section was provided by using a 55 W submersible pump. Two four (4) W light emitting diode (LED) lights were positioned over the aquaculture tank. These lights operated for a period of four hours nightly.

The submersible pump chosen, which requires a power supply from a 220 voltage, is readily available, reliable, robust and cost effective. The only disadvantage of choosing AC equipment is that an inverter is required. However, it was imperative to use reliable technology to minimise the risk of failure and fatality to the fish, which would happen if the circulation of water failed and dissolved oxygen ran out.

- Sizing of the PV array

Solar irradiance/radiation: The quantity of power per unit area coming from the sun is known as irradiance. The energy produced by a photovoltaic module is directly related to the availability of solar energy, which in turn is dependent on geographical location (El Mays *et al.*, 2017).

In sizing the PV system, the sum of the electrical energy load, supplemented by the various losses described in Table 2.2, was required. The minimum number of irradiation hours available to meet this requirement was chosen as the shortest daylight hours during winter months.

- Electrical load

$$\text{Pump:} \quad 55W \times 24h = 1320 Wh$$

$$\text{LED Lights:} \quad 4W \times 2 \times 4h = 32 Wh$$

$$(L_R) = 1320 + 32 = 1352 Wh$$

Where: L_R is the total Watt hour load required per day.

- Considering the various losses from PV panels

Temperature losses: The high temperatures that the PV panels attain are mainly due to exposure to high solar radiation and heat absorbed from the ambient surrounds (Michael *et al.*, 2015). PV panels are normally specified at 25° C and radiation at 1000 W/m² (Ceylan *et al.*, 2014; Micheli *et al.*, 2015). The cell voltage decreases by approximately 2.2 mV with every 1° C increase in temperature. The efficiency of the crystalline PV energy generating cells drops by 0.5% (Moharram *et al.*, 2013). For crystalline modules, a typical temperature reduction in efficiency could be in the range of 11% (Court & Ramon, 2001).

Soiling of the PV panels: Dust accumulation, leaves, bird droppings and dirt can cause soiling of solar panels. This accumulated dirt causes shading of the cells and thus reduces the available power generation. Annual losses caused by this soiling range from 1.5 to 6.2% depending on the location of the PV plant (Maghami *et al.*, 2016).

Tilt losses: The energy output from a PV module, made from crystalline silicon cells, is maximum if the sunlight is incident with a perpendicular angle on it (Maghami *et al.*, 2016; Loschi *et al.*, 2015). Some of the most important factors potentially impacting the output from the PV systems are dependent on the installation of their components. For example, some are related to the cables, the orientation of the panel and the mismatch of equipment. These losses should be kept at minimum, but it is difficult to keep them below 3% for any PV system. An average reduction factor for these losses is 95% (Court & Ramon, 2001).

Ageing or degradation losses: Manufacturers of PV panels (crystalline silicon modules) typically provide a warranty period ranging from 20 to 25 years (Kuitche, 2013). Manufacturers consider a PV module degraded when its power reaches a level below 80% of its initial power (Wohlgemuth *et al.*, 2005). Considering degradation as an output loss factor, which will only become a full reality at the end of a warranty period, is in fact over sizing the panel at the design stage.

The PV loss factors are summarised Table 2.2.

Table 2.2: Photovoltaic loss factors

	Efficiency	Losses
Temperature loss	0.89	11%
Soiling	0.94	6%
Tilt	0.95	5%
Ageing	0.80	20%

Using the information listed in Table 2.2, the PV total loss factor was determined:

$$PV \text{ total loss factor} = 0.89 \times 0.94 \times 0.95 \times 0.8 = 0.64$$

- PV generator factor

The PV generator factor (PV_{gf}) taking into account losses and average daylight hours of irradiation (normally during winter months) was determined using Equation 2.1.

$$PV_{gf} = S_l \times T_{hrs} \quad (2.1)$$

Where: PV_{gf} PV generator factor
 S_l PV losses factor
 T_{hrs} Average daily winter irradiation hours (5.5 hrs)

$$PV_{gf} = 0.64 \times 5.5 = 3.35$$

- Determining the number of PV panels

The total power required from the PV panels was determined using Equation 2.2.

$$P_a = \frac{L_R}{PV_{gf}} \quad (2.2)$$

Where: P_a Total array power required
 L_R Load required per day
 PV_{gf} PV generator factor

The total power required of the PV panel was determined

$$P_a = \frac{1352}{3.35} = 403.58 \text{ W.}$$

The number of panels required was determined by dividing the total power required by the power available for the selected PV panel. The commercially available PV panels have a nominal output power of 235 W_p. Table 2.3 shows the selected PV panel specifications.

$$P_n = \frac{P_a}{W_p} \quad (2.3)$$

Where: P_n Number of panels required
 P_a Total power required
 W_p PV panel's rated power

From Equation 2.3, the number of PV panels required is as follows:

$$P_n = \frac{403.58}{235} = 1.7, \text{ hence select 2 panels}$$

Table 2.3: Selected PV panel specifications

Rated power (P_{max})	235 W _p
Rated voltage (V_{mp})	30 V
Rated current (I_{mp})	7.83 A
Open circuit voltage (V_{oc})	37 V
Short circuit current (I_{sc})	8.25 A

- Battery sizing

Deep cycle batteries: In this application, deep cycle batteries were used to store and supply energy when required.

Flooded lead acid batteries, the more common battery type, have been developed for more than 150 years. Having proven their reliability in the automotive industry, they have found their way into renewable energy storage systems. In applications similar to this one, the use of deep cycle batteries is prominent but it does have drawbacks. During the charge cycle, these batteries vent hydrogen and oxygen gasses to the atmosphere and therefore need to be topped-up with distilled water on a regular basis, therefore requiring constant maintenance (Tantichanakul *et al.*, 2013). More modern types incorporate valve regulated lead-acid batteries (VRLA) which are sealed batteries. These batteries have pressure-relieve valves that allow gases to escape when internal pressures are exceeded. Gases are recaptured during the charge cycle

and recombined with the electrolyte, minimising water losses (Tantichanakul *et al.*, 2013). VRLA batteries were the obvious and clear choice.

Maintaining the correct state of charge (SoC) is important as the life of the battery is dependent on it (Marom *et al.*, 2015). The life span of a battery is determined through its depth of discharge. The depth of discharge is the fluctuation between the discharging and charging of the battery from fully charged to 20% discharge and vice versa. As the depth of discharge increases, subsequently the life of the battery decreases. The standard depths of discharge vary: in practice the common rate of 80% for deep cycle batteries could give a seven to eight year life expectancy (El Shenawy *et al.*, 2017). For the selected VRLA battery, the depth of discharge of up to 70% is feasible (Appendix E). Battery loss factors range from 80 to 85% (Kulworawanichpong & Mwambeleko, 2015; El Shenawy *et al.*, 2017).

The calculation for the battery was done with the provision of two days of autonomy. Batteries are assumed to be fully charged at the start-up. During adverse weather conditions (the charge will be minimal due to low solar irradiation) or possible mishaps such as failure of ancillary equipment, the battery will be able to supply power for two days without receiving any charge. In the work of Kulworawanichpong and Mwambeleko (2015), one of the arguments was that it would be uneconomical to design a rural stand-alone PV house system for two or three autonomous days since there will always be sunshine available to supply charge to the batteries throughout the year. However, in the case of the MSPAS, the lives of the fish are at stake. The author has therefore decided to apply two days of autonomy to rectify a mishap or find an alternative power source.

Battery calculation (24 V output):

- Assumed two days of autonomy
- Load of 1352 Wh/day as previously determined
- Depth of discharge of 70% (Appendix E)
- Battery loss factor of 80% (Kulworawanichpong & Mwambeleko, 2015)

$$I_B = \frac{L_R}{L_B \times C_D \times V_{nB}} \times n_{ad} \quad (2.4)$$

Where:

I_B	Battery capacity in Ah
L_R	Total Watt-hours per day used by appliances
L_B	Battery loss factor
C_D	Depth of discharge

V_{nB} Nominal battery voltage

n_{ad} The number of days of autonomy (number of days that the system operates should there be no power produced by the PV panels)

The battery capacity required for the 24 V system was found to be as follows:

$$I_B = \frac{1352}{0.8 \times 0.7 \times 24} \times 2 = 201 \text{ Ah.}$$

Readily available VRLA lead-acid deep cycle batteries rated at 12 V and 100 Ampere hours were selected. The schematic diagram in Figure 2.12 depicts a typical 12 V batteries set-up for a 24 V 200Ah output.

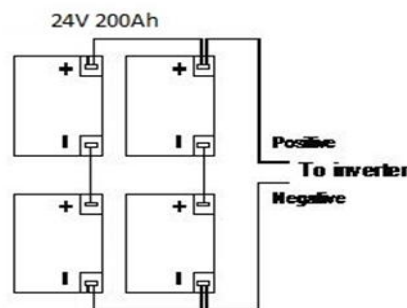


Figure 2.12: Typical 12 V batteries set-up for 24 V 200 Ah output

- Charge controller selection

The success of any off-grid PV system depends to a large extent on the long-term performance of the batteries. For a system to operate well and have a long lifetime, the batteries must be charged properly and maintained at a high level of charge. A charge controller's function is to regulate the voltage and current from the solar arrays to the battery to prevent overcharging and over discharging (Kulworawanichpong & Mwambeleko, 2015). According to Leonics (n.d.), a microgrid expertise specialist company, the standard practice for sizing a solar charge controller is to take the short circuit current (I_{sc}) of the PV array and multiply it by 1.3. (system losses are taken to be 30%).

The charge controller size was determined using Equation 2.5.

$$I_{cc} = n_{pv} \times I_{sc} \times 1.3 \quad (2.5)$$

Where:

I_{cc} Charge controller's rating

n_{pv} Number of PV panels

- I_{sc} Short circuit current of the PV array/panel (Table 2.3)
- 1.3 Energy lost in the system standard practice (Leonics, n.d.)

The capacity that the charge controller required was found to be:

$$I_{cc} = 2 \times 8.25 \times 1.3 = 21.45 \text{ A.}$$

A standard 24 V charge controller was selected that could handle 30 A.

- Inverter selection

An inverter was included in the stand-alone solar PV system to convert the DC into AC electricity. The inverter must meet two requirements: peak (or surge) power and continuous power. Some appliances, particularly those with electric motors, need a much higher power level at start-up than they do when running (Foster & Ghassemi, 2010).

The inverter size should be 25-30% bigger than the total Watts of appliances. In case of an electric motor or compressor, the inverter size should be a minimum of three times the capacity of the appliances and must be added to the capacity of the inverter to handle surge current during starting (Leonics, n.d.).

The total wattage that the inverter would require to maintain the electrical load had to be determined. A start-up rating of three (3) was assigned to the class of machine (centrifugal pump) in use in the system; this accounts for the momentary spike in power required to start the pump. The efficiency of the inverter was assumed to be 90% (Fouad *et al.*, 2017).

Pump power: $55 \text{ W} \times 3 \text{ (startup rating)} = 165 \text{ W}$

Lights: $4 \text{ W} \times 2 \times 1.3 = 10.4 \text{ W}$

Where 1.3 is the industry practice/system loss (Leonics, n.d.)

The inverter size was determined using Equation 2.6

$$P_i = \frac{\sum P_T}{\eta} \quad (2.6)$$

- Where:
- P_i Inverter's power
 - P_T Watts used per day by the equipment

assuming/applying an Inverter efficiency of 90%:

$$P_i = \frac{165 + 10.4}{0.9} = 195 \text{ W}$$

A standard 200 W inverter which can accept 24 V direct current supplied by the battery bank and deliver an output of 220 V and alternating current at a frequency of 50 Hz, would suffice. A 1500 W inverter was secured which was greatly oversized; however, this inverter was reasonably priced and readily available.

- The power cable sizing for the PV system

Selecting the correct size and type of wire would enhance the performance and reliability of the PV system. Voltage drop through incorrectly sized cables is one of the most common faults of an electrical system.

The cross sectional area of the DC cable was determined by using the online calculator for the various components, as described in Table 2.4 (Solar-wind, 2019). Sizing is based on maximum cable length and electrical current requirements.

Table 2.4: PV panel specifications

Cable size between PV and charge controller	$I = 21.45 \text{ A}$	$l = 1.5 \text{ m}$	$A_c = 4 \text{ mm}^2$
Cable size between charge controller and battery	$I = 30.00 \text{ A}$	$l = 1.5 \text{ m}$	$A_c = 4 \text{ mm}^2$
Cable size between battery and inverter	$I = 69.44 \text{ A}$	$l = 1.5 \text{ m}$	$A_c = 10 \text{ mm}^2$
Cable size between inverter and the AC load	$I = 6.82 \text{ A}$	$l = 3 \text{ m}$	$A_c = 1 \text{ mm}^2$

2.2.3 SWH design

The temperature of the water for the tilapia fish to grow optimally is between 25 to 30° C (Elfeky, 2019). To improve the control of the temperature of the water, a conventional flat plate solar energy collector was selected (Table 2.5) based on a readily available SWH that could fit the prototype. The design covers the performance of this SWH, taking into consideration a typical day in summer and winter. The initial calculations were used to predict the performance of the collector by considering thermosiphon induced flow through the collector. The results proved that the temperatures required were obtained during summer with a slight improvement of the water temperature during the winter months (further expanded in the paragraphs below Figure 2.13). According to Rakocy *et al.* (2004), fish consumed more feed at 29° C as opposed to 24° C (U.S. Virgin Islands summer and winter water temperatures). It was decided to use forced (pumped) water supply, regulating the flowrate to obtain the required constant 29° C output from the SWH.

Table 2.5: Flat plate solar collector specifications

Part number SBS1.5 V	
Appeture mrea	1.45 m ²
Dimensions (L x W x H) (mm)	1840 x 840 x 76
Absorber	Copper - ultrasonically welded
Header material	22 mm copper tube
Riser material	9.53 mm copper tube
Glass cover - low iron clear tempered glass	4 mm
Frame	0.65 mm aluminium grade 5052
Insulation	50 mm glass wool
Absorber coating	Selective black chrome coating

- SWH flat plate collector performance

The following section deals with the prediction of the performance of the chosen SWH. By making use of existing software such as PVSyst v6.5 and Kolektor v2.2, data was obtained for the ideal summer and winter day. A summer day is characterised with high irradiation and low-moderate wind speeds whereas a winter day has low irradiation and high wind speeds.

- Meteorological Data

Meteorological input data for summer and winter was obtained from the PVSyst (Tables 2.6 & 2.7). This software provides typical hourly ambient temperatures and wind speeds and is able to compute GHI on an inclined plane (40° to the horizontal) over a 12-hour period.

Table 2.6: Summer day with high irradiation and low-moderate wind

Time	Solar irradiation (W/m ²)	Ambient temperature (° C)	Wind speed (m/s)
6:00	66,7	15,3	1,6
7:00	201,2	16,8	1,2
8:00	444,1	18,5	2,2
9:00	668,1	20,2	2,9
10:00	848,8	21,7	4,2
11:00	962,7	23	4,5
12:00	999,1	24,1	4,2
13:00	967	24,9	3,4
14:00	866,5	25,3	3,4
15:00	700,5	25,5	3,6
16:00	482,1	25,2	3,8
17:00	241,9	24,6	4,8
18:00	74,7	23,6	4,3

Table 2.7: Winter day with low irradiation and high wind

Time	Solar irradiation (W/m ²)	Ambient temperature (° C)	Wind speed (m/s)
6:00	0	11,6	6,4
7:00	0,7	11,9	8,6
8:00	31,6	12,2	6
9:00	64,4	12,6	7,3
10:00	105,8	13,3	7,9
11:00	139,2	13,9	7,9
12:00	116,8	14,1	6,9
13:00	246,4	14,8	6,6
14:00	191,5	15,2	6,6
15:00	165,2	15,3	7,3
16:00	76	15,1	7,6
17:00	35,7	14,8	7,6
18:00	0,3	14,8	6,9

- Kolektor

The data from PVSyst, together with dimensions and characteristics of the SWH, were the input for the Kolektor software to compute the heat transfer loss coefficients for conduction, convection and radiation (Matuska & Zmrhal, 2009) (see Appendix F for Kolektor details). Also, the following conditions for the system and environment were included as input data:

A constant mass flow rate of 0.008 kg/s (Hamed *et al.*, 2014)

A constant inlet water temperature of 20° C for summer and 15° C for winter

A constant relative humidity of 66% for summer and 70% for winter

- SWH's performance prediction

From the results obtained through the use of the Kolektor and PVSyst, results could be predicted, firstly by making use of the steady-state energy balance Equation 2.8:

$$Q_u = GA_a(\tau\alpha) - U_t A_g(T_{abs} - T_a) - U_b A_b(T_{abs} - T_a) \quad (2.8)$$

Where:	Q_u	Useful energy gain of the SWH
	G	Solar radiation absorbed by the solar collector (W/m ²)
	A_a	Aperture area, A_b is the bottom area; A_g is the gross area of the collector (m ²)
	τ	Solar radiation transmittance of the collector's cover (glazing)
	α	Solar radiation absorptance of the collector's absorber
	U_t, U_b	Top and bottom collector's overall heat transfer loss coefficient due to conduction, convection and radiation (W/m ² K)
	T_{abs}	Mean absorber plate temperature (K)
	T_a	Ambient temperature (K)

The overall heat transfer loss coefficient for the top section (facing the sun) of the collector can be expressed in terms of its conduction, convection and radiation coefficients as follows:

$$U_t = \frac{1}{\frac{1}{(h_{pg}+h_{sg})} + \frac{1}{h_v} + \frac{1}{(h_{pa}+h_{sa})}} \quad (2.9)$$

Where:	h_{pg}	is the natural and forced convection at the exterior surface of glazing
	h_v	heat conduction through the glazing
	h_{sg}	radiation between the surface of glazing and sky
	h_{pa}	radiation between absorber and interior surface of the glazing
	h_{sa}	natural convection between absorber and interior surface of the glazing

Heat transfer coefficients for the bottom of the collector can be determined in a similar way.

The predicted results for the output water temperature from the SWH were determined as depicted on the graph for both summer and winter conditions (Figure 2.13 & Appendix G for input data analysis).

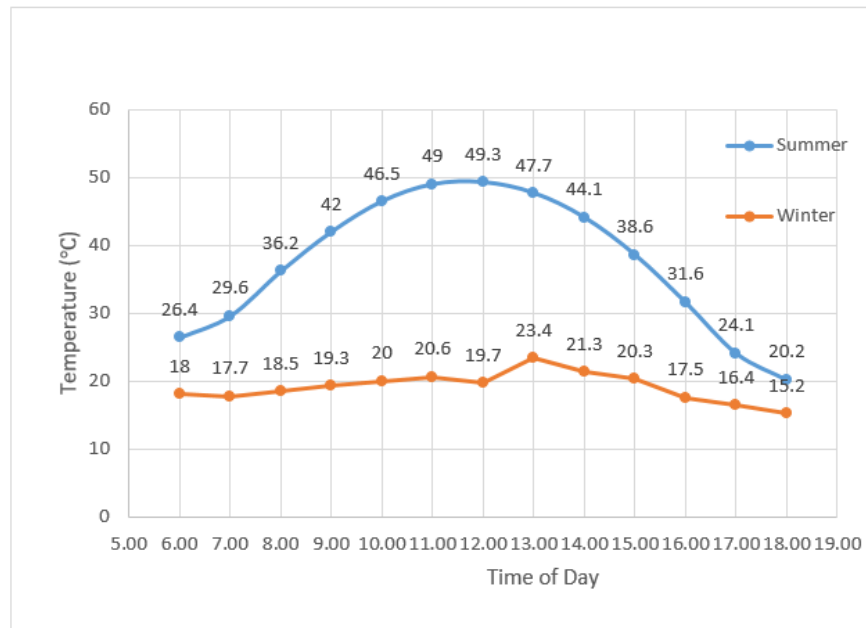


Figure 2.13: Predicted output temperature for summer and winter days

The predicted values in Figure 2.13 indicate that outlet temperatures of the water can reach up to 49° C which is greater than 29° C required for the tilapia. To circumvent this, the flow rate through the SWH can be adjusted according to the solar radiation, which fluctuates throughout the day. This can be achieved by using the hand control valve and pump to regulate the water flow through the SWH.

A slight increase in temperature was noticed during winter, where water temperature could be raised from 15° C to an average of 19.1° C, with a maximum of 23.4° C just after midday. Thus, an auxiliary water heater is recommended to supplement the shortcomings during winter months.

The following section will discuss the necessary adjustments required to maintain a constant 29° C for the outlet water temperature from the SWH.

- Controlling the water flow rate through the SWH

The following analytical modelling demonstrates how to determine the volumetric flow rate through the SWH to maintain a constant water temperature output of 29° C. The analytical model was used and compared to experimental data.

The following section is a snapshot of the modelling for a specific time (solar noon) in summer. Figure 2.14 shows the ambient conditions that could affect the performance of the SWH.

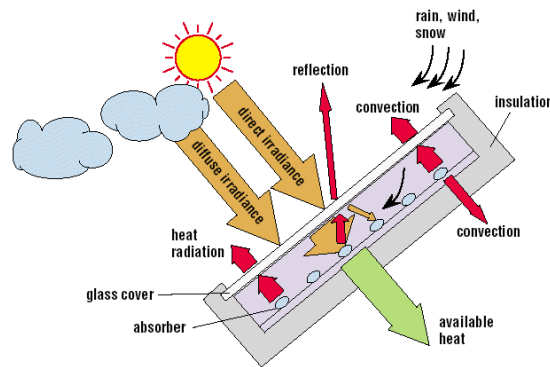


Figure 2.14: Effects of ambient conditions on the performance of the SWH (Wang et al., 2015)

The condition chosen for the sample calculation, as shown here, were those of solar noon on a summer day which provided the following data:

Incoming solar radiation	$G_s = 999.1 \text{ W/m}^2$
Collector area	$A = 1.45 \text{ m}^2$
Ambient temperature	$T_a = 24.1 \text{ }^\circ\text{C} = 297.25 \text{ K}$
Glass temperature	$T_g = 26 \text{ }^\circ\text{C} = 299.15 \text{ K}$
Inlet water temperature	$T_{inlet} = 20 \text{ }^\circ\text{C} = 293.15 \text{ K}$
Outlet water temperature	$T_{outlet} = 29 \text{ }^\circ\text{C} = 302 \text{ K}$
Wind Speed	$u_w = 4.2 \text{ m/s}$
Glass transmittance-absorptivity product	$\tau\alpha = 0.874$
Glass emissivity	$\varepsilon = 0.85$

An energy balance was used to determine the thermal energy gained by the water in the collector:

$$\dot{Q}_w = \dot{Q}_{col} - (\dot{Q}_{conv} + \dot{Q}_{rad}) \quad (2.10)$$

Where: \dot{Q}_w Heat gain in the water

\dot{Q}_{col} Heat gain in the collector

\dot{Q}_{conv} Heat loss by convection

\dot{Q}_{rad} Heat loss by radiation

The incoming solar radiation impinging on the collector plate considering optical and absorptive losses:

$$\dot{Q}_{collector} = G_s(\tau \alpha)A \quad (2.11)$$

$$\dot{Q}_{collector} = (0.874)(999.1)(1.45)$$

$$\dot{Q}_{collector} = 1257.53 \text{ W}$$

To determine the heat transfer loss by convection above the collector:

$$\dot{Q}_{conv} = h_c A (T_g - T_a) \quad (2.12)$$

The heat transfer coefficient is determined by using an empirical model (Watmuff & Proctor, 1977) developed by winds speeds less than 7 m/s:

$$h_c = 2.8 + 3.0 u_w \quad (2.13)$$

$$h_c = 14.6 \text{ W/m}^2 \text{ K}$$

The heat loss from convection Equation 2.12 was determined to be:

$$\dot{Q}_{conv} = 14.6(1.45)(299.15 - 297.25)$$

$$\dot{Q}_{conv} = 40.2 \text{ W}$$

To determine the heat transfer loss by radiation:

$$\dot{Q}_{rad} = \varepsilon \sigma A (T_g^4 - T_{sky}^4) \quad (2.14)$$

The sky temperature is determined by using model developed by Swinbank (1963):

$$T_{sky} = 0.0552 T_a^{1.5} \quad (2.15)$$

$$T_{sky} = 282.89 \text{ K}$$

The heat transfer loss from radiation Equation 2.14 was determined to be:

$$\dot{Q}_{rad} = (0.8)(5.670 \times 10^{-8})(1.45)[(299.15)^4 - (282.89)^4]$$

$$\dot{Q}_{rad} = 104.46 \text{ W}$$

The total heat transfer losses neglecting conduction loss through the glazing is determined by:

$$\dot{Q}_{loss} = \dot{Q}_{conv} + \dot{Q}_{rad} \quad (2.16)$$

$$\dot{Q}_{loss} = 144.66 \text{ W}$$

The heat gain to the water can be calculated as follows:

$$\dot{Q}_{water} = \dot{Q}_{collector} - \dot{Q}_{loss} \quad (2.17)$$

$$\dot{Q}_{water} = 1112.87 \text{ W}$$

The mass flow rate required to maintain the water at 29°C is

$$\dot{Q}_{water} = \dot{m}_{water} Cp (T_{out} - T_{in}) \quad (2.18)$$

The density of water is a function of the water temperature and can be expressed as:

$$\rho = 1.0005776 \times 10^3 - 7.0629371 \times 10^{-2} t_w - 3.5666433 \times 10^{-3} t_w^2 \quad (2.19)$$

The specific heat capacity of water is also a function of the water temperature and can be expressed as:

$$Cp = (4.2152727 - 1.6342424 \times 10^{-3} t_w + 1.651515 \times 10^{-5} t_w^2) \times 10^3 \quad (2.20)$$

$$\dot{m}_{water} = \frac{1112.87}{Cp (302 - 293)}$$

$$\dot{m}_{water} = 0.02958 \text{ kg/s}$$

To obtain the flow rate in litres per minute:

$$\dot{V} = \frac{\dot{m}_{water}}{\rho} \times 1000 \times 60 \quad (2.21)$$

$$\dot{V} = 1.79 \text{ l/min}$$

The predicted results for the volumetric flow rate to maintain the 29° C are presented in Table 2.8.

Table 2.8: Design flow rate for summer

Time	Solar irradiation (W/m²)	Ambient temperature (° C)	Wind speed (m/s)	Flow rate (l/min)
6,00	66,7	15,3	1,6	Na
7,00	201,2	16,8	1,2	0.1972
8,00	444,1	18,5	2,2	0.676
9,00	668,1	20,2	2,9	1.12
10,00	848,8	21,7	4,2	1.48
11,00	962,7	23	4,5	1.74
12,00	999,1	24,1	4,2	1.79
13,00	967	24,9	3,4	1.78
14,00	866,5	25,3	3,4	1.61
15,00	700,5	25,5	3,6	1.22
16,00	482,1	25,2	3,8	0.79
17,00	241,9	24,6	4,8	0.233
18,00	74,7	23,6	4,3	Na

It should be noted in Table 2.8 that at 6:00 and 18:00, the solar radiation would be too low to obtain the desired water outlet temperature.

CHAPTER THREE: THE MSPAS EXPERIMENTS

3.1 Aquaponics experimental set-up

This chapter covers the various experiments undertaken to validate the design parameters discussed in Chapter Two. These experiments included aquaponics experimental set-up, solar collector orientation, PV equipment performance and SWH capacity of the MSPAS.

3.1.1 Experimental set-up of the aquaponics section

The main components of the aquaponics section of the MSPAS comprised the hydroponics and aquaculture sections. The equipment, content and function are explained in the paragraphs that follow and Figure 3.1 shows the schematic layout of the aquaponics (combination of hydroponics and aquaculture) system.

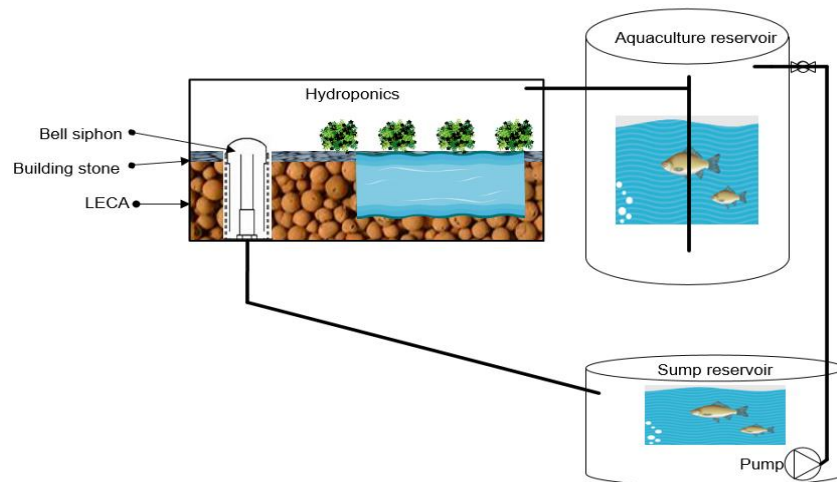


Figure 3.1: Aquaponics schematic

- Hydroponics grow-bed

The hydroponics grow-bed was filled with LECA to a depth 300 mm. The top layers of LECA were mixed with building stone (19 mm) to weigh it down (Figure 3.2). Water filled the crevices between the LECA and stone to just below the stand pipe opening of the bell siphon.

A constant flow rate (18 l/min) of water was allowed via the overflow from the aquaculture grow-out reservoir for the experiment.



Figure 3.2: Hydroponics grow-bed

- Siphon

The ebb tide was regulated by the siphon located in the grow-bed. The flow rate of the water entering the grow-bed triggered a siphon action at intervals of 11 minutes. The dimensions of the siphon are shown in the schematic diagram, Figure 3.3.

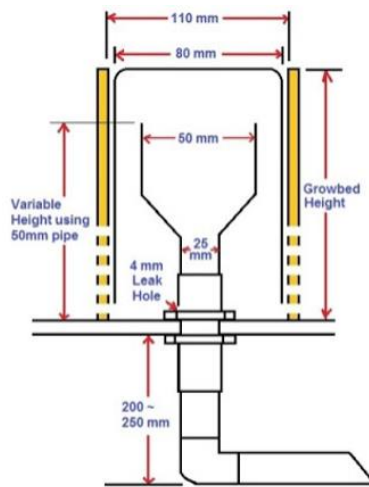


Figure 3.3: The siphon

- Vegetation growth

Seedlings were planted in the prototype MSPAS with growth rate monitored by weekly height measurements (Figure 3.4).

Tomato, spinach, lettuce and basil seedlings were planted in the grow-bed and their growth was measured once weekly with a steel ruler.



Figure 3.4: Method of measuring plant growth

- Fish growth

Prior to adding the fish, the system stood for two weeks to remove chemicals, such as chlorine, normally found in municipal water. This also allowed sufficient time for the bacteria to develop in the hydroponics porous LECA.

Monitoring the fish growth rate was carried out by attaching a control tank to the existing pilot system wherein the fish were added (Figure 3.5). A 20 x 20mm PVC grid was placed at the bottom of the tank. The procedure was to take photos on a regular basis to determine the growth (size of the fish). This procedure alleviated unnecessary stress on the fish if required to temporarily remove them from the tank to measure their length.

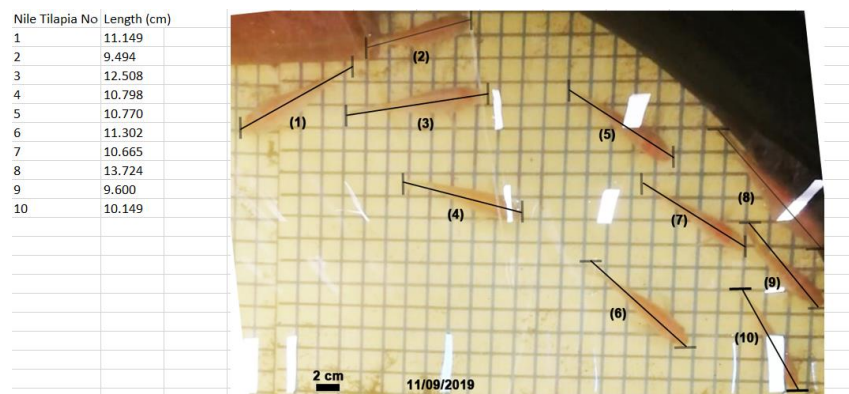


Figure 3.5: Fish photographed swimming over the 'background' grid in the control tank

Fish were carefully weighed prior to commencing the experiment. Ten fish with a total weight of 250 g were placed in the control tank. The fish feed was also weighed so that a feed-to-weight ratio was applied according to Table 3.1.



Figure 3.6: Fish and feed weight

Table 3.1: Tilapia growth and feeding rate

Month	Start weight (g)	End weight (g)	Growth rate (g/day)	Feeding weight (% weight)
1	1	5	0.2	15-10
2	5	20	0.5	10-7
3	20	50	1.0	7-4
4	50	100	1.5	4-3.5
5	100	165	2.0	3.5-2.5
6	165	250	2.5	2.5-1.5
7	250	350	3.0	1.5-1.25
8	350	475	4.0	1.25-1.0
9	475	625	5.0	1.0

After the anticipated completion of the growth period, the fish were carefully weighed and measured.

Prior research showed growth rates of tilapia fish in an aquaponics system (Rakocy *et al.*, 2012). Male mono-sex Nile tilapia were stocked at 77 fish/m³ and Red tilapia at 154 fish/m³ (Table 3.2).

Table 3.2: Fish growth rate (Rakocy *et al.*, 2012)

Tilapia	Harvest weight per tank (kg)	Harvest weight per unit volume (kg/m ³)	Initial weight (g/fish)	Final weight (g/fish)	Growth rate (g/day)	Survival (%)
Nile	480	61.5	79.2	813.8	4.4	98.3
Red	551	70.7	58.8	512.5	2.7	89.9

The plants and fish and the livestock were borrowed from the Pilot Project implemented at the community centre in Belhar (nearby the CPUT campus). Issues relating to fish welfare and transportation from the community centre to CPUT's Bellville campus are contained in a document in Appendix H.

3.2 Sun path orientation for experiments of solar collector alignment

The sun paths for winter and summer conditions were determined by online software, with Figures 3.7 and 3.8 illustrating the sun path for winter and summer, respectively (Sunearthtools, 2019). The yellow line indicates the sun track daylight hours specific to the area where the MSPAS was located.



Figure 3.7: Sun's path at CPUT's Bellville campus for winter (Sunearthtools, 2019)



Figure 3.8: Sun's path at CPUT's Bellville campus for summer (Sunearthtools, 2019)

3.1.1 The basic operation of the tracker

The tracker was designed to automatically align the photovoltaic panel with the sun. A cost-effective mechanism was developed to be deployed at low-income communities in the future. Standard off the shelf equipment was sourced and adapted to develop the tracking system that controls the PV panel to track the sun from sunrise till noon and thereafter remain stationary till sunset. At sunrise, the light sensor was triggered and elevated the panel to face the sun.

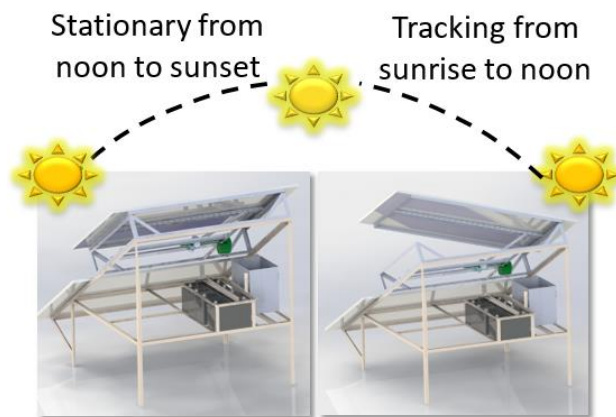


Figure 3.9: Operation of PV panel solar tracker

3.1.2 Experimental procedure for tracking vs stationary PV

The experiment was set up at CPUT to compare the performance of a stationary PV panel/solar collector to one that was tracking.

The data in Tables 3.3 and 3.4 were downloaded to assist in setting up the test and understanding the location of the sun relative to the position where the test was being conducted.

Table 3.3: Sun position (Sunearthtools, 2019)

Sun position	Elevation	Azimuth	Latitude	Longitude
20/05/2015 20:45 GMT1	-36.14°	271.14°	33.93242 05° S	18.640644 6° E
Twilight	Sunrise	Sunset	Azimuth Sunrise	Azimuth Sunset
twilight -0.833°	07:33:59	17:49:40	66.37°	293.74°
Civil twilight - 6°	07:07:07	18:16:29	70°	290.12°
Nautical twilight -12°	06:36:41	18:46:55	73.95°	286.19°
Astronomical twilight -18°	06:06:50	19:16:45	77.72°	282.43°
Daylight	hh:mm:ss	diff. dd+1	diff. dd-1	Noon
20/05/2015	10:15:41	-00:01:16	00:01:19	12:41:49

Table 3.4: Sun position day tracking (Sunearthtools, 2019)

Date	20/05/2015 GMT1	
Coordinates	-33.9324205, 18.6406446	
Location	Engineering Way, Bellville South Industrial, Cape Town, 7530, South Africa	
Hour	Elevation	Azimuth
7:33:59	-0.833°	66.37°
8:00:00	4.03°	62.67°
9:00:00	14.57°	53.17°
10:00:00	23.75°	41.83°
11:00:00	30.9°	28.13°
12:00:00	35.19°	12.09°
13:00:00	35.93°	354.77°
14:00:00	32.98°	338.03°
15:00:00	26.86°	323.36°
16:00:00	18.39°	311.14°
17:00:00	8.32°	300.99°
17:49:40	-0.833°	293.74°

One of the two identical PV panels was mounted onto the single axis solar tracker. The solar tracker was aligned with the sun throughout the testing procedure. According to the literature, a fixed solar collector in South Africa facing north, with a tilt angle of 30° to the horizontal, should be able to capture 98% of the maximum annual solar insolation (Le Roux, 2016). The highest yearly energy (HYE) can be obtained for this tilt angle in the Cape Town area (Bekker, 2007). During winter months, as this angle would represent the worst-case scenario, it was decided to set up the tracking experiment at this angle. The entire mechanism was set up north facing tilted 30° (with reference to the horizontal) to align with the zenith angle (Figure 3.10). The fixed collector was also set up north facing and tilted at 30° to the horizontal throughout the test.



Figure 3.10: Solar tracking set-up at CPUT Bellville campus

At sunrise, the tracking mechanism was opened to its maximum position and then slowly closed as it tracked the sun moving across the sky until approximately solar noon. At this point the tracking mechanism was at its maximum closed position.

3.2 Solar photovoltaic electricity supply experiment: introduction

This section describes the design and assembly of the equipment with relevant instrumentation and the experimental protocol used for the PV experiment. The aim of the experiment was to validate that the PV system would provide electricity for the pump and lights needed in the MSPAS. The pump had to run continuously (24 hrs) while the lights had to be on for a duration of four hours at night.

3.2.1 Experimental set-up and equipment used

The PV system's main components included PV panels, a charge controller, four deep cycle lead acid batteries, an inverter, submersible pump and two light emitting diode (LED) lights. The components and their function are explained in the paragraphs that follow; Figure 3.11 shows the schematic layout of the system.

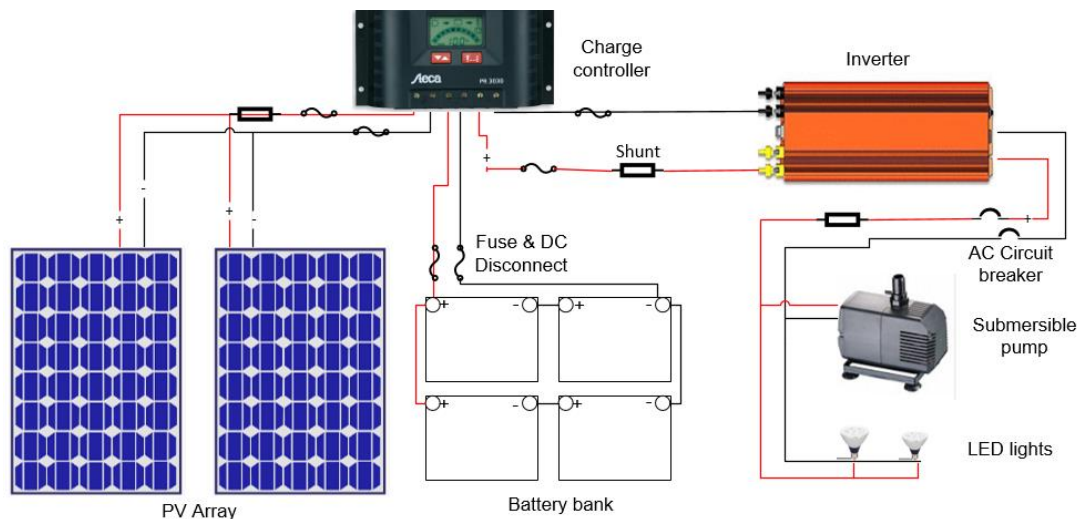


Figure 3.11: Schematic illustration of the PV system

- The PV array

In the prototype PV system, there are two polycrystalline PV panels connected in parallel (SETSOLAR M2200P, Appendix I). The dimensions of each panel are 1480 x 991 mm, with a panel area of 1.47 m². The maximum peak power per panel chosen was 235 W_p. The combination of the two panels can produce up to 470 W_p.

- Battery storage and use

The 24 V battery bank installed in the PV system consisted of four deep cycle 12 V, 100 Ah lead acid batteries, made by Ceil Power Safe ATX (Figure 3.12 & Appendix E for specification). Two batteries connected in series constitute a 24 V string whereby the two strings were connected in parallel to the charge controller.



Figure 3.12: Prototype battery bank

These batteries have a standard rating of 100 Ah @ 20 hr rate, meaning that the battery will discharge after 20 hours if a 5 A load is applied continuously. Reserve capacity minutes (RCM) for these batteries, also referred to as reserve capacity (RC), has a minimum stated electrical load; it is defined as the time (in minutes) that a 12 V lead-acid battery at 27° C will continuously deliver 25 A before its voltage drops below 10.5 V. The recommended charging current is 10 A for this type of battery.

- Protecting the batteries

The PV array was connected to a charge controller to prevent damage to the batteries and prolong their life expectancy.

The Steca PR 3030 12/24 V PWM charge controller was employed to control the charging and discharging of the batteries (Figure 3.13 & Appendix J for specifications).



Figure 3.13: Steca PR 3030 12/24 V

As the charge controller has an automatic voltage detection feature, it was therefore important that the battery bank be connected prior to connecting the PV array. This was to ensure that the charge controller detects the correct system voltage (24V) and to set the operating parameters accordingly. This charge controller consumed a current less than four mA for its own operation and could manage a current of up to 30 A.

- DC to AC conversion

An inverter was connected to the battery bank to convert the DC to AC voltage supply as required to power the submersible pump and LED lights.

The most appropriate choice was a pure sine wave inverter which could run motors more efficiently. The pure sine-wave inverter KS-1500P (pictured in Figure 3.14 & Appendix K for specifications), 1500 W 24 V, was connected to the battery bank to convert the 24 V DC to 240 V AC.



Figure 3.14: KS-1500P 1500 W 24 V inverter

- AC submersible pump

The submersible pump model was a B.I.C.I.S.A 2500. It had a power rating of 55 W and could deliver water to a maximum head of 2.5 m and a flow rate of 2000 l/h.



Figure 3.15: Submersible pump

- AC LED lights

The 2 x LED lights each had a power rating of four (4) W, input voltage 230 V/240 V, input current 65 mA, luminous flux of 320 in the warm white light spectrum.



Figure 3.16: 4 W LED light bulb

- Lights' timer switch

The 'Major Tech' 24-hour programmable timer acquired could handle loads up to 3500 W, 16 A, operating temperature -10 to +40° C with an accuracy of ±1 minute per month. The timer was set to switch on the lights at 8:00 pm and off at 12:00 pm daily.



Figure 3. 17: Programmable timer

3.2.2 Instrumentation for the PV experiment

In this section, a brief description of the instrumentation used to measure the PV system's performance is provided.

- Data Logger

Voltage drop readings across the shunts were recorded using a data logger (Agilent 34972A, Figure 3.18). The 34972A features 6.5 digits (22 bits) of resolution, 0.004% basic DC V accuracy, and ultra-low reading noise with scan rates of up to 250 channels/sec.



Figure 3.18: Agilent data logger model 34972A

- Shunt

Two shunts were connected to the PV system to measure the incoming power from the PV array and power consumed by the load. The type of shunt supplied was from Murata Power Solutions 50 A 50 mV. The 50 mV output was connected to the Agilent data logger to compute the power supplied and consumed.

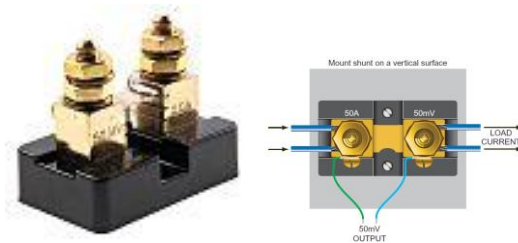


Figure 3.19: 50 A 50 mV shunt

- Battery tester

The TestMate battery tester assessed the state of health, state of charge and CCA capability of the 12 V batteries used.



Figure 3.20: Battery analyser

- Clamp meter

The amperage drawn from the various components was measured with the Iso-Tech (ICM 136R) clamp meter. The accuracy typically for DC is between 0A~60A is $\pm 1.5\%$ and for AC $\pm 1.9\%$ as specified at $23^{\circ}\text{C} \pm 5^{\circ}\text{C}$ and $\leq 80\%$ R.H.



Figure 3.21: Clamp meter

3.2.3 Battery bank autonomy experiment

An experiment to ascertain how long the batteries could last without any charge was performed in the laboratory (Figure 3.22).

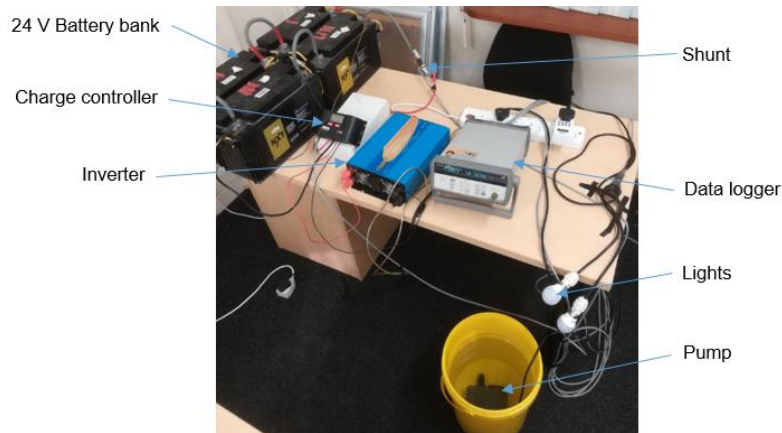


Figure 3.22: Battery autonomy set-up

The following measurements were recorded:

- Battery's charge state at the start and end of the experiment.
- Voltage drop across the shunt.
- Power consumed by the inverter in a stand-alone state.
- Pump's voltage requirement (the pump ran continuously).
- Voltage supplied to the lights (the light switch timer was set to activate at 20:00 and switch off at 24:00).

3.2.4 PV system experimental procedure

All the equipment and instrumentation described in sections 3.2.1 and 3.2.2, respectively, were connected to the MSPAS prototype and the experiment started.

- The light switch timer was set to activate at 20:00 and switch off at 24:00.
- The submersible pump was switched on and ran continuously. The submersible pump feeds water from the sump reservoir to the upper reservoir as explained in the aquaculture section of Chapter Two.
- The data logger was set to record readings of incoming solar power at the PV array and power consumed, or drawn, from the battery bank via the shunts.
- Pump operation and water levels were monitored regularly.

3.3 Solar water heating experiment: introduction

This section describes the procedure, components, equipment and instrumentation that were used for the solar water heating experiment. This experiment was to validate the predictions from the analytical model.

The aim of the experiment was to investigate the capability of the SWH panel to heat the water to a temperature of 29° C (daily) as required for the fish. The SWH experiment, forming part of the aquaculture section, was isolated from the hydroponics section. The focus was on the performance of the SWH during sunny, partly cloudy and cloudy conditions. The tests were conducted between December 2018 and March 2019.

3.3.1 Experimental set-up

The MSPAS equipment used for the experiment comprised the flat SWH panel, feed water tanks/reservoirs, a top tank, submersible pump and throttle valve. Figure 3.23 shows the test rig schematic and Figure 3.24 a photograph of the actual set-up. The components and their function are explained in the paragraphs that follow.

The water flow rate through the SWH panel had to be controlled to obtain the desired temperatures at the outlet. Two feed water tanks (reservoirs 1 and 2) were filled with municipal water (together contained 800 litres). It was required that this amount of water circulated at least once per day through the SWH panel.

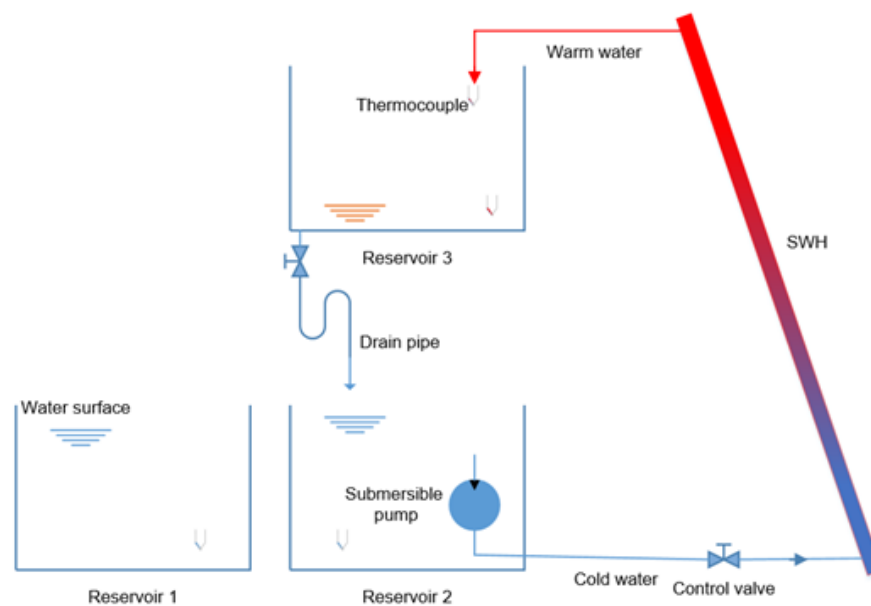


Figure 3.23: Schematic illustration of the SWH set-up

The warm water exiting the SWH panel was collected in the top tank (reservoir 3). Upon reaching its capacity (usually just after midday) the water was drained back to the feed water tank (reservoir 2) where it originated from, and remained there until the following day. The submersible pump was then manually relocated from reservoir 2 to the feed water reservoir 1 and together with the throttling valve ensured that water was fed at the required flow rate through the SWH panel to reach the desired temperature. The process continued until the tank ran empty or there was insufficient solar radiation to heat the water to the required temperature.

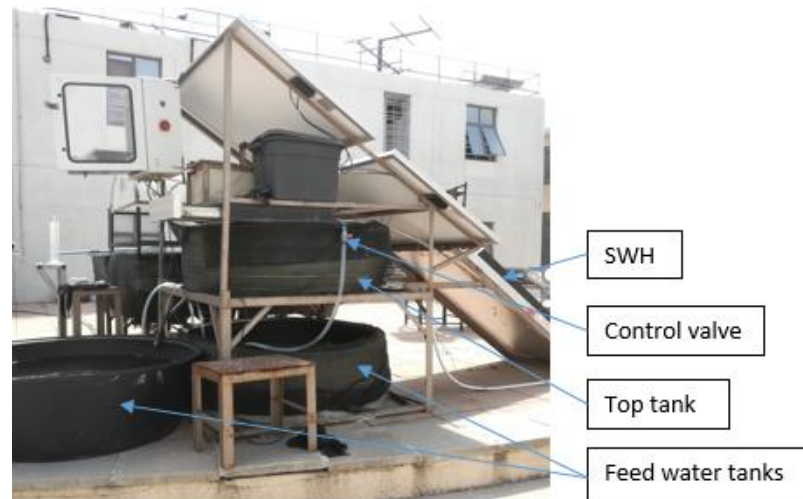


Figure 3.24: SWH experimental set-up

Type T thermocouples were attached at various locations on the SWH panel, such as on the absorber fins, absorber riser tubes, glazing, bottom of the panel and suspended between the glazing and absorber. Thermocouples were also placed at the inlet and outlet of the footer and header tubes of the absorber, all reservoirs and suspended in the air to measure ambient conditions. Figure 3.25 shows the attachment of the thermocouples to the absorber riser tube and glazing. The thermocouple's end was immersed in a blob of heat transfer paste which was covered with a piece of masking tape and then sealed off by epoxy resin.



Figure 3.25: Thermocouple set-up

3.3.2 Instrumentation for the SWH experiment

In this section, a brief description of the equipment used to measure the system's performance is provided. The temperatures of the ambient, the inlet and outlet of the water at the SWH panel, and plate were measured. Also, measurements of the solar incident radiation, wind speeds and the flow rate of water through the system were obtained.

- Temperature measurements

The various temperatures (mentioned above) were measured using type T thermocouples. The type T thermocouple, illustrated in Figure 3.26, known as copper constantan (55% copper & 45% nickel), produces a relatively high sensitivity of about $43 \mu\text{V}/^\circ\text{C}$.

These thermocouples have a good resistance to corrosion and moisture. Its tolerance class is superior to other thermocouples where type T thermocouple accuracy is standard $\pm 1.0^\circ\text{C}$. This accuracy can be improved by re-calibration by using the two-point calibration method.

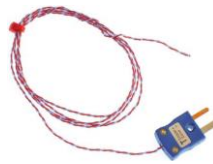


Figure 3.26: T Type thermocouple

- Thermocouple calibration

As a standard procedure in the laboratory, all the thermocouples were individually tested using the data logger, prior to connecting them in their positions. The data logger was configured to read T-Type thermocouples that automatically convert the millivolt potential difference to temperature. The thermocouples were connected to the data logger circuit board as shown in Figure 3.27.



Figure 3.27: Agilent data logger circuit board (24 channel multiplexer)

The thermocouples were checked at the boiling point of water, and at close to 0° C. The high temperature was measured using a kettle filled with water which was allowed to boil with its lid open. The thermocouple was immersed into the boiling water and the temperature read off the data logger. All the thermocouples were within the expected range of 100° C at sea level (Figure 3.28). The low temperature was measured by filling a bucket with water and ice, and the results recorded were within the expected range of 0° C.



Figure 3.28: Thermocouples Inserted in boiling water in the kettle



Figure 3.29: Thermocouple's calibration in water and ice mixture in a bucket

The thermocouples were found to be within a maximum error of 0.4° C or 0.4% within the working range of 0 to 100° C.

- Measurement of water flow rate through the SWH

A flow meter was installed at the outlet of the header tube of the SWH (Figure 3.30). The flow meter uses a pinwheel to measure liquid flow rate by generating a pulse every 2.25 ml flow rate.



Figure 3.30: Flow meter

Flow rates through the meter were verified with a beaker, collecting water and timed with a stop watch. The beaker, made by Searle to British Standard 604, has a maximum permitted error between 0.8% and 2%. Flow rates were recorded in litres/minute (l/min).



Figure 3.31: Beaker collecting water flowing through a device

- Flow rate calibration through the pump and siphon

To calibrate the flow rate of the pump and siphon, the two-bucket method was set up, whereby the submersible pump was employed to circulate water between the two buckets, and a valve was used to regulate the flow rate (Figure 3.32).

A variable area flow meter was installed and its output data was verified by the beaker and stop watch method prior to its use in the two-bucket method described above (Figure 3.33).



Figure 3.32: Flow rate test calibration set-up



Figure 3.33: Flow rate measurement using beaker, stop watch and variable area flow meter

Table 3.5: Typical results using beaker and stop watch and variable flow meter

Time taken to fill five litre beaker (seconds)	Calculated flow (l/h)	Flow meter reading (l/h)
59.88	300,6	300
35.66	504,8	500
17.78	1012,3	1000
11.84	1520,2	1500
8.95	2011,2	2000

- Wind speed measurement

Wind speed was measured by making use of the hand held Kestrel 2000 anemometer, having a range of 0.6 – 40 m/s with a 0.1 m/s resolution (see Appendix L for the certificate of conformance).



Figure 3.34: Anemometer

- Solar radiation measurement

Solar radiation was measured using a solar power meter (TES-1333). This meter is commonly used in meteorology, solar radiation measurement, solar power research, physics and optical laboratories and was determined as suitable for this study. The accuracy is typically within $\pm 10 \text{ W/m}^2$ [$\pm 3 \text{ Btu} / (\text{ft}^2 \times \text{h})$] or $\pm 5\%$, whichever is greater in sunlight; additional temperatures induced error $\pm 0.38 \text{ W/m}^2/\text{°C}$ [$\pm 0.12 \text{ Btu} / (\text{ft}^2 \times \text{h})/\text{°C}$] from 25°C.



Figure 3.35: Solar radiation meter

- Data logger

Temperatures and flow rate readings were recorded using a data logger (Agilent 34972A) also described in the SWH experiment (section 3.2.2).

3.3.3 Solar water heating experimental procedure

The tests began in the mornings and lasted until the late afternoons. The cold water was fed through the inlet of the SWH panel via a 55 W submersible centrifugal pump. The flow rate of the water through the solar panel was regulated by a throttling valve which was throttled to obtain the desired water temperature at the SWH panel's outlet (Figure 3.36).

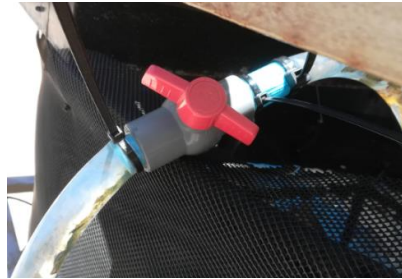


Figure 3.36: Throttling valve

Prior to commencing the experiment, the following was ensured:

The SWH panel's glass aperture was clean, free from dust, dirt or bird droppings and the feed water reservoirs 1 and 2 were filled to a total capacity of 800 litres of clean municipal water.

The following steps, as discussed in paragraph 3.3.1, describe the experimental procedure:

1. The submersible pump was positioned in reservoir 1 and switched on.
2. The flow rate of the water was regulated by adjusting the control valve. The desired temperature was reached at the outlet of the SWH panel. The water was collected in reservoir 3. Note: When reservoir 3 is filled reservoir 1 should be empty and water can then be siphoned from reservoir 3 back to reservoir 1.
3. When reservoir 1 became empty, the pump was placed in reservoir 2 and the water in reservoir 3 was siphoned in reservoir 1 where it remained until the following day.
4. The process continued with the pump in reservoir 2 pumping water through the SWH panel at the correct flow rate to yield the desired temperature. The test ended when reservoir 2 emptied, or if insufficient radiation could not heat the water to the required temperature.

5. At the end of the experiment the water from reservoir 3 was siphoned back to reservoir 2. Both reservoirs (1 & 2) were left full and ready for testing on a different occasion.

Note: Heating the water as it flows through the SWH panel is dependent on the incident solar radiation on the glass aperture of the SWH and can only be adjusted once sufficient radiation is received. Therefore, incident radiation readings should be taken at 30-minute intervals on the hour by placing the pyrometer perpendicular to the glass aperture of the SWH (Figure 3.37 shows the SWH mounted just below the PV panel in the same plane).



Figure 3.37: Pyrometer reading

Similarly, all relevant temperature, water flow rate and wind speed readings should be taken at 30-minute intervals on the hour. Place the anemometer perpendicular to the glass aperture to measure the updraft (Figure 3.38). The updraft is caused by natural wind and/or convection from heat dissipated by the panel.



Figure 3.38: Anemometer reading

CHAPTER FOUR: DISCUSSION OF RESULTS

4.1 Overview

The project culminated in the experimental study described in Chapter Three which attempted to assess the functionality and performance of the MSPAS. The experiments were conducted in the courtyard at CPUT's Mechanical Engineering department. The 1st experiments determined the growth rate of leafy greens. The 2nd determined the optimum solar collector orientation towards the sun, and included some basic tracking in the morning hours. The 3rd experiment determined the autonomy of the batteries or the expected time these batteries could operate without receiving any charge. The 4th experiment determined that the PV system could power the MSPAS continuously. The 5th experiment determined whether the SWH system could provide the necessary heating capacity to the aqueous medium.

4.2 Growth rate of leafy greens

In four weeks, the lettuce grew 130 mm, the ruby chard grew 170 mm, the spinach grew 180 mm, the rocket grew 300 mm and the cherry tomatoes grew 515 mm. The lettuce was harvestable just after 35 days compared to 50 to 60 days when planted in soil (Organised seeds, 2013). The chard, rocket and tomatoes grew notably quicker than the specified harvest time when planted in soil (Figure 4.1).

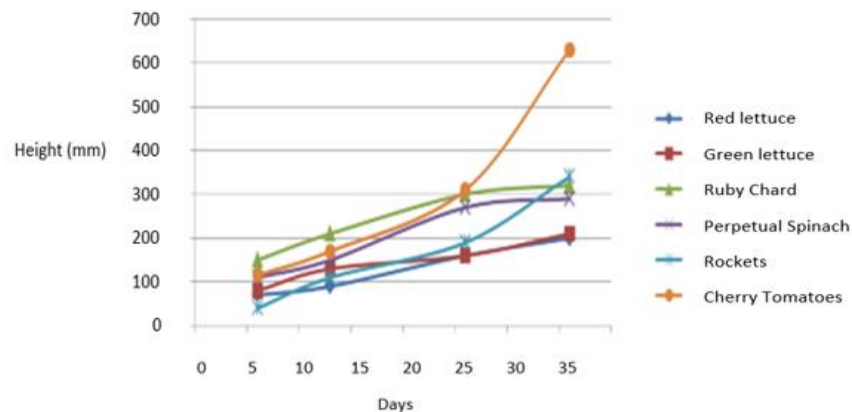


Figure 4.1: Plant growth rates

4.3 Growth rate of fish

Growth rate of fish, model explanation: Recently, a range of growth models to describe the size and the mass of fish as a function of time have been developed (MacNeil *et al.*, 2017). In this work, the model that uses equations to display the size and mass during the lifespan of an organism, developed by Von Bertalanffy (1957), was adopted. The von Bertalanffy growth function (VBGF) is an expression of fish growth whereby the size-at-age data can theoretically be used to estimate fish growth rates (Renner-Martin *et al.*, 2018). Following on that, what is known of the generalised Von Bertalanffy growth model (GVBGM) for the mass of the fish (during their lifespan) was used (Essington *et al.*, 2001):

$$m(t) = m_{\infty} \left(1 - \exp \left(- \left(\frac{k}{3} \right) \cdot (t - t_0) \right) \right)^3 \quad (4.1)$$

Where m is the mass of the fish; t is the time in days; m_{∞} is the full-grown mass of the fish; k is the energy loss constant; and t_0 is the age at which $m = 0$.

The GVBGM can be expressed in terms of fish length through the length–mass relationship since empirical evidence for fish suggests that the mass may be related to length (da Costa *et al.*, 2018).

In this work the mass of the fish was approximated by the third power of their length similar to what was reported previously in the literature (Essington *et al.*, 2001). An expression for the length of the fish (during their lifespan) was obtained (Essington *et al.*, 2001):

$$L(t) = L_{\infty} \left(1 - \exp \left(- \left(\frac{k}{3} \right) \cdot (t - t_0) \right) \right) \quad (4.2)$$

Where L is the length of the fish; and L_{∞} is full grown length.

This form of the GVBGM is noteworthy in that it is equivalent to the empirically derived growth curve most commonly used in growth studies (Essington *et al.*, 2001).

Growth rate of fish, results and discussion: Equations 4.1 and 4.2 were used with data of the fish grown at the MSPAS (Figure 4.2a & b). From an aquaculture perspective, the maximum mass and length (i.e., m_{∞} and L_{∞}) of the fish species used should be known, especially as these values influence the variance (De Graaf & Prein, 2005). In the present study, a value for m_{∞} and L_{∞} of 426 g and 27 cm were used, respectively. The fish will reach a mass of about 400 g and a length of ~ 26 cm in about

nine (9) months, after which a slow growth was observed, both experimentally and theoretically (Figure 4.2a & b). The results indicated that the growth rate reduced to almost zero after about 400 days, with the fish reaching a mass and length of about 470 g and 27 cm respectively, which conforms to the model's value of $m_{\infty} = 426 \text{ g}$ and $L_{\infty} = 27 \text{ cm}$.

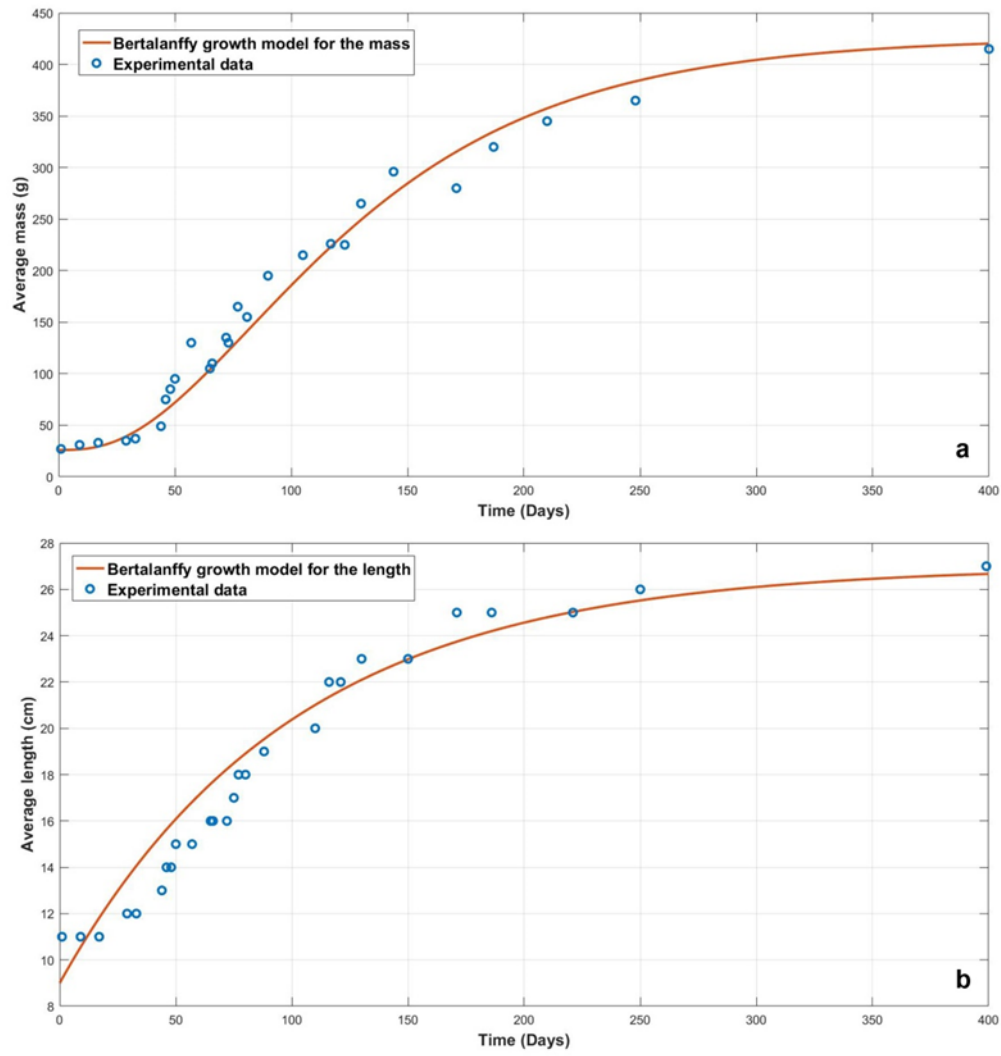


Figure 4.2: Mass- and length-at-age data of fish grown at the MSPAS (a) fish mass and (b) fish length. For both figures, the best fitting GVBGM is indicated by the solid lines

4.4 Orientation experiments of solar collector

Figure 4.3 presents the data (power produced at 15-minute intervals) by the tracking and fixed PV panels as described in Chapter Three section 3.1.2. The graphical format depicts the power produced by the panels, showing the advantage of tracking compared to that of the fixed PV collector.

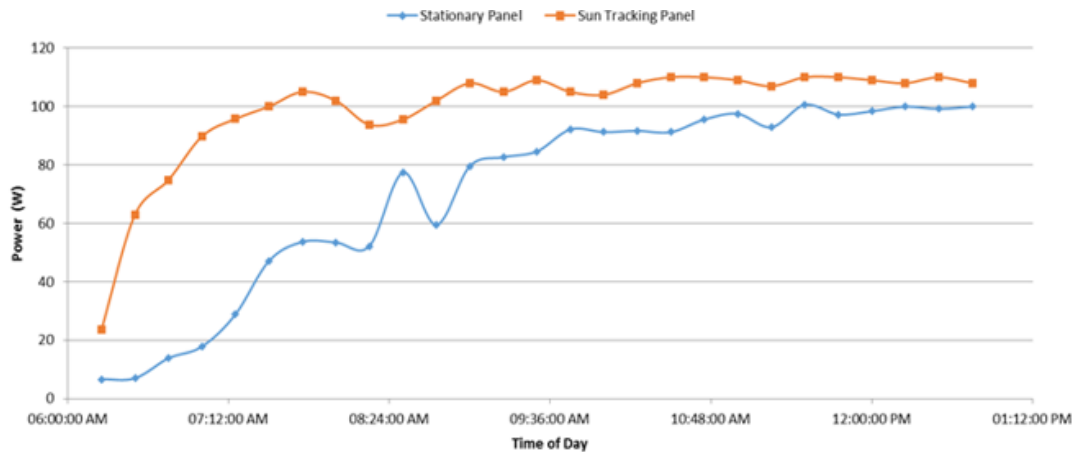


Figure 4.3: Comparative power output for stationary vs tracking collectors

The results are in line with prior solar tracking literature (Al-Mohamad, 2004). An overall of 40% increase for the tracking panel was noted when compared to the stationary collector. However, it must be noted that tracking the sun requires energy, and with moving parts, regular maintenance (a level of sophistication not suited for the chosen or intended operating environment of a low-income community). Optimum, fixed sun facing angles can be allocated for the solar collectors based in the Cape Town area and their elevation could be adjusted manually to accommodate seasonal conditions.

4.5 PV experimental results

This section covers the battery autonomous test and PV system design.

4.5.1 Battery autonomy experiment

The battery autonomy experiment was conducted to establish how long the system could run on battery power only. This will be useful to know in times when cloudy and sparse sun reaches the PV panels. It is important that the pump runs continuously so that the cycle balance remains constant and does not harm the fish (most vulnerable) in the system. The graph in Figure 4.4 depicts the overall voltage drop and current consumed during the experiment. The pump ran continuously and the lights were switched on for four hours nightly.

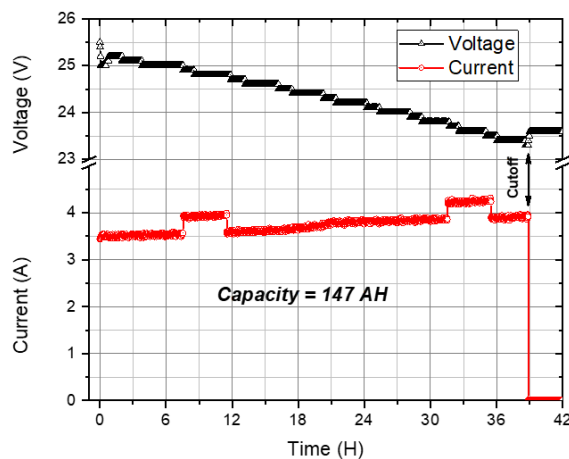


Figure 4.4: Battery capacity

The following results were noted:

- At the start of the experiment, the solar charge controller indicated the state of charge (SOC) of the battery bank to be 97%.
- The battery supplied power to the load for a total of 38 hrs.
- The battery bank capacity used was determined to be 147 Ah just before the load disconnected.
- At the end of the experiment, the charge controller switched off the load at 18% SOD.

The design capacity for the battery bank was 200 Ah for a 24 V connection (Chapter Two Figure 2.12). A shortfall of ten hours was noted which could be attributed to losses such as ageing of the batteries (four years old) and the inverter being over specified and not operating at its efficient capacity range. Overall, these results were not too alarming as it was able to power the load for the duration of the experiments.

4.5.2 MSPAS PV system experiment

The PV system's experiment proved the functionality of the electricity supply to the load. According to Bekker (2007), when charging batteries for a stand-alone PV system, the highest minimum daily energy (HMDE) calculation for a five-day period is required. This is enough time to simulate a system where batteries would be able to supply the load for five days with minimum recharging. It was decided to carry out the experiment over an eight-day period, during winter, to determine the worst-case scenario.

Figure 4.5 depicts the PV array power generated over the eight-day period whereby clear, cloudy and worst-case stormy weather was experienced. An average energy input of 1167 Wh/day was recorded, for this is strongly dependent on the length of the period and the weather. This is a slight under performance compared to the design criteria of 1352 Wh/day. The stored energy capacity of the batteries was sufficient to supplement the shortcoming as demanded from the load. The load operated continuously. The PV panels collected adequate energy from the sun during the day to keep the batteries charged maintaining the load during the day, night and moderate to low solar radiance conditions. It was anticipated that in summer conditions the amount of energy produced by the PV array will supply the required load.

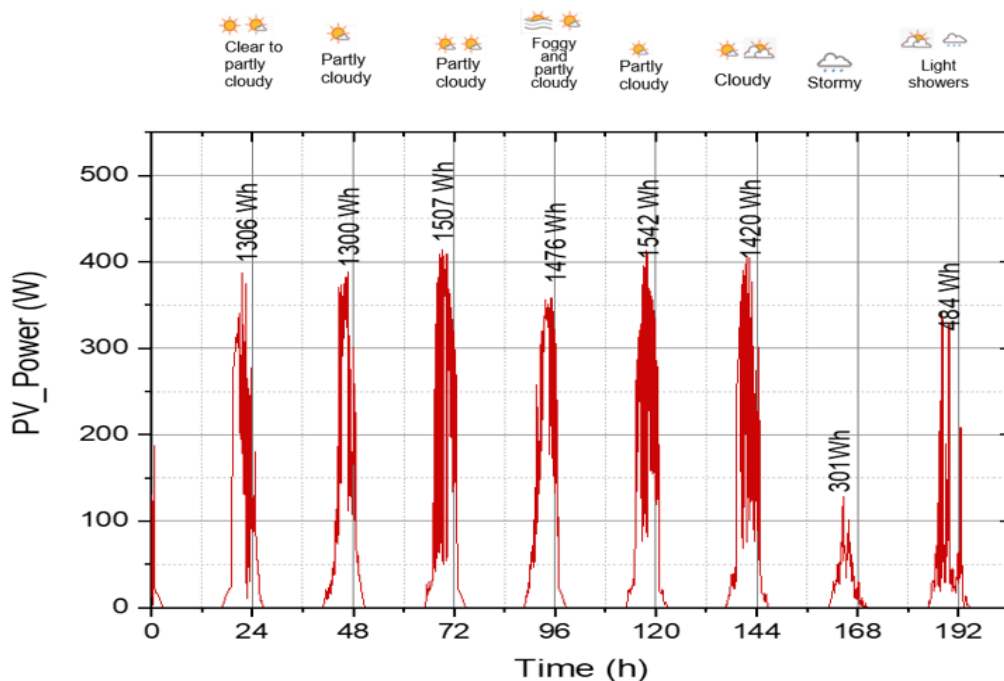


Figure 4.5: PV system power performance

Figure 4.6 shows the energy distribution a typical test period. The energy generated by the PV array was stored in the batteries and released on demand to the inverter. The

graph shows losses between the output energy from the inverter to that of the load. These losses could be attributed to the load operating at the lower efficiency band of the oversized inverter. The pump's power factor was determined to be 55% (using the three voltmeters method) (Hambley, 2014).

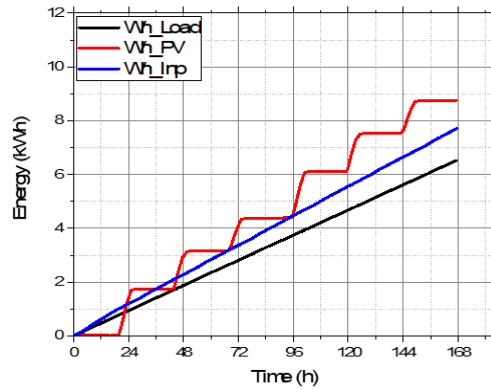


Figure 4.6: Energy system power performance

Figure 4.7 shows a typical snapshot of the system's power performance. The continuous running of the pump and periodic switching on and off of the lights were evident. The average load noted for the pump was approximately 38 W which was mainly due to its low power factor.

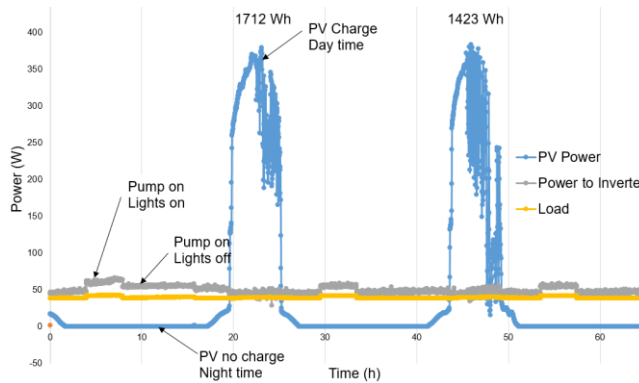


Figure 4.7: Typical system power performance

Meteorological data obtained from Meteo Cape Town (2018) yielded an average solar radiation value of 586 W/m^2 . The average daylight hours amounted to 7.24 hrs and the aperture total area of the array was 3.25 m^2 . The array produced 1.167 kWh as stated before. The total energy produced by the sun that was transferred to the array amounted to 13.8 kWh for this period. The efficiency for the PV array was determined to be 8.5%.

4.6 SWH experimental results

The SWH experiments determined volumetric flow rates required to maintain the 29° C in the fish reservoirs and to see if the experimental results could validate the analytical predictions. Figure 4.8 depicts the conditions achieved where the experimental results are compared to the analytical data and the actual radiation values taken on the day. The experiment for the clear day showed a consistent radiation curve. This was expected as no clouds meant no shadows cast over the solar collectors. The highest radiation recorded for the day was 1070 W/m² with an average radiation of 979 W/m² between 12:00 and 16:00. The average flow rate for this period was 1.78 l/min.

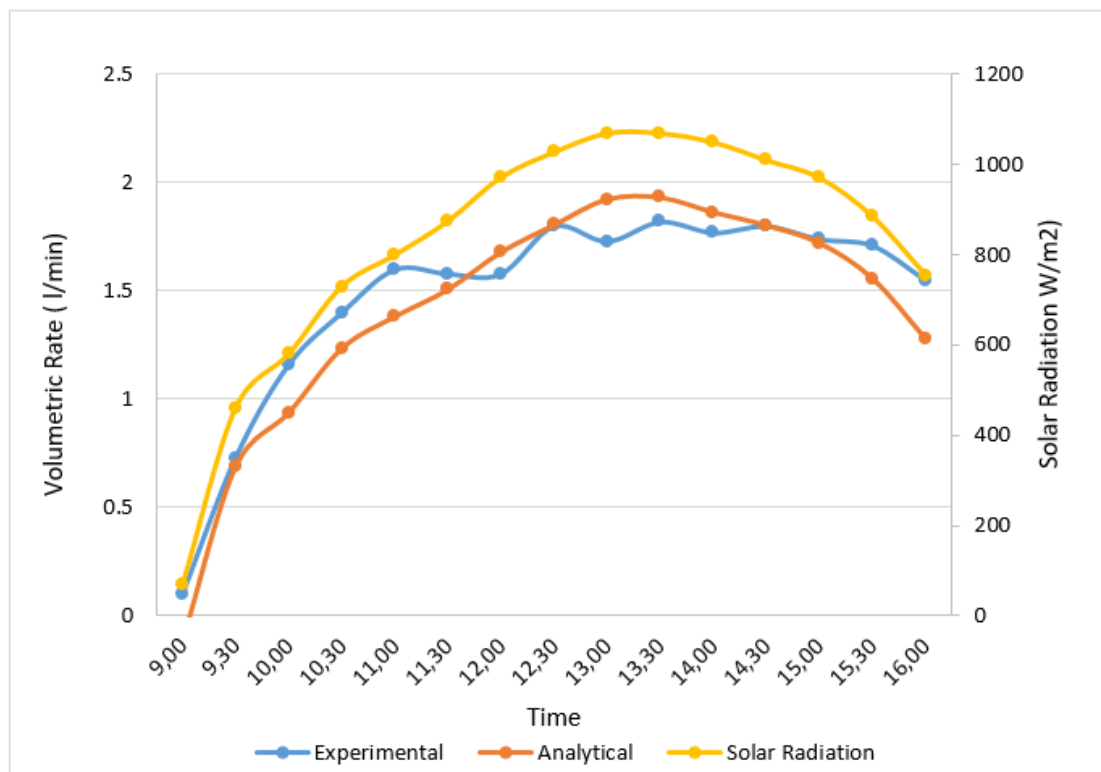


Figure 4.8: Comparison of experimental and analytical results (clear day)

The experimental and analytical data for the clear day showed a close correlation to one another making the analytical method fairly reliable for future predictions. It was possible to maintain a temperature close to the required 29° C at the outlet of the collector (Table 4.1). Due to temperature losses to the atmosphere and surrounding environment, a slight deviation of approximately 2° C can be noted in the temperature of the top reservoir to what is exiting the collector. The average temperature from 12:00 to 16:00 was found to be 27.3° C in the top reservoir.

The flow rate of the water through the SWH could be adjusted accordingly (continuously or periodically) to harness the heat energy optimally throughout the day, for example via a control system (if developed in the future). Temperature losses in the top reservoir could be compensated for by adjusting the throttle valve accordingly.

Table 4.1: Data collected on a clear sunny day

Time	Ambient Temp °C	Solar Radiation (W/m ²)	Temp Collector Outlet °C	Temp Inlet (BotReservoir) °C	Top Reservoir temp °C	Flow Rate (L/min)
09:00	20.4	68	23.4	19.4	17.6	0.1
09:30	23.8	460	28.1	20.5	19.1	0.73
10:00	27.2	580	29	20.6	22.3	1.16
10:30	28.5	730	28.4	20.5	24.8	1.6
11:00	28.4	800	29.3	20.5	25.8	1.58
11:30	27	875	29.4	20.6	26.1	1.58
12:00	28.7	972	29.2	20.8	26.4	1.93
12:30	27.5	1028	29.6	20.6	26.8	1.88
13:00	26.9	1070	29.8	20.3	26.5	1.73
13:30	26.4	1070	29.8	20.5	26.6	1.82
14:00	27	1050	29.9	20.7	27.3	1.77
14:30	27.8	1010	29.9	21	27.9	1.8
15:00	26.8	971	29.6	21.6	27.9	1.74
15:30	27.3	885	29.8	22.1	28	1.71
16:00	27.7	755	29.2	22.8	27.9	1.76

The data collected for Figure 4.8 and Table 4.1 were for a clear sunny day, 06 March 2019.

CHAPTER FIVE: COMMUNITY ENGAGEMENTS

5.1 The low-income community Pilot Project

The author assisted with the construction and development of the MSPAS Pilot Project at the Belhar Early Childhood Development Community Centre located in the Western Cape in SA, near CPUT. Equipment and processes proven successful on the prototype were implemented in the Pilot Project at the Belhar Community. Four fish tanks (total 4000 l) and ten grow-beds (total area 18 m²) were erected (Figure 5.1).

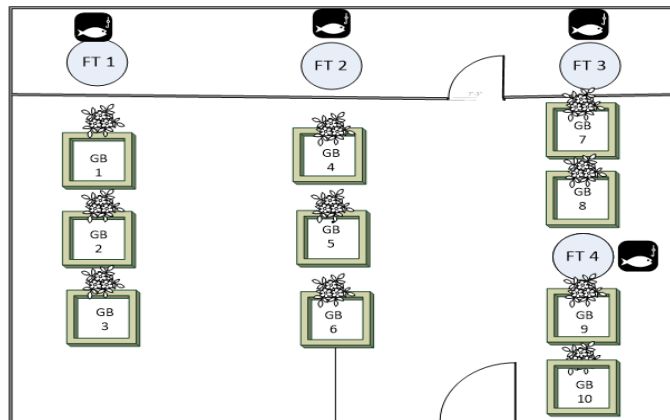


Figure 5.1: Pilot Project schematic lay-out

Plants such as basil, cherry tomatoes, Italian parsley, mint, lettuce and spinach were planted and harvested on a regular basis (Figure 5.2).



Figure 5.2: Grow-beds

The four fish tanks at the community centre accommodate the tilapia fish. Harvests have not yet taken place, as fish are still in the growing stage (Figure 5.3).



Figure 5.3: Fish tanks

The aquaponics pilot system was also used for educational purposes for the community centre’s children (Figure 5.4).

The Belhar Community Centre sponsors an early childhood development programme for approximately 125 toddlers, aftercare for 25 scholars, and a small Internet access hub for community members. Toddlers are taught how to take care of the environment through the MSPAS pilot. The idea is to develop these toddlers into future environmentally friendly and self-sustainable individuals. Currently in this environment most children are facing a community riddled with drug abuse, poverty and unemployment. With the assistance of teachers, these children are taught how to germinate seeds, grow seedlings and later replant these seedlings into the MSPAS grow-out beds. They also assist with feeding the fish located in the MSPAS pilot which has a calming and caring effect on them (see Appendix K for progress report).



Figure 5.4: Teaching activities at the community centre

The acceptance of the technology of the Pilot Project, while remarkable within the community, has not been without challenges. For example, training on the RE system and failsafe devices had to be established after one of the inverters was blown when the community members accidentally overloaded the system with power tools.

5.2 Scholarly and general community outputs

The research work on the prototype at CPUT in conjunction with the outcomes from the Pilot Project operating in the Belhar Community, yielded material that was publicized as cited below:

1. F. Ismail, J. Gryzagoridis, O. Nemraoui and M.W. Schouw, *Experimental Analysis of an integrated aquaponics and stand-alone solar photovoltaic system*, International Conference on the Industrial Use of Energy (ICUE), Cape Town, RSA, 2019, DOI 10.2139/ssrn.3638163
2. Presentation: F. Ismail, *Use of solar energy to enhance an aquaponics project at a low-income community*, U6 international conference, Cape Town, South Africa, September 2018
3. F. Ismail and J. Gryzagoridis, *Optimising photovoltaic system by direct cooling and transferring heat to aquaculture medium to boost aquaponics food production in low income communities*, International Conference on the Domestic Use of Energy (DUE), Cape Town, RSA, 2017, pp. 187-192, ISBN 978-0-9946759-2-7
4. F. Ismail and J. Gryzagoridis, *Sustainable development using renewable energy to boost aquaponics food production in low income communities*, International Conference on the Industrial Use of Energy (ICUE), Cape Town, RSA, 2016, pp. 185-190, ISBN 978-0-9946759-1-0
5. F. Ismail and J. Gryzagoridis, *Sustainable design; an example of Modular Solar Powered Aquaponics System*, International Conference on Sustainable Energy for All by Design, Proceedings of the Lenses Conference, Cape Town, RSA, 2016, pp. 15-22, ISBN 978-88-95651-24-8
6. Key note address at the Lenses international conference by F. Ismail (September 2016)
<http://www.lensesconference.polimi.it/keynote-and-invited-speakers/fareed-ismail-south-africa/> <https://www.youtube.com/watch?v=hqNXEP5rKQY>
7. Presentation: F. Ismail, *Sustainable development through engineering solutions: An example of Modular Solar Powered Aquaponics*, Future Force Conference, hosted by The Dutch Minister of Defence and the Dutch Chief of Defence, World Forum, The Hague, Netherlands, 2017

8. Presentation and discussions: F. Ismail, *Sustainable development through engineering solutions: An example of Modular Solar Powered Aquaponics (A Project Overview)*, Regional Sharefair on Gender and Resilience (Women Resilience in Agriculture), hosted by UN Women, Nairobi, Kenya, November 2016
9. Presentation: F. Ismail, *Modular solar powered aquaponics*, SATN 9th Annual international conference, Cape Town, South Africa, October 2016
10. Presentation and lecture session on RE. F. Ismail, *Modular solar powered aquaponics*, 20th Habitable Planet Workshop, CPUT, Cape Town, South Africa, 2016
11. Presentation and mini paper: F. Ismail, *Modular solar powered aquaponics*, SAIMECHE, Bellville, South Africa, 2015
12. Exhibit model and presentation at side event: F. Ismail, *Modular solar powered aquaponics*, SAIREC, CTICC, Cape Town, South Africa, 2015
13. Exhibited model at the Spice Mecca Radio 786 Ramadan Expo (5th-7th June 2015). This led to a follow-up 30-minute Radio 786 broadcast.
14. Newspaper publication: TANYA FARBER | 01 July, 2015. *The Times* visited the author at CPUT and the low-income community and published an article in print and on their website about this project.
<http://www.timeslive.co.za/thetimes/2015/07/01/Cape-scientist-creates-perfect-miniature-world>
15. Presented (18 August 2015) the renewable energy powered aquaponics system to the CPUT Directors and visiting Professor Wilfried Zörner from Germany
16. Author received CPUT Outstanding Community Project/Community Outreach Award 2015
17. The acceptance of the technology and involvement by the community has been remarkable. They have been awarded South Africa's Social Developmental Department first prize for their Early Childhood Development programme in the Western Cape Province (17 February 2016) and later the National first prize competition (04 May 2016).

CHAPTER SIX: CONCLUSIONS AND RECOMMENDATIONS

6.1 Conclusions

The aquaponics unit has already provided a productive indication of vegetable yield where crops such as lettuce, ruby chard, rocket, spinach, tomatoes, cucumbers, cauliflower, cabbage and radish were successfully grown in the MSPAS. For example, in four weeks, the lettuce grew 130 mm, the ruby chard grew 170 mm, the spinach grew 180 mm, the rocket grew 300 mm and the cherry tomatoes grew 515 mm. Lettuce grew particularly quicker in this system where it took 35 days to grow to harvest compared to 50 days when grown by conventional farming methods. The pilot system located in the community centre is currently producing a successful vegetable harvest and the community has embarked on small-scale entrepreneurship. The centre has partnered with a company called Pure Good Food and are now providing rotational crop harvest for this company. Harvest not sold is processed and fed to the children in the ECD at the centre.

While fish harvest has not taken place yet, a good balance between the fish stock and vegetable growth is evident from the vegetable harvest produced thus far. The choice of farming with tilapia came to fruition after discussions with the community members. Tilapia look closest to fish found in the sea with which people in the Western Cape are familiar. The fish growth was carefully monitored and compared to the Von Bertalanffy growth model. The results indicated that the growth rate reduced to almost zero (0) after about 400 days, with the fish reaching a mass and a length of about 470 g and 27 cm respectively, which conforms to the model's value of mass = 426 g and length = 27 cm, respectively. It is safe to recommend fish harvest (for fully grown fish) after a nine-month growth period, where the mass of about 400 g and a length of ~ 26 cm can be expected. Popular retail outlets are currently selling tilapia, with the average fish weight about 300 g and priced at approximately ZAR 40/kg. This seem to be a popular plate size fish for a meal. According to the growth model, these fish took approximately six months to grow.

The PV system proved to be reliable and able to sustain the load of 1352 Wh/day for the operation of the aquaponics pump and the four hours of night lights required during moderate to adverse weather conditions. An experiment was conducted prior to installing the PV system, whereby a comparison between the power produced by a sun tracking to a stationary panel showed a 40% advantage. However, tracking the sun requires the initial cost of moving parts and maintenance and thus is not suitable for a low-income community. It was decided to fix the panels at sun facing angle of 50° (with respect vertical), as suggested by Bekker (2007). This angle is most suited for

achieving the highest minimum daily energy (HMDE), for stand-alone fixed panel systems, throughout the year for Cape Town. The energy output for the stand-alone PV system was monitored over an eight-day period during winter, whereby clear, cloudy and worst-case stormy weather was experienced. An average energy of 1167 Wh/day was recorded for this period. This average slightly underperformed the design criteria of 1352 Wh/day. The stored energy capacity of the batteries (designed for two days' autonomy, but with a shortfall of ten hours due to aged batteries) was sufficient to supplement the shortcoming as demanded from the load. The load operated continuously and uninterrupted. Such stand-alone PV systems would be viable when implemented in aquaponics farming methods but also could be rolled out (with necessary modifications for greater power requirements) to socio-economically deprived communities where grid power is lacking or unavailable.

The SWH system design proved to be adequate during clear sunny days but lacking in capacity during adverse weather conditions (prominent in winter months). The experimental and analytical data for the clear day showed a close correlation to one another, rendering the analytical method fairly reliable for future predictions. It was possible to maintain a temperature close to the required 29° C at the outlet of the collector during ideal weather conditions. Maintaining an average flow rate of 1.78 l/min proved adequate to allow most of the water (~750 l) to pass through the solar collector in one day (~7 hours of sunlight). During winter months, the model predicted a slight increase in temperature, where water temperature could be raised from 15° C to an average of 19.1° C, with a maximum of 23.4° C just after midday. Thus, an auxiliary water heater is recommended to supplement the shortcomings during winter months. The SWH system could be scaled up, but this would lead to a redundancy of power during the summer months; hence, the extra solar collectors would need to be isolated to prevent the water from overheating. Redundancies would also mean extra costs and will defeat the objective of keeping the system affordable. For now, the little improvement in heating the water during winter months will have to suffice until further developments can occur.

Numerous problems were experienced as community members fiddled with the valve settings which regulated the flow rates within the aqueous medium. Training the community members had to take place as this was imperative to avoid accidents and damage. Members of the community also became overexcited and attempted to show initiative and inventiveness. For example, they added extra fish tanks to the pilot unit during one of the university's holiday periods, while the author was away on holiday. This created an imbalance to the aquaponics system which resulted in too few plants available to filter the water. They also used underground water which had low levels of

oxygen (1.9 mg/l) compared to the required five (5) mg/l. This resulted in some fish fatalities. Thankfully, as a result of additional training offered to community members, the system is currently performing well.

The economics of aquaponics systems hinge on specific site conditions and markets. It would be inaccurate to make far-reaching generalisations since material costs, construction costs, operating costs and market prices vary by location. For example, an outdoor tropical system would be less expensive to build and operate than a controlled-environment greenhouse system in a temperate climate. Nevertheless, the economic potential of aquaponics systems looks promising based on studies as reported by Rakocy *et al.* (2012). The addition of the solar system will further enlarge the initial capital expenditure of the overall cost, but could be offset against the free energy to run the system over a period of time and could prove viable. This would make an interesting topic for future research.

6.2 Recommendations

One of the shortcomings of the system is to supply the required heat to the aqueous medium throughout the entire year in a cost-effective manner. Work has started on modifying existing PV panels to PV/T by direct cooling methods making use of the aqueous medium. In so doing, heat generated by the PV panel is absorbed into the aqueous medium and carried to the fish tanks, thereby extending the required temperature of 29° C during the late afternoons and even the winter months. More about this can be read in the authors' publication (Ismail & Gryzagoridis, 2019).

An automated flow control device needs to be developed that will allow the correct temperature control directly proportional to the sun's radiation received on the SWH.

Nutritional values of vegetables and fish can be investigated in the current existing system which can lead to other post graduate studies in different faculties.

The social impact on the children at the community centre could also be monitored to determine the effectiveness of the exposure through fun learning techniques utilising the pilot system.

An economic viability study of such systems could be conducted. Such a study should not only include the yield of produce but also the educational and technology transfer benefits to socio-economically deprived communities.

REFERENCES

- Al-mohamad, A. 2004. APPLIED Efficiency improvements of photo-voltaic panels using a Sun-tracking system. , 79: 345–354.
- Aliyu, A.K., Modu, B. & Tan, C.W. 2018. A review of renewable energy development in Africa: A focus in South Africa, Egypt and Nigeria. *Renewable and Sustainable Energy Reviews*, 81(February 2016): 2502–2518.
<https://doi.org/10.1016/j.rser.2017.06.055>.
- Alternative energy, T. 2019a. evacuated-tube-collector @ www.alternative-energy-tutorials.com. <http://www.alternative-energy-tutorials.com/solar-hot-water/evacuated-tube-collector.html> 22 August 2019.
- Alternative energy, T. 2019b. flat-plate-collector @ www.alternative-energy-tutorials.com. <http://www.alternative-energy-tutorials.com/solar-hot-water/flat-plate-collector.html> 22 August 2019.
- Aquaponichowto. 2009. 89b71344b2eff50cdfbac3341a09f86681cb053d @ aquaponichowto.com. <http://aquaponichowto.com/commercial-aquaponic-farming-how-it-is-possible-to-master-aquaponics/> 30 August 2019.
- Badamasi, Y.A. 2014. The working principle of an Arduino. *Proceedings of the 11th International Conference on Electronics, Computer and Computation, ICECCO 2014*.
- Badiola, M., Basurko, O.C., Piedrahita, R., Hundley, P. & Mendiola, D. 2018. Energy use in Recirculating Aquaculture Systems (RAS): A review. *Aquacultural Engineering*, 81(November 2017): 57–70. <https://doi.org/10.1016/j.aquaeng.2018.03.003>.
- Bah, M.M. & Azam, M. 2017. Investigating the relationship between electricity consumption and economic growth: Evidence from South Africa. *Renewable and Sustainable Energy Reviews*, 80(February): 531–537. <http://dx.doi.org/10.1016/j.rser.2017.05.251>.
- Bazilian, M., Onyeji, I., Liebreich, M., MacGill, I., Chase, J., Shah, J., Gielen, D., Arent, D., Landfear, D. & Zhengrong, S. 2013. Re-considering the economics of photovoltaic power. *Renewable Energy*, 53: 329–338.
<http://dx.doi.org/10.1016/j.renene.2012.11.029>.
- Bekker, B. 2007. Irradiation and PV array energy output, cost, and optimal positioning estimation for South Africa. *Journal of Energy in Southern Africa*, 18(2): 16–25.

- Belton, B., van Asseldonk, I.J.M. & Thilsted, S.H. 2014. Faltering fisheries and ascendant aquaculture: Implications for food and nutrition security in Bangladesh. *Food Policy*, 44: 77–87. <http://dx.doi.org/10.1016/j.foodpol.2013.11.003>.
- Berka, R. 1986. *The transport of live fish. A review*.
http://www.flyingsharks.eu/literature/fao_iata/Transport_of_live_fish_FAO.pdf.
- Von Bertalanffy, L. 1957. THE QUARTERLY REVIEW OF BIOLOGY. , 32(3): 333–406.
- Brew-Hammond, A. & Kemausuor, F. 2009. Energy for all in Africa - to be or not to be?! *Current Opinion in Environmental Sustainability*, 1(1): 83–88.
- Buker, M.S. & Riffat, S.B. 2015. Building integrated solar thermal collectors - A review. *Renewable and Sustainable Energy Reviews*, 51: 327–346.
<http://dx.doi.org/10.1016/j.rser.2015.06.009>.
- Butti, K. & Perlin, J. 1980. *A Golden-Thread : 2500 Years of Solar Architecture and Technology*. United States of America.
- Ceylan, I., Gürel, A.E., Demircan, H. & Aksu, B. 2014. Cooling of a photovoltaic module with temperature controlled solar collector. *Energy and Buildings*, 72: 96–101.
- El Chaar, L., Lamont, L.A. & El Zein, N. 2011. Review of photovoltaic technologies. *Renewable and Sustainable Energy Reviews*, 15(5): 2165–2175.
<http://dx.doi.org/10.1016/j.rser.2011.01.004>.
- da Costa, M.R., Tubino, R. de A. & Monteiro-Neto, C. 2018. Length-based estimates of growth parameters and mortality rates of fish populations from a coastal zone in the Southeastern Brazil. *Zoologia*, 35: 1–8.
- Court, N. & Ramon, S. 2001. PV Installation Guide A GUIDE TO PHOTOVOLTAIC (PV). , (June): 1–39.
- DoE. 2014. r_solar @ www.energy.gov.za.
http://www.energy.gov.za/files/esources/renewables/r_solar.html 21 August 2019.
- Duffie, J.A. & Beckman, W.A. 2013. *Solar Engineering of Thermal Processes*. Fourth. Canada: Wiley.
- Elfeky, A. 2019. Performance of Nile Tilapia (*Oreochromis niloticus*) Fingerlings . II . Influence of Different Water Temperatures. , (January 2009).
- Essington, T.E., Kitchell, J.F. & Walters, C.J. 2001. The von Bertalanffy growth function,

- bioenergetics, and the consumption rates of fish. *Canadian Journal of Fisheries and Aquatic Sciences*, 58(11): 2129–2138.
- Fin24. 2019a. eskom-sa-on-brink-of-further-load-shedding-20190821 @ www.fin24.com. <https://www.fin24.com/Economy/eskom-sa-on-brink-of-further-load-shedding-20190821> 30 August 2019.
- Fin24. 2019b. just-in-eskom-posts-net-loss-after-tax-of-r207-billion-20190730 @ www.fin24.com. <https://www.fin24.com/Economy/Eskom/just-in-eskom-posts-net-loss-after-tax-of-r207-billion-20190730>.
- Foster R, Ghassemi M, C.A. 2010. *Solar energy: renewable energy and the environment*. CRC Press.
- Fouad, M.M., Shihata, L.A. & Morgan, E.S.I. 2017. An integrated review of factors influencing the performance of photovoltaic panels. *Renewable and Sustainable Energy Reviews*, 80(May): 1499–1511. <http://dx.doi.org/10.1016/j.rser.2017.05.141>.
- Fox, B.K., Howerton, R. & Tamaru, C.S. 2010. Construction of Automatic Bell Siphons for Backyard Aquaponic Systems. *college of Tropical Agricultural and Human Resources (CTAHR)*, 10(June): 1–11. www.ctahr.hawaii.edu/freepubs.
- Fuller, R.J. 2007. Solar heating systems for recirculation aquaculture. *Aquacultural Engineering*, 36(3): 250–260.
- Goddek, S. & Keesman, K.J. 2018. The necessity of desalination technology for designing and sizing multi-loop aquaponics systems. *Desalination*, 428(May 2017): 76–85. <https://doi.org/10.1016/j.desal.2017.11.024>.
- Goldblatt, A. 2011. Agriculture: Facts and Trends South Africa. *World Wide Fund for Nature (WWF)*: 2–26. http://awsassets.wwf.org.za/downloads/facts_brochure_mockup_04_b.pdf.
- De Graaf, G. & Prein, M. 2005. Fitting growth with the von Bertalanffy growth function: A comparison of three approaches of multivariate analysis of fish growth in aquaculture experiments. *Aquaculture Research*, 36(1): 100–109.
- Graber, A. & Junge, R. 2009. Aquaponic Systems: Nutrient recycling from fish wastewater by vegetable production. *Desalination*, 246(1–3): 147–156. <http://dx.doi.org/10.1016/j.desal.2008.03.048>.
- Gulati, M., Jacobs, I., Jooste, A., Naidoo, D. & Fakir, S. 2013. The Water–energy–food

- Security Nexus: Challenges and Opportunities for Food Security in South Africa. *Aquatic Procedia*, 1: 150–164.
<https://linkinghub.elsevier.com/retrieve/pii/S2214241X1300014X>.
- Hambley, A.R. 2014. *Electrical Engineering : Principles and Applications*. 6th ed. United States of America: Pearson.
- Hambrey. 2013. The relevance of aquaponics to the New Zealand aid programme, particularly in the Pacific Commissioned Report Prepared by Hambrey Consulting for New Zealand Aid Programme Ministry of Foreign Affairs and Trade. , (December).
- Hamed, M., Fella, A. & Ben Brahim, A. 2014. Parametric sensitivity studies on the performance of a flat plate solar collector in transient behavior. *Energy Conversion and Management*, 78: 938–947. <http://dx.doi.org/10.1016/j.enconman.2013.09.044>.
- Ismail, F. & Gryzagoridis, J. 2019. Optimising photovoltaic system by direct cooling and transferring heat to aquaculture medium to boost aquaponics food production in needy communities. *Proceedings of the Conference on the Industrial and Commercial Use of Energy, ICUE*, 2018-Augus: 1–6.
- japanaquaponics. 2019. bell-siphon-guide @ www.japan-aquaponics.com.
<http://www.japan-aquaponics.com/bell-siphon-guide.html> 30 August 2019.
- Kalogirou, S.A. 2004. *Solar thermal collectors and applications*.
- Kuitche. 2013. 濟無No Title No Title. *Journal of Chemical Information and Modeling*, 53(9): 1689–1699.
- Kulworawanichpong, T. & Mwambeleko, J.J. 2015. Design and costing of a stand-alone solar photovoltaic system for a Tanzanian rural household. *Sustainable Energy Technologies and Assessments*, 12: 53–59.
<http://dx.doi.org/10.1016/j.seta.2015.10.001>.
- Kyaw, T.Y. & Ng, A.K. 2017. Smart Aquaponics System for Urban Farming. *Energy Procedia*, 143: 342–347. <https://doi.org/10.1016/j.egypro.2017.12.694>.
- Lapere, P. 2010. A Techno-Economic Feasibility Study into Aquaponics in South Africa by. *Master Thesis*, (December).
- Lennard, W. 2012. Aquaponic System Design Parameters : Fish to Plant Ratios (Feeding Rate Ratios). *Aquaponic Solutions*, 1(1): 1–11. <http://www.aquaponic.com.au/Fish> to

plant ratios.pdf.

- Leonics. articles2_12j_en @ www.leonics.com. *How to Design Solar PV System*.
http://www.leonics.com/support/article2_12j/articles2_12j_en.php 2 June 2020.
- Liang, F. & Xia, X.A. 2005. Long-term trends in solar radiation and the associated climatic factors over China for 1961-2000. *Annales Geophysicae*, 23(7): 2425–2432.
- Loschi, H.J., Iano, Y., León, J., Moretti, A., Conte, F.D. & Braga, H. 2015. A Review on Photovoltaic Systems: Mechanisms and Methods for Irradiation Tracking and Prediction. *Smart Grid and Renewable Energy*, 06(07): 187–208.
- Love, D.C., Fry, J.P., Li, X., Hill, E.S., Genello, L., Semmens, K. & Thompson, R.E. 2015. Commercial aquaponics production and profitability: Findings from an international survey. *Aquaculture*, 435: 67–74. <http://dx.doi.org/10.1016/j.aquaculture.2014.09.023>.
- MacNeil, M., Chong-Seng, K., Pratchett, D., Thompson, C., Messmer, V. & Pratchett, M. 2017. Age and Growth of An Outbreking *Acanthaster cf. solaris* Population within the Great Barrier Reef. *Diversity*, 9(1): 18.
- Maghami, M.R., Hizam, H., Gomes, C., Radzi, M.A., Rezadad, M.I. & Hajjighorbani, S. 2016. Power loss due to soiling on solar panel: A review. *Renewable and Sustainable Energy Reviews*, 59: 1307–1316. <http://dx.doi.org/10.1016/j.rser.2016.01.044>.
- Marom, R., Ziv, B., Banerjee, A., Cahana, B., Luski, S. & Aurbach, D. 2015. Enhanced performance of starter lighting ignition type lead-acid batteries with carbon nanotubes as an additive to the active mass. *Journal of Power Sources*, 296: 78–85.
<http://dx.doi.org/10.1016/j.jpowsour.2015.07.007>.
- Matuska, T. & Zmrhal, V. 2009. Kolektor 2.2. *Environmental Engineering*.
- El Mays, A., Ammar, R., Hawa, M., Akroush, M.A., Hachem, F., Khaled, M. & Ramadan, M. 2017. Improving Photovoltaic Panel Using Finned Plate of Aluminum. *Energy Procedia*, 119: 812–817. <http://dx.doi.org/10.1016/j.egypro.2017.07.103>.
- Mchunu, N., Lagerwall, G. & Senzanje, A. 2018a. Aquaponics in South Africa : Results of a national survey. *Aquaculture Reports*, 12(March): 12–19.
<https://doi.org/10.1016/j.aqrep.2018.08.001>.
- Mchunu, N., Lagerwall, G. & Senzanje, A. 2018b. Aquaponics in South Africa: Results of a national survey. *Aquaculture Reports*, 12(August): 12–19.

<https://doi.org/10.1016/j.aqrep.2018.08.001>.

Mchunu, N., Odindo, A. & Muchaonyerwa, P. 2018. The effects of urine and urine-separated plant nutrient sources on growth and dry matter production of perennial ryegrass (*Lolium perenne*. L). *Agricultural Water Management*, 207(August): 37–43. <https://doi.org/10.1016/j.agwat.2018.05.023>.

Merwe, C. Van Der. 2011. Key Challenges for Ensuring Food Security in South Africa's Inner Cities. *Africa Institute of South Africa*, (36): 1–8.

Meteo Cape Town. 2018. Local Weather-Table View.

Meyer, I. 2018. Western Cape Budget Speech 2018 / 19. <https://www.westerncape.gov.za/speech/western-cape-budget-speech-2018-19>.

Michael, J.J., S, I. & Goic, R. 2015. Flat plate solar photovoltaic-thermal (PV/T) systems: A reference guide. *Renewable and Sustainable Energy Reviews*, 51: 62–88. <http://dx.doi.org/10.1016/j.rser.2015.06.022>.

Micheli, L., Reddy, K.S. & Mallick, T.K. 2015. Plate micro-fins in natural convection: An opportunity for passive concentrating photovoltaic cooling. *Energy Procedia*, 82: 301–308.

Milkwood. 2014. b9e5362e701e4f85fbf82c9b8fd16d7a95f1c2a2 @ www.milkwood.net. <https://www.milkwood.net/2014/01/20/aquaponics-a-brief-history/> 30 August 2019.

Moharram, K.A., Abd-Elhady, M.S., Kandil, H.A. & El-Sherif, H. 2013. Enhancing the performance of photovoltaic panels by water cooling. *Ain Shams Engineering Journal*, 4(4): 869–877. <http://dx.doi.org/10.1016/j.asej.2013.03.005>.

Mulvaney, R.L., Khan, S.A. & Ellsworth, T.R. 2009. Synthetic Nitrogen Fertilizers Deplete Soil Nitrogen: A Global Dilemma for Sustainable Cereal Production. *Journal of Environment Quality*, 38(6): 2295.

Nako, K. 2010. Ke NaKo. *Chief Executive*.

Nelson, R. & Pade, J. Methods of Aquaponics. <https://aquaponics.com/methods-of-aquaponics/#> 2 September 2019.

Palz, W. 2014. *Solar Power for the World*. Pan Stanford Publishing.

Pan, C.A. & Dinter, F. 2017. Combination of PV and central receiver CSP plants for base load power generation in South Africa. *Solar Energy*, 146: 379–388.

- <http://dx.doi.org/10.1016/j.solener.2017.02.052>.
- Pattillo, D.A. 2017. Technical Bulletin Series An Overview of Aquaponic Systems: Hydroponic Components. , (March): 1–10.
- Prasad, D. & Snow, M. 2005. *Designing with Solar Power :A Source Book Building Integrated Photovoltaics*.
- Rakocy, J. E., Bailey, D. S., Shultz, R. C., & Thoman, E.S. 2004. Update on tilapia and vegetable production in the UVI aquaponic system. New dimensions on farmed tilapia. *Proceedings from the 6th International Symposium on Tilapia in Aquaculture*, 000: 1–15.
- Rakocy, J.E. 1989. Tank Culture of Tilapia. *Screen*, 17(282): 523–529.
http://www.ncbi.nlm.nih.gov/entrez/query.fcgi?cmd=Retrieve&db=PubMed&dopt=Citation&list_uids=7836875.
- Rakocy, J.E., Masser, M.P. & Losordo, T.M. 2012. Aquaponics — Integrating Fish and Plant Culture. : 1–16. <http://pods.dasnr.okstate.edu/docushare/dsweb/Get/Document-10215/SRAC-454web.pdf>.
- Rawlins, J. 2019. Political economy of water reallocation in South Africa: Insights from the Western Cape water crisis. *Water Security*, 6(February): 100029.
<https://doi.org/10.1016/j.wasec.2019.100029>.
- Renner-Martin, K., Brunner, N., Kühleitner, M., Nowak, W.G. & Scheicher, K. 2018. On the exponent in the Von Bertalanffy growth model. *PeerJ*, 2018(1): 1–25.
- Rizal, A., Dhahiyat, Y., Zahidah, Andriani, Y., Handaka, A.A. & Sahidin, A. 2018. The economic and social benefits of an aquaponic system for the integrated production of fish and water plants. *IOP Conference Series: Earth and Environmental Science*, 137(1).
- Le Roux, W.G. 2016. Optimum tilt and azimuth angles for fixed solar collectors in South Africa using measured data. *Renewable Energy*, 96: 603–612.
<http://dx.doi.org/10.1016/j.renene.2016.05.003>.
- RSA & Department of Agriculture Forestry and Fisheries. 2012. Production guidelines for Tomato. *Production Guideline*: 1–13.
- SA Yearbook. 2008. SA YEARBOOK 2008/09 K 2008/09 AGRICULTURE AND LAND AFFAIRS. : 46–73.

- <https://www.gcis.gov.za/sites/default/files/docs/resourcecentre/yearbook/2009/chapter3.pdf>.
- Sabiha, M.A., Saidur, R., Mekhilef, S. & Mahian, O. 2015. Progress and latest developments of evacuated tube solar collectors. *Renewable and Sustainable Energy Reviews*, 51: 1038–1054.
- Sampaio, P.G.V. & González, M.O.A. 2017. Photovoltaic solar energy: Conceptual framework. *Renewable and Sustainable Energy Reviews*, 74(December 2016): 590–601.
- Schroeder, D. V. 2011. The Sun and the Seasons.
<https://physics.weber.edu/schroeder/ua/sunandseasons.html> 2 September 2019.
- El Shenawy, E.T., Hegazy, A.H. & Abdellatef, M. 2017. Design and optimization of stand-alone PV system for Egyptian rural communities. *International Journal of Applied Engineering Research*, 12(20): 10433–10446.
- Skelton, P. 2001. *A complete guide to the freshwater fishes of Southern Africa*. Second Edi. Struik Publisher.
- Solar-wind. 2019. dc-cable-sizing-tool @ www.solar-wind.co.uk. <https://www.solar-wind.co.uk/info/dc-cable-sizing-tool> 30 August 2019.
- solarelectricityhandbook. 2019. solar-angle-calculator @ www.solarelectricityhandbook.com. <http://www.solarelectricityhandbook.com/solar-angle-calculator.html> 23 August 2019.
- Solargis. 2019. south-africa @ solargis.com. <https://solargis.com/maps-and-gis-data/download/south-africa> 22 August 2019.
- Somerville, C., Cohen, M., Pantanella, E., Stankus, A. & Lovatelli, A. 2014. *Small-scale aquaponic food production. Integrated fish and plant farming*.
- Sunearthtools. 2019. Pos_Sun @ [Www.Sunearthtools.Com](http://www.Sunearthtools.Com).
http://www.sunearthtools.com/dp/tools/pos_sun.php#top 31 August 2019.
- Swanson, R.. 2006. A Vision for Crystalline Silicon Photovoltaics. *Progress in Photovoltaics: Research and Applications*, 17: 443–453.
- Swinbank, W.C. 1963. Long-wave radiation from clear skies. *Quarterly Journal of the Royal Meteorological Society*, 89(381): 339–348.

- Tantichanakul, T., Chailapakul, O. & Tantavichet, N. 2013. Influence of fumed silica and additives on the gel formation and performance of gel valve-regulated lead-acid batteries. *Journal of Industrial and Engineering Chemistry*, 19(6): 2085–2091. <http://dx.doi.org/10.1016/j.jiec.2013.03.024>.
- Tessema, Z., Mainali, B. & Silveira, S. 2014. Mainstreaming and sector-wide approaches to sustainable energy access in Ethiopia. *Energy Strategy Reviews*, 2(3–4): 313–322.
- du Toit, D.C. 2011. *Department of agriculture forestry and fisheries*.
- Vermaak, H.J. 2014. Techno-economic analysis of solar tracking systems in South Africa. *Energy Procedia*, 61: 2435–2438. <http://dx.doi.org/10.1016/j.egypro.2014.12.018>.
- Wang, C. & Lu, Y. 2015. Solar Photovoltaic Efficiency. : 1–7.
- Wang, Z., Yang, W., Qiu, F., Zhang, X. & Zhao, X. 2015. Solar water heating: From theory, application, marketing and research. *Renewable and Sustainable Energy Reviews*, 41: 68–84. <http://dx.doi.org/10.1016/j.rser.2014.08.026>.
- Watmuff, J. & Proctor, D. 1987. Solar and wind induced external coefficients - Solar collectors. , (May).
- Wohlgemuth, J.H., Cunningham, D.W., Nguyen, A.M. & Miller, J. 2005. Long term reliability of PV modules. *Proceedings of the 20th European PV Solar Energy Conference*: 1942–1948. <http://citeseerx.ist.psu.edu/viewdoc/download;jsessionid=F0050C879CAA1F0BD54880F4EE1AEC40?doi=10.1.1.496.984&rep=rep1&type=pdf>.
- Yang, Y., Kim, K.A., Blaabjerg, F. & Sangwongwanich, A. 2019. *Advances in Grid-Connected Photovoltaic Power Conversion Systems*. First Edit. Elsevier B.V.
- Yilmaz, S., Ozcalik, H.R., Kesler, S., Dincer, F. & Yelmen, B. 2015. The analysis of different PV power systems for the determination of optimal PV panels and system installation - A case study in Kahramanmaraş, Turkey. *Renewable and Sustainable Energy Reviews*, 52: 1015–1024. <http://dx.doi.org/10.1016/j.rser.2015.07.146>.

APPENDIX A: Ethical Clearance: University



**CAPE PENINSULA UNIVERSITY OF TECHNOLOGY ANIMAL ETHICS COMMITTEE
(CPUT-AEC)**
Registration Number NHREC: To be confirmed

P.O. Box 1906 • Bellville 7535 South Africa
Symphony Road Bellville 7535
Tel: +27 21 959 6917
Email: besterd@cput.ac.za

DATE 25 February 2019
REC Approval Reference No:
CPUT/AEC 2019/01

Dear Mr Ismail

Re: APPLICATION TO THE CPUT-AEC FOR ETHICS CLEARANCE

Approval was granted by the Cape Peninsula University of Technology Animal Ethics Committee to Fareed Ismail for ethical clearance on 25 February 2019. This approval is for research activities related to student research in the Department of Mechanical Engineering at the Cape Peninsula University of Technology.

TITLE: Use of solar energy to control the environment for aquaponics in low income communities.

Supervisor: Prof Gryzagoridis

Comment: The issuing of this certificate is supported by the appropriate permits from the Provincial Government of the Western Cape.

Approval will not extend beyond 01 March 2020. An extension should be applied for 6 weeks before this expiry date should data collection and use/analysis of data, information and/or samples for this study continue beyond this date.

The investigator(s) should understand the ethical conditions under which they are authorized to carry out this study and they should be compliant to these conditions. It is required that the investigator(s) complete an **annual progress report** that should be submitted to the CPUT-AEC in December of that particular year, for the CPUT-AEC to be kept informed of the progress and of any problems you may have encountered.

Kind Regards

A handwritten signature in blue ink, appearing to read "Dirk Bester".

Dr Dirk Bester
Chairperson – Animal Ethics Committee
Cape Peninsula University of Technology

APPENDIX B: Ethical Clearance: Faculty



P.O. Box 1906, Bellville 7535 South Africa,
Tel: +27 21 959 6666 E-Mail: greenf@cput.ac.za

ENGINEERING FACULTY

On 19 June 2018, the Chairperson of the Engineering Ethics Committee of the Cape Peninsula University of Technology granted ethics approval to **FAREED ISMAIL: 200736191** for research activities related to his **DOCTOR OF ENG IN MECHANICAL ENG** studies at the Cape Peninsula University of Technology.

Title of thesis:

Use of solar energy to control the environment for aquaponics in low income communities

~~Comment~~

- Data collection is not required
 Data collection required – permission letter attached



19/6/2018

Prof R Haldenwang
Faculty of Engineering Ethics Committee Chairperson. (Acting)

Date

APPENDIX D: Tracking code for Arduino

```
#include <Servo.h> // include Servo library

Servo horizontal; // horizontal servo
int servoh = 90; // stand horizontal servo

Servo vertical; // vertical servo
int servov = 90; // stand vertical servo

// LDR pin connections
// name = analogpin;
int ldr1t = 0; //LDR top left
int ldr1r = 1; //LDR top right
int ldr1l = 2; //LDR down left
int ldr1d = 3; //ldr down right

void set-up()
{
  Serial.begin(9600);
  // servo connections
  // name.attach(pin);
  horizontal.attach(9);
  vertical.attach(10);
}

void loop()
{
  int lt = analogRead(ldr1t); // top left
  int rt = analogRead(ldr1r); // top right
  int ld = analogRead(ldr1l); // down left
  int rd = analogRead(ldr1d); // down right

  int dtim = analogRead(4)/20; // read potentiometers
  int tol = analogRead(5)/4;

  int avt = (lt + rt) / 2; // average value top
  int avd = (ld + rd) / 2; // average value down
  int avl = (lt + ld) / 2; // average value left
  int avr = (rt + rd) / 2; // average value right

  int dvert = avt - avd; // check the diffirence of up and down
  int dhoriz = avl - avr; // check the diffirence og left and right

  if (-1*tol > dvert || dvert > tol) // check if the diffirence is in the tolerance else change
  vertical angle
  {
    if (avt > avd)
    {
      servov = ++servov;
      if (servov > 180)
      {
        servov = 180;
      }
    }
  }
}
```

```

}
else if (avt < avd)
{
servov= --servov;
if (servov < 0)
{
servov = 0;
}
}
vertical.write(servov);
}

if (-1*tol > dhoriz || dhoriz > tol) // check if the difference is in the tolerance else change
horizontal angle
{
if (avl > avr)
{
servoh = --servoh;
if (servoh < 0)
{
servoh = 0;
}
}
else if (avl < avr)
{
servoh = ++servoh;
if (servoh > 180)
{
servoh = 180;
}
}
else if (avl == avr)
{
// nothing
}
horizontal.write(servoh);
}
delay(dtime);
}

```

APPENDIX E: Battery specifications



Introduction:

After 10 years of experience in VRLA with Shin Kabe, Exide (INDIA) has finally launched new Ceil Powersafe NXT with the cycle life unmatched with competition nationally and internationally with its unique feature of 5 hours quick recharge option.

Features:

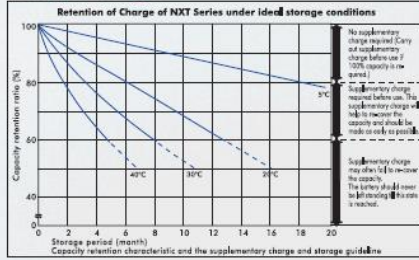
- Deep cycle application
- Fast recovery from deep discharge
- Extended cycle life
- Fast recharge capability
- Excellent charge retention
- International size
- Free from orientation constraints
- Eco-friendly

Specification Table

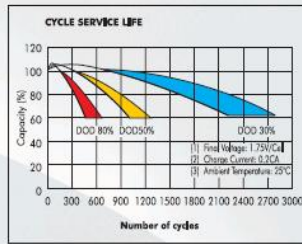
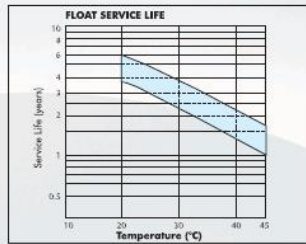
Battery Type	Nominal Voltage (V)	Rated Capacity (Ah) at 27°C										Dimensions (mm)				Weight (kg) ±0.2%	Internal Resistance (mohm)	Maximum Discharge Current (Amps)
		20hr	10hr	5hr	3hr	2hr	90 mins	40 mins	30 mins	Overall Height up to +J2	Length +J2	Width +J2	Height up to +J2	Length +J2	Width +J2			
NXT 17-2	12	17	15.5	14.0	13.0	12.0	11.0	9.5	7.5	167	167	181	76	5.90	15	235		
NXT 26-2	12	26	23.5	21.0	19.5	18.0	17.0	14.5	11.5	175	175	166	125	9.60	10	390		
NXT 42-2	12	42	38.0	34.0	31.5	29.5	27.5	23.0	19.0	170	170	197	165	13.80	8	420		
NXT 65-2	12	65	58.5	52.5	49.0	45.5	43.0	36.0	29.5	174	174	350	166	22.00	8	500		
NXT 100-2	12	100	90.0	81.0	75.0	70.0	66.0	55.0	45.0	235	235	407	173	35.00	6	600		
NXT 150-2	12	150	135.0	121.5	112.5	105.0	99.0	82.5	67.5	240	240	557	172	50.00	6	900		
NXT 200-2	12	200	180.0	162.0	150.0	140.0	132.0	110.0	90.0	240	240	533	250	67.00	5	1200		

Note: Batteries are despatched from factory at minimum 90% state of charge. Full capacity is achieved after a minimum ten numbers of charge - discharge cycle at full depth or 3 months of continuous float operation.

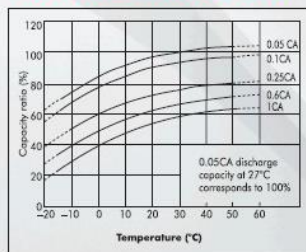
CAPACITY RETENTION



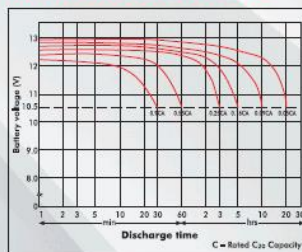
NXT SERVICE LIFE



EFFECT OF TEMPERATURE ON CAPACITY



NXT DISCHARGE CHARACTERISTICS



NOTES ON OPERATIONS:

Charging Characteristics:

a) Normal Recharge:

Batteries to be recharged in conv model only.

Mode of operation	Voltage setting per 12V unit for ambient temperature 20 ± 30 °C	Current setting
Float	13.7V ± 0.1V	Maximum : 0.3 CA Minimum : 0.1 CA
Cyclic	14.7V ± 0.1V	

Temperature Compensation : (Reference 25°C)
 Float : + 18mV / °C / 12V unit
 Cyclic : - 30mV / °C / 12V unit

b) Fast Recharge option:

During operation, if the battery bank is subjected to regular (daily) deep discharge in excess of 50% (cumulative basis), the fast recharge option may be exercised.

Fast recharge, following pattern to be followed:

- Step 1: 0.3C - 14.5V
- Step 2: 0.1C - 14.5V
- Step 3: 0.05C - 14.5V
- Step 4: 0.02C - 14.5V

Total duration for the four steps shall be 5.0 hours for a recharge after a 70% DOD. However, this mode of recharge will require an equalization once a month at the recommended float voltage for a period of 12 hours uninterrupted.

Caution on Ripple: The maximum limits of the A.C. content of the D.C. shall be 5A.A.C. (rms) per 100 Ah C20 capacity during float charge. The A.C. current induced battery temperature rise should be below 3°C. At all times the average D.C. float current must be kept positive.

Heat Dissipation: A VRLA battery under normal float condition shall dissipate heat into the atmosphere. For the overall heat load calculation, taking into account a worst case operation, the rate of heat dissipation may be taken as 0.45 Watts/100 Ah C20 capacity/Cell.

Hydrogen Evolution: Hydrogen gas evolved by a lead acid battery may be estimated from the following formula:

$$\text{Hydrogen gas evolved per hour} = 0.45 \times 10^{-4} \times n \times i \times C \text{ m}^3 \text{ at N.T.P.}$$

Where, n = number of 2V cells

i = 0.2 A/100 Ah for a VRLA cell

C = C20 capacity of Cell

To design for the ventilation (air flow) requirement so that the hydrogen percentage in the air is always below 4% (Lower Explosive Limit), the air flow rate may be estimated as:

$$Q = d \times s \times 0.45 \times 10^{-4} \times n \times i \times C \text{ m}^3 / \text{hr}$$

Where, d = dilution ratio $(100 - 4) / 4 = 24$

s = factor of safety, eg.5

For a VRLA, the above may be simplified as:

$$Q = 0.0108 \times n \times C$$

Paralleling of Battery Strings: (a) Paralleling of a maximum of three strings is allowed provided they are all of the same make and Ah capacity and of same age. (b) Adequate care shall be taken in ensuring that all inter-unit connecting cables have equal length and cross-section. All cables to the system, from each of the strings, shall also be of same length and cross-section. (c) Total charging current, in the case of parallel strings, to be taken care of so that each of the strings get the recommended level of Amperes = minimum 10% and maximum 30% of the rated C20 capacity of each of the 12V blocks.

For inter-block connection flexible copper cable with suitable lugs are recommended. Cable cross section may be estimated at 2.8A/mm² at the maximum anticipated discharge load.

Even though the Cell Powersafe NXT batteries are designed to perform anywhere between -40 to +50°C, for optimum battery life avoid prolonged operation in ambient in excess of 35°C.

Above 27°C, for every 8°C rise of weighted average operating temperature, battery life is reduced by 50%.

Test discharge on installation and commissioning, if necessary, should be conducted only after 48 hours of uninterrupted float charge with load disconnected.

Ensure that batteries are put to recharge immediately after any discharge. Under no circumstance the gap between the end of discharge and initiation of recharge should be more than 24 hours.

Standard Maintenance Recommendations: (a) Visual check every 3 months to note any physical abnormality like bulge, crack or leakage etc. (b) Measure float voltage of individual units once in 3 months and record the data. (c) Test discharge the battery bank at least once in 12 months to check battery health. (d) Keep the battery top clean with the help of a dry cotton cloth periodically. Inspect the inter-unit connection points for any corrosion etc. The inter-unit connection area to be checked for tightness once a year. (e) If battery bank is placed on steel racks / cabinets ensure an insulation between the battery base and the steel tray. This could be a coat of durable (acid-resistant) paint or any other insulating medium. Steel racks should preferably be well grounded.

Statutory Notice:

All batteries contain lead, which is harmful for human beings and environment. As per statutory requirements, the used battery must be returned to the authorized dealer, manufacturer or at the designated collection centres.



HEAD OFFICE: Exide Industries Limited, Exide House, 59C Chowringhee Road, Kolkata - 700 020, India
 Phone +91 33 2283 2120 / 2133, Fax +91 33 2283 2637 / 2283 2632

CORPORATE MARKETING OFFICE: SA Hasibagan Road, Entally, Kolkata - 700 014, India
 Phone +91 33 2286 9158 / 59, Fax +91 33 2286 6186
 visit us at: www.exideindustrialbatteries.com/www.exideind.com

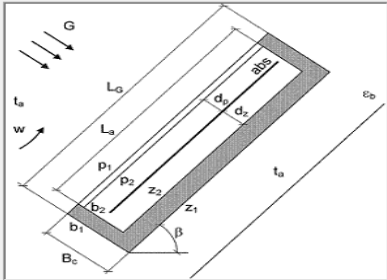
APPENDIX F: SWH “KOLEKTOR” software application

Kolektor 2.2
File Calculation Help

Design parameters | Absorber | Glazing and insulation | Calculation

Operation and climatic conditions

Input fluid temperature	t_{in}	20	°C
Specific fluid mass flow rate	m'	0.011	kg/s/m ²
Global solar irradiation	G	597	W/m ²
Ambient temperature	t_a	19.3	°C
Ambient relative humidity	ϕ_a	40	%
Wind velocity	w	3.3	m/s
Collector slope	β	30	deg
Adjacent frontal surface emissivity	ϵ_{as}	0.8	-



Collector dimensions

Gross height	L_g	1.84	m
Gross width	H_g	0.84	m
Gross area	A_g	1.55	m ²
Aperture height	L_a	1.82	m
Aperture width	H_a	0.79	m
Aperture area	A_a	1.44	m ²

Type of collector installation

Separate
 Integrated into building envelope

Collector depth

Absorber-glazing gap thickness	d_p	12.5	mm
Absorber-frame gap thickness	d_z	12.5	mm
Collector depth	B	0.08	m
Edge sides area	A_b	0.42	m ²

VZTech

Kolektor 2.2
File Calculation Help

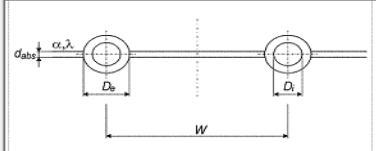
Design parameters | Absorber | Glazing and insulation | Calculation

Absorber parameters

Material	Copper	Solar absorbance	α_{abs}	0.95	-		
Thermal conductivity	λ_{abs}	390	W/mK	Front surface emissivity	$\epsilon_{abs,p}$	0.05	-
Thickness	d_{abs}	0.2	mm	Back surface emissivity	$\epsilon_{abs,z}$	0.5	-

Pipe register parameters

Length of riser pipes	L	1.82	m	Collector mass flow rate	M'	0.0158	kg/s
Number of riser pipes	n_{tp}	10	pcs	Pipe mass flow rate	M_1'	0.00151	kg/s
Distance between riser pipes (fin)	W	79	mm	Heat transfer fluid			
Pipe external diameter	D_e	9.53	mm	Fluid type	Water	Water	
Pipe internal diameter	D_i	7.73	mm	Mixing ratio	0	100	%
Type of bond	Middle						
Average bond width	a	0.9	mm	Freezing temperature	t_f	0	°C
Average bond thickness	b	0.9	mm				
Bond thermal conductivity	λ_{sp}	300	W/mK				
Bond thermal conductance	C_{sp}	300	W/mK				



VZTech

Kolektor 2.2

File Calculation Help

Design parameters Absorber Glazing and insulation Calculation

Glazing parameters

Material: Glass

Thickness: d_{gl} 4 mm

Normal solar transmittance: τ_n 0.92 -

Normal solar reflectance: ρ_n 0.06 -

Diffuse solar reflectance: ρ_d 0.6 -

External surface emissivity: ε_{p1} 0.85 -

Internal surface emissivity: ε_{p2} 0.85 -

Thermal properties

Thermal conductivity

Thermal resistance

Thermal conductivity (polynomic): $\lambda = \lambda_0 + \lambda_1 t + \lambda_2 t^2$

λ : 0.8 W/mK

λ_1 : 0 W/mK²

λ_2 : 0 W/mK³

Frame / insulation parameters

Material: Mineral wool

Thickness: d_{fr} 50 mm

Thermal conductivity: λ_{fr} 0.045 W/mK

Thermal resistance: R_{fr} 1.11 m²K/W

External frame surface emissivity: $\varepsilon_{f,z1}$ 0.5 -

Internal frame surface emissivity: $\varepsilon_{f,z2}$ 0.5 -

Gas filling of collector interior

Type of gas: Air

Gas pressure: 101 kPa

Optical efficiency of collector

Effective $\tau\alpha$ product: 0.874 -

VZTech

Kolektor 2.2

File Calculation Help

Design parameters Absorber Glazing and insulation Calculation

GLAZING ABSORBER FRAME / INSULATION

t_a 19 °C t_{p1} 20.40 °C t_{p2} 20.52 °C $t_{out} = 30.6$ °C t_{z2} 28.79 °C t_{z1} 19.71 °C t_a 19 °C

Radiation p1 - a: Berdahl, Martin h_s 4.421 W/m²K

Radiation abs - p2: $F'' = 0.965$, $F_b = 0.933$, h_s 0.299 W/m²K

Radiation abs - z2: h_s 2.101 W/m²K

Radiation z1 - a: h_s 2.526 W/m²K

Convection p1 - a: McAdams h_p 17.18 W/m²K for all w

Convection abs - p2: Hollands h_p 2.044 W/m²K for slope 0 - 60°

Convection abs - z2: Correlation A1 h_p 2.068 W/m²K for any slope

Convection z1 - a: McAdams h_p 17.18 W/m²K

$t_{in} = 20$ °C $t_{stg} = ??$ °C

Forced convection in pipes: Laminar: Shah, Turbulent: Sieder-Tate, h_i (Laminar) 381 W/m²K

Iteration: Number of loops 10

Calculation: For given t_{in} , Efficiency curve calculation

Calculate

VZTech

APPENDIX G: SWH flat plate collector design summer and winter day

	A	B	C	D	E	F	G	H	I	J
4	Summer Day (High Radiation & LowModerate Wind Speeds)									
5										
6			solar Ira	Ambien	wind speed		Qu	Qu()	Tabs	Delta T
7		6.00	66.7	15.3	1.6		96.048	83.94595	21.7	6.4
8		7.00	201.2	16.8	1.2		289.728	253.2223	26.4	9.6
9		8.00	444.1	18.5	2.2		639.504	558.9265	34.7	16.2
10		9.00	668.1	20.2	2.9		962.064	840.8439	42.2	22
11		10.00	848.81	21.7	4.2		1222.286	1068.278	48.2	26.5
12		11.00	962.7	23	4.5		1386.288	1211.616	52	29
13		12.00	999.1	24.1	4.2		1438.704	1257.427	53.4	29.3
14		13.00	967	24.9	3.4		1392.48	1217.028	52.6	27.7
15		14.00	866.5	25.3	3.4		1247.76	1090.542	49.4	24.1
16		15.00	700.5	25.5	3.6		1008.72	881.6213	44.1	18.6
17		16.00	482.1	25.2	3.8		694.224	606.7518	36.8	11.6
18		17.00	241.9	24.6	4.8		348.336	304.4457	28.7	4.1
19		18.00	74.7	22.6	4.3		107.568	94.01443	22.8	0.2

K	L	M	N	O	P	Q
	Glass	K	0.8			
		T	0.004			
Top Losses						
hs(p1-a)	hp(p1-a)	hv(p1-p2)	hs(abs-p2)	hp(abs-p)	Up	QUp
4.652	11.708	200	0.28	2.005	1.985067	18.29437
4.731	9.62	200	0.29	2.025	1.973761	27.28527
4.83	13.22	200	0.306	2.149	2.137969	49.87454
4.931	15.74	200	0.322	2.447	2.41244	76.42608
5.012	20.42	200	0.335	2.673	2.654158	101.2827
5.084	21.5	200	0.334	2.77	2.741367	114.4795
5.145	20.42	200	0.348	2.76	2.733239	115.3208
5.188	17.54	200	0.348	2.662	2.623126	104.6313
5.175	17.54	200	0.342	2.521	2.510622	87.12861
5.182	18.26	200	0.332	2.239	2.290362	61.34506
5.146	18.98	200	0.318	2.08	2.157668	36.04169
5.096	22.58	200	0.303	2.052	2.147025	12.67603
4.986	20.78	200	0.291	2.027	2.104301	0.606039

S	T	U	V	W	X	Y
Insulation	K	0.045				
	T	0.05				
Bottom Losses						
hs(z1-a)	hp(z1-a)	hv(z1-z2)	hs(abs-z2)	hp(abs-z2)	Uz	Quz
2.423	11.708	0.9	1.927	2.018	0.696688	6.911144
2.463	9.62	0.9	2.019	2.045	0.694476	10.3338
2.509	13.22	0.9	2.184	2.091	0.709922	17.82613
2.555	15.74	0.9	2.342	2.132	0.719795	24.54501
2.594	20.42	0.9	2.472	2.164	0.729785	29.97593
2.629	21.5	0.9	2.56	2.185	0.733513	32.97139
2.659	20.42	0.9	2.593	2.193	0.733469	33.31052
2.682	17.54	0.9	2.576	2.189	0.7297	31.32968
2.68	17.54	0.9	2.505	2.172	0.727601	27.17954
2.693	18.26	0.9	2.391	2.144	0.724982	20.90124
2.681	18.98	0.9	2.239	2.105	0.720731	12.95875
2.662	22.58	0.9	2.076	2.061	0.718159	4.563903
2.607	20.78	0.9	1.961	2.028	0.711967	0.22071

AB	AC	AD	AE	AF
Quseful	Coll_Eff	F'	Fr	Tout
58.74043	61%	0.932	0.877	26.4
215.6032	74%	0.933	0.877	29.6
491.2258	77%	0.929	0.87	36.2
739.8728	77%	0.923	0.86	42
937.0197	77%	0.918	0.851	46.5
1064.165	77%			49
1108.796	77%	0.916	0.848	49.3
1081.067	78%	0.919	0.852	47.7
976.2341	78%			44.1
799.375	79%			38.6
557.7513	80%			31.6
287.2057	82%	0.928	0.87	24.1
93.18768	87%	0.929	0.871	20.2

22									
23	Winter Day (Low Radiation & High Wind Speeds)								
24									
25									
26									
27		solar Ira	Ambien	wind speed	Qu	Qu()	Tabs	Delta T	
28		6.00	0	11.6	6.4	0	0	14.6	3
29		7.00	0.7	11.9	8.6	1.008	0.880992	14.6	2.7
30		8.00	31.6	12.2	6	45.504	39.7705	15.7	3.5
31		9.00	64.4	12.6	7.3	92.736	81.05126	16.9	4.3
32		10.00	105.8	13.3	7.9	152.352	133.1556	18.3	5
33		11.00	139.2	13.9	7.9	200.448	175.1916	19.5	5.6
34		12.00	116.8	14.1	6.9	168.192	146.9998	18.8	4.7
35		13.00	246.4	14.8	6.6	354.816	310.1092	23.2	8.4
36		14.00	191.5	15.2	6.6	275.76	241.0142	21.5	6.3
37		15.00	165.2	15.3	7.3	237.888	207.9141	20.6	5.3
38		16.00	76	15.1	7.6	109.44	95.65056	17.6	2.5
39		17.00	35.7	14.8	7.6	51.408	44.93059	16.2	1.4
40		18.00	0.3	14.8	6.9	0.432	0.377568	15	0.2
41									

Top Losses

hs(p1-a)	hp(p1-a)	hv(p1-p2)	hs(abs-p2)	hp(abs-p)	Up	QUp
4.238	27.52	200	0.263	1.971	2.065622	8.923487
4.426	34.65	200	0.264	1.972	2.092846	8.136983
4.257	26.17	200	0.266	1.981	2.070808	10.43687
4.269	30.49	200	0.268	1.983	2.091978	12.95353
4.291	32.43	200	0.271	1.988	2.105679	15.16089
4.31	32.43	200	0.271	1.988	2.105742	16.9807
4.315	29.18	200	0.273	1.992	2.099269	14.20785
4.343	28.19	200	0.281	2.008	2.115909	25.59404
4.352	28.19	200	0.279	2.003	2.109965	19.1416
4.353	30.49	200	0.278	2.001	2.116451	16.15275
4.342	31.47	200	0.273	1.99	2.106084	7.581902
4.332	31.47	200	0.27	1.985	2.099119	4.231823
4.33	29.18	200	0.268	1.981	2.085576	0.600646

Bottom Losses

hs(z1-a)	hp(z1-a)	hv(z1-z2)	hs(abs-z2)	hp(abs-z2)	Uz	Quz
2.327	27.52	0.9	1.795	1.977	0.709357	3.298512
2.334	34.65	0.9	1.796	1.978	0.712697	2.982637
2.342	26.17	0.9	1.816	1.984	0.709551	3.849314
2.532	30.49	0.9	1.837	1.991	0.712948	4.751798
2.37	32.43	0.9	1.865	1.999	0.714977	5.541074
2.385	32.43	0.9	1.887	2.006	0.71597	6.214624
2.39	29.18	0.9	1.875	2.002	0.71392	5.200904
2.408	28.19	0.9	1.957	2.027	0.71695	9.334692
2.418	28.19	0.9	1.925	2.017	0.715584	6.987674
2.42	30.49	0.9	1.909	2.013	0.716092	5.882694
2.414	31.47	0.9	1.854	1.996	0.7141	2.767138
2.406	31.47	0.9	1.828	1.998	0.713267	1.547789
2.406	29.18	0.9	1.8071	1.981	0.710856	0.220365

Quseful	Coll_Eff			Tout
0	#DIV/0!			18
-12.222	-1098%			17.7
-10.23863	53%			18.5
25.48431	72%			19.3
63.34594	78%			20
112.4537	80%			20.6
151.9962	80%			19.7
127.5911	82%			23.4
275.1805	83%			21.3
214.885	83%			20.3
185.8787	82%			17.5
85.30152	81%			16.4
39.15098	-103%			15.2

APPENDIX H: Method of transporting fish



Department Of Mechanical Engineering

Modular Solar Powered Aquaponics System (MSPAS)

**Issues relating to transporting and welfare of fish from the Belhar community centre
to the CPUT Bellville campus**

Date: 20 November 2018

Compiled by:

Name :	Student Number :	Signature :
Fareed Ismail	200736191	
Stijn Burmanje	4458451	
Matthew Schouw	209150998	

Contents

1. Introduction.....	2
2. Quality of fish.....	2
3. Oxygen required	2
4. Water Quality	3
5. Stock fish/water ratio.....	3
6. The system of transport.....	3
7. Before the trip to CPUT	4
8. The loading phase	4
9. The transport	4
10. The unloading phase.....	4
11. Discussion.....	5
12. Procedures.....	5
12.1 Loading phase:.....	5
13. Welfare and monitoring of fish growth	6
13.1 Site conditions:.....	6
13.2 Clinical signs of ill fish will be monitored :	6
13.3 Nutrition:.....	7
13.4 Growth monitoring:.....	7
14 Prevention Strategy for Invasive species into local waters:	7

1. Introduction

The research proof of concept requires fish to be added to the MSPAS. The environment will be adjusted so as to make it comfortable and conducive for the fish.

The Belhar Community Centre are currently farming with tilapia and has agreed to borrow some of their fish to be added to the MSPAS prototype at CPUT BV campus.

This document will serve as a guideline for the transportation and welfare monitoring of the fish.

2. Quality of fish

The fish should be of good quality before they can be transported on long journeys. Weaker fish are less likely to survive (Harmon, 2009). Furthermore, according to the recommendations in (Berka, 1986), the water temperature difference should not be greater than 12-15 °C. Another aspect to take into consideration is the digestive status of the fish: "The fish with full digestive tracts also need more oxygen, are more susceptible to stress and produce excrements which take up much of the oxygen of the water." (Berka, 1986). "Due to this mechanism, feed withdrawal, for 2-4 days before transport, is a way to improve the water quality (Murray, 1986, Hjeltnes et al., 2008) in the transport haul and must be regarded as a best practice" (Rosten, 2011)

3. Oxygen required

Providing the fish an adequate level of oxygen is critical for a good and least stressful way of transport (Harmon, 2009). The level of the oxygen metabolism of the fish is dependent on the weight of the fish and water temperature (Berka, 1986). "From the point of view of fish transport, for each 0.5 °C rise in temperature, the fish load should be reduced by about 5.6%." (Piper, 1982). Furthermore, the amount of oxygen consumed by the fish is also dependent on the level of oxygen available. When there are high levels of oxygen available, fish will consume more oxygen (Berka, 1986). Accordingly, at low levels, the fish will lower their O₂ intake. During transport the oxygen does not fully satisfy, causing the fish to use stored oxygen from within their body. This causes for "an oxygen "debt" which must be repaid when favourable oxygen conditions are experienced." (Berka, 1986).

"Best practice (RSPCA Std.) would recommend enough O₂ available for 150 % of journey requirement." (Rosten, 2011).

4. Water Quality

The quality of the water is dependent on the pH, which is directly influenced by the CO₂ level and proportions of toxic ammonia. Ideally, the pH-level should be neutral (e.g. 7-8) (Hamon, 2009). The longer the transport, the more CO₂ will be emitted causing the pH-level to drop. According to Berka (1986): "If the CO₂ level increases rapidly, as with heavy fish loads, fish become distressed. However, elevated concentrations of CO₂ can be tolerated if the rate of buildup is slow." As previously explained, lowering the digestion of the fish will decrease the excretion rates of the fish. The excretion of NH₃ is also dependent on the metabolism of the fish (Berka, 1986). Lowering the water temperature will decrease the metabolism and therefore the production of the NH₃. According to the Berka (1986): "the generally applicable zones of optimum temperatures for transported fish are 6–8 °C for cold-water fishes and 10–12 °C for warm-water fishes in summer, 3–5 °C for cold-water fishes and 5–6 °C for warm-water fishes in spring and autumn, and 1–2 °C for all in winter." A good ventilation will further limit the risk of a sudden increase in the metabolites (Rosten, 2011).

5. Stock fish/water ratio

The fish/water ratio should also be taken into account. According to Pecha, Berka and Kouril (1983), "parent fish can be transported: water/weight ratio of 1:2 to 1:3, but with smaller organisms this ratio could decrease to 1:100 to 1:200." However, these ratios are also dependent on the kind of fish and the level of activity of the fish. When the fish are being transported, they usually show a large amount of muscular activity (Erikson et al., 1997, Iversen et al., 2005) which requires a large amount of oxygen and thus also more space. Transporting more fish will also require more "muscle-activity" space. Therefore, it is recommended to make the loading process as smooth as possible, without hurting the fish (Rosten, 2011).

6. The system of transport

Transporting live fish can be done in two basic methods: via a closed system (e.g. fish contained in a plastic bag) or an open system (e.g. a container). In a closed system, the sealed surrounding provides the requirements for self-survival, whereas the open system requires external help in the form of supplying oxygen (Berka, 1986). The successful and least stressful

method of transport relies on the quality of the fish, amount of oxygen, water quality and the density of the stock (Berka, 1986). For this research, the fish will be transported a closed system.

7. Before the trip to CPUT

As previously mentioned, it is important to stop feeding the fish 4 days prior to the transport. Also, the water temperature of the fish tank at the Community Centre should be relatively low, so that the fish can be transported in cold water as well (around 15 degrees Celsius). Packing the fish should be done at the latest moment (Rosten, 2011).

8. The loading phase

Because the fish are relatively small (the fingerlings at the Community Centre are a couple of centimetres), it is recommended to transport the fish in a 5-gallon bucket. As a rule of thumb, there should be 25 kilograms of tilapia per 1000L water (Hess, 2018) Assuming that fingerlings weigh around 15 grams, 525 grams of tilapia will be transported to the university. This would require 21 litres of water. The difference of water temperature between the "tank water" and the "transport water" should not be greater than 12-15 degrees. According to Berka (1986), the container to transport the fish should be filled with $\frac{2}{3}$ of water and $\frac{1}{3}$ of oxygen. This would mean that a 30-litre bucket should be filled with 20 litres of water of around 15 °C. When the transport is ready, the fish can be taken out of the fish tank via a fine mesh fish net and transported into the bucket.

9. The transport

Because of the short travel distance (3 kms), there is no need to add extra oxygen to the bucket while driving (Harmon, 2009). The bucket should be placed in a dark and well-supported place, keeping the level of shocks during transport at a minimum. This will be essential for the lowest amount of stress (Berka, 1986).

10. The unloading phase

Unloading fish generate a high stress-response (Erikson et al., 1997) and is the most critical phase of the transport. According to Berka (1986), a new environment with different characteristics (e.g. water temperature, pH-level, amount of gasses, etc.) can cause a level of stress beyond what the fish can stand. It is therefore important to make sure the water quality

and temperature are at the same level as the "transport water". When this is confirmed, the bucket can be placed inside the fish tank underwater, after which the lid can be opened and the fish are free to swim out of the bucket.

11. Discussion

Because of the short travel distance (around 3 kms), the fish will not need extra oxygen and the build-up of CO₂ and NH₃ will be of lesser impact (Hamon, 2009). The most important element is the quantity, quality and temperature of the transported water and the water at the destination. As previously mentioned, these new environments will have a great impact on the metabolism of the fish and therefore directly affect their stress levels.

According to Noga (2000), the stress level of the fish is dependent on the severity and the duration of the stress as well as the health of the fish. Given that the fish at the Community Centre are in good health and the travel distance is relatively short, the level of stress can be reduced to a minimum, keeping the water quality in mind.

12. Procedures

The fish growth monitoring will take place from January to April 2019. The fish will be transported from the community centre in Belhar to the CPUT Bellville campus which spans a distance of less than 3 kms. Due to the short distance it is recommended to use a closed transport system. Transporting the fish will be done in three phases: the loading, transport and the unloading.

12.1 Loading phase:

- Stop feeding the fish 4 days prior to the transport. The water temperature of the fish tank at the Community Centre should be approximately 15 °C.
- Packing the fish should be done just prior to transporting using a fine mesh fish net. The fine mesh will prevent fins and spines from being tangled in the net.
- 35 fish fingerlings will be loaded into an 80 litre container of which the lid will be sealed with a minimum 50mm air gap between the water and the lid. External oxygen supply is not required due to the short travel distance. It is important to seal the lid tightly, so no fish or water can escape during the transport.

12.2 Transport phase:(Cheng & Hammond, 2017)

- The transport of the fish will be done by the community leaders SUV.
- Stress during the transportation will be minimized by placing the bucket in a dark and secure place and ensuring an ease of transport to prevent water splashing.

12.3 Unloading phase:

- The water quality and temperature of the water in the new environment should be of a similar quality as the transport water.
- The container with the fish will be immersed in the new tank at CPUT BV allowing them to swim out freely.

13. Welfare and monitoring of fish growth

The Welfare and monitoring of fish growth were based on the literature by (Johansen et al., 2006; Martins et al., 2012) as guidelines.

13.1 Site conditions:

- Water levels to be consistently monitored daily.
- Water clarity/turbidity
- The following water conditions will be measured by using a standard pool test kit on a weekly basis:
 - pH levels should be between (7-8) neutral
 - Acidity
 - Alkalinity
 - Chlorine content should be zero
- Temperature of the water will be monitored and adjusted gradually to the comforted levels required for the fish.

13.2 Clinical signs of ill fish will be monitored :

- Fish swimming on their sides and erratically.
- Colour change and fin/appendage loss
- Mucous on fins: indicates the presence of pathogens

- Aggression: fish attacking one another or being territorial.
- An indication of low dissolved oxygen will show when the fish starts gasping at the surface of the water. To ensure the prevention of low dissolved oxygen the system allows for continuous flow of water and siphoning through the grow bed. This system has been proven adequate at the community centre. Additional air pumps can be added if required.
- Sick fish will be quarantined while being treated or medicated.

13.3 Nutrition:

- The fish will be fed commercially available fish feed.
 - Fish will be fed twice per day after sunrise and before sunset.
 - Fish feed for tilapia must contain 25 % protein.
 - 5 - 10 g of tilapia fingerlings require 10 – 5% feed of bio mass.

13.4 Growth monitoring:

- A water filled transparent container will be weighed and thereafter the fish placed inside measuring the difference to determine the fish weight before placing into the tank and at the end of the trial.
- The growth length of the fish will be determined on averaged by placing a grid-marked base in the tank and allowing the fish to swim over the 20 mm square markings and photographing them on a weekly basis.

14 Prevention Strategy for Invasive species into local waters:

The information used to educate the relevant individuals will be disseminated using the following documents:

- *Risk assessment for Nile tilapia Oreochromis niloticus in South Africa*
- *Introduction To Invasive Alien Species*

The following strategies will be implemented:

- Verbal communication

The community leader will be educated regarding the implications of foreign fish into local waters and dams.

- Visual Display

A4 Signs will be designed and displayed around the MSPAS prototype at CPUT and at the community center to inform individuals and students that the Tilapia should not be removed and introduced into local waters.

Bibliography

Berka, R. (2018). The transport of live fish A review. EIFAC TECHNICAL PAPER, [online] 48. Available at: <http://www.fao.org/docrep/009/af000e/af000e00.htm#TOC> [Accessed 20 Nov. 2018].

Cheng, V.K.M. & Hammond, G.P. 2017. Life-cycle energy densities and land-take requirements of various power generators: A UK perspective. *Journal of the Energy Institute*, 90(2): 201–213. <http://dx.doi.org/10.1016/j.joei.2016.02.003>

Erikson, U., Sigholt, T. and Seland, A. (1997). Handling stress and water quality during live transportation and slaughter of Atlantic salmon (*Salmo salar*). *Aquaculture*, 149(3-4), pp.243-252.

Harmon, T. (2009). Methods for reducing stressors and maintaining water quality associated with live fish transport in tanks: a review of the basics. *Reviews in Aquaculture*, [online] 1(1), pp.58-66. Available at: <http://citeseerx.ist.psu.edu/viewdoc/download?doi=10.1.1.502.4939&rep=rep1&type=pdf> [Accessed 19 Nov. 2018].

Hess, J. (2018). *How many tilapia can I stock my tank with? – Ichthys Aquaponics*. [online] ichthysaquaponics.co.za. Available at: <https://www.ichthysaquaponics.co.za/how-many-tilapia-can-i-stock-my-tank-with/> [Accessed 20 Nov. 2018].

Introduction To Invasive Alien Species.

http://www.issg.org/pdf/publications/GISP/GISP_TrainingCourseMaterials/Management/ManaginginvasivesModule1.pdf[Accessed 04 Dec. 2018].

Johansen, R., Needham, J.R., Colquhoun, D.J., Poppe, T.T. & Smith, A.J. 2006. Guidelines for health and welfare monitoring of fish used in research. *Laboratory Animals*, 40(4): 323–340.

Martins, C.I.M., Galhardo, L., Noble, C., Damsgård, B., Spedicato, M.T., Zupa, W., Beauchaud, M., Kulczykowska, E., Massabuau, J.C., Carter, T., Planellas, S.R. & Kristiansen, T. 2012. Behavioural indicators of welfare in farmed fish. *Fish Physiology and Biochemistry*, 38(1): 17–41.

Noga EJ (2000) *Fish Disease: Diagnosis and Treatment*. Iowa State University Press, Ames

Piper, R. G. (1982). *Fish hatchery management*. Washington, D.C.: U.S. Gov. Print. Off.

Rosten, T. W. (2011). Transport of Live Fish. *Aquaculture Engineering*, 256-265. doi:10.1002/9780470995945.ch18

Risk assessment for Nile tilapia Oreochromis niloticus in South Africa
https://www.environment.gov.za/sites/default/files/docs/niletilapia_riskassessment.pdf
[Accessed 04 Dec. 2018].

APPENDIX I: PV specifications



SETSOLAR M2200P HIGH EFFICIENCY PHOTOVOLTAIC SOLAR MODULE

SETSOLAR assembles its own photovoltaic modules using guaranteed and certified materials.

This module meets industry standards for consumer safety and reliability and is covered by a comprehensive 20 year warranty.

Low-iron tempered glass is designed to resist impact and increase light transmittance, thus improving daily power generation.

Encapsulating the solar cells between Tempered Glass / EVA / Tedlar guarantees a durable protection for the cells during extreme weather conditions.

The strong aluminium frame with pre-drilled mounting holes allow for easy installation.

Each solar module is equipped with a pre-wired IP65 junction box, which includes MC equivalent connectors and protective bypass diodes.

Furthermore is each solar module submitted to an individual quality inspection, certifying product quality and output power performance.

Modules designed and manufactured according to IEC 61215 & IEC 61730 standards.

APPLICATIONS

- Water pumping
- Rural Electrification
- Telecommunication
- Billboard illumination
- Grid Connection Systems

CONTACT US

Unit 8, 98b Bofors Circle, Epping Ind. 2
Cape Town, South Africa, 7460
Tel: 021 535 1978 or 021 535 1741
Admin Fax: 021 534 0233
Sales Fax: 021 534 5730
Int: +27 21 535 1978
Info@setsolar.co.za
www.setsolar.co.za



Issued: FEB 2012



*Image for illustration purposes only

** Data sheet in accordance with the industry requirements - EN50530

SETSOLAR M2200P

TYPICAL PERFORMANCE CHARACTERISTICS								
Typical power (Wp)	195	200	205	210	215	220	225	230
Tolerance (%)	± 5%							
Voltage at max.power (V)	27.0	27.2	27.4	27.7	28.0	28.3	28.5	28.8
Current at max.power (A)	7.20	7.40	7.50	7.60	7.70	7.8	7.90	8.00
Open circuit voltage (Voc)	33.2	33.4	33.6	33.8	34.0	34.4	34.6	34.9
Short circuit current (Isc)	7.60	7.80	8.00	8.10	8.20	8.30	8.40	8.50

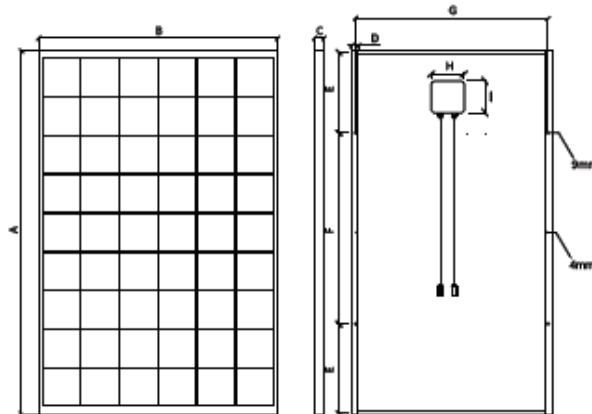
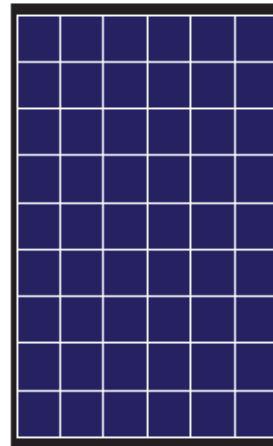
Standard test conditions: 1000W/m², AM1.5G and 25 degree C

TEMPERATURE COEFFICIENTS	
Voltage	-115.30mV / degree C
Current	+4.50mA / degree C
Power	-0.46% / degree C
NOCT (degrees)	45

CELLS	
Type	Texturized multicrystalline
Dimensions	156mm x 156mm
Layout	54 cells (6rows x 9cells)

GENERAL INFORMATION	
Maximum System voltage	840V
Diodes	3 x 10A bypass
Type of connection	Pre-wired IP65 junction box with MC equivalent connectors
Frame	35mm black anodized aluminium
Weight (kg)	20
Packaging	2 modules per carton box

WARRANTY	
Product	5 years
Power output	Terrestrial: 20 years / 80% yield Marine: 10 years / 90% yield



DIMENSIONS	
A	1480
B	991
C	35
D	30
E	340
F	800
G	947
H	93
I	93

Dimensions in mm
(tolerance ±4mm)

SETSOLAR reserves the right to modify all data without notice, due to continuous product development.



APPENDIX J: Charge controller specifications

SOLARLADEREGLER

Steca
ELECTRONIK

Steca PR

1010, 1515, 2020, 3030

Die Steca PR 10-30-Laderegler-Serie ist das Highlight unter den Solarladeregler. Die neuesten Ladetechnologien verbunden mit einer Ladezustandsbestimmung ergeben eine optimale Batteriepflege und Kontrolle. Ein großes Display informiert den Nutzer mit Hilfe von Symbolen über alle Betriebszustände. Der Ladezustand wird in der Art einer Füllstandsanzeige visuell dargestellt. Daten wie z. B. Spannung, Strom und Ladezustand können auch digital als Zahl auf dem Display angezeigt werden. Zudem verfügt der Regler über einen Energiezähler, den der Nutzer selbst zurücksetzen kann.

CLASSIC



Produktmerkmale

- Shunt-Topologie mit MOSFETs
- Ladezustandsberechnung durch Steca AtonIC (SOC)
- Automatische Spannungsanpassung
- PWM-Regelung
- Mehrstufige Ladetechnologie
- SOC-abhängige Lastabschaltswelle
- Automatische Lastabschaltung und -wiedereinschaltung
- Temperaturkompensation
- Negative Erdung einer oder positive Erdung mehrerer Klemmen möglich
- Integrierter Datenlogger (Energiezähler)
- Abend-, Nacht- und Morgenlichtfunktion
- Selbsttestfunktion
- Monatliche Ausgleichsladung

Elektronische Schutzfunktionen

- Überladeschutz
- Tiefentladeschutz
- Verpolschutz von Modul, Last und Batterie
- Automatische elektronische Sicherung
- Kurzschlusschutz von Last und Modul
- Überspannungsschutz am Moduleingang
- Leerlaufschutz ohne Batterie
- Rückstromschutz bei Nacht
- Übertemperatur- und Überlastschutz
- Lastabschaltung bei Batterieüberspannung

Anzeigen

- Grafiq-LC-Display
- für Betriebsparameter, Störmeldungen, Selbsttest

Bedienung

- Einfache menügeführte Bedienung
- Programmierung durch Tasten
- Manueller Lastschalter

Optionen

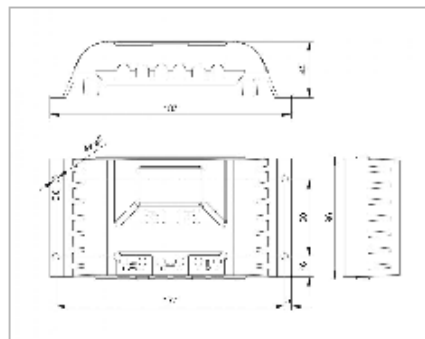
- Alarmkontakt

Zertifikate

- Weltbankzertifikat für Nepal
- CE-konform
- RoHS-konform
- Made in EU
- Hergestellt unter ISO 9001 und ISO 14001

Zubehör

- Externer Temperatursensor Steca PA TS10



	PR 1010	PR 1515	PR 2020	PR 3030
Charakterisierung des Betriebsverhaltens				
Systemspannung	12 V (24 V)			
Eigenverbrauch	12,5 mA			
DC-Eingangsspannung				
Leerlaufspannung Solarmodul (bei minimaler Betriebstemperatur)	< 47 V			
Modulstrom	10 A	15 A	20 A	30 A
DC-Ausgangsspannung				
Laststrom	10 A	15 A	20 A	30 A
Wiedereinschaltspannung (SOC / LMR)	> 50 % / 12,8 V (5,2 V)			
Tiefentladeschutz (SOC / DVD)	< 30 % / 11,1 V (2,2 V)			
Batteriewerte				
Ladenspannung	13,9 V (27,8 V)			
Bocilladenspannung	14,4 V (28,8 V)			
Ausgleichsladung	14,7 V (29,4 V)			
Eingestellter Akkutyp	flüssig (einstellbar über Menü)			
Umgebungsbedingungen				
Umgebungstemperatur	-10 °C ... +50 °C			
Ausstattung und Ausführung				
Anschlußklemmen (Ein- / einzeileitig)	16 mm ² / 25 mm ² - AWG 6 / 4			
Schutzart	IP 31			
Abmessungen (K x Y x Z)	187 x 96 x 44 mm			
Gewicht	350 g			

- Technische Daten bei 25 °C / 77 °F
- Wechselrichter dürfen nicht an den Lastausgang angeschlossen werden.

Version 2019-03-29 13:12

Steca Elektronik GmbH | Mammostraße 1 | 87700 Memmingen | Germany | info@steca.de | www.steca.de

APPENDIX K: Inverter specification



2 Samantha Street, Strijdom Park, Randburg, Johannesburg, 2194
 Tel: (+27) 11 896-7874 | Fax: (+27) 11 767 0178
 sales@sinotech.co.za | www.sinotech.co.za

COTEK S-SERIES PURE SINE WAVE INVERTER 1500W

FEATURES:

- Pure sine wave output (THD < 3%)
- RS-232 interface / Remote control port
- Input & output fully isolated
- Thermo controlled fan
- Output Voltage & Frequency can be adjusted by means of a DIP switch
- Input Protection: Reverse Polarity (Fuse) / Under Voltage / Over Voltage
- Output Protection: Short Circuit / Overload / Over Temperature
- Built-in LED indicator for battery voltage & power status
- Power saving mode to conserve energy
- UL approved



	S1500-112	S1500-124	S1500-148	S1500-212	S1500-224	S1500-248
OUTPUT						
AC Voltage	100 / 110 / 120VAC ±5%			220 / 230 / 240VAC ±3%		
Rated Power	1500W					
Surge Power	2000W					
Wave Form	Pure sine wave (THD < 3%)					
Frequency	50 / 60 Hz ± 0.05%					
Voltage Regulation	100 / 110 / 120 V RMS -10% / +4%			220 / 230 / 240 V RMS -10% / +4%		
Peak Current	25A			11A		
Power Factor Allowed	COSφ-90° ~ COSφ+90°					
Standard Receptacles	NEMA5-15R / GFCI			Schuko / UK / Australia / Universal		
Led Indicator	Input voltage level, output load level and fault status					
INPUT						
No Load Current Draw	0.87A	0.43A	0.23A	0.83A	0.43A	0.22A
DC Voltage	12VDC	24VDC	48VDC	12VDC	24VDC	48VDC
Voltage Range	10.0-16.0VDC	20.0-32.0VDC	40.0-62VDC	10.0-16.0VDC	20.0-32.0VDC	40.0-62VDC
Efficiency (typ.)	87.0%	90%	92.0%	90%	93%	94%
Fuse	35A x 2	20A x 2	10A x 2	35A x 2	20A x 2	10A x 2
Remote Control	By external switch					
PROTECTION						
Bat. Low Alarm	10.2VDC	20.4VDC	41.6VDC	10.2VDC	20.4VDC	41.6VDC
Bat. Low Shutdown	9.5V	19.3VDC	38.6VDC	9.5V	19.3VDC	38.6VDC
Over Load	Shut off output voltage, restart to recover					
Over Voltage	17.1VDC	34.1VDC	63.0VDC	17.1VDC	34.1VDC	63.0VDC
Over Temperature	Shut off output voltage, recovers automatically after temperature goes down					
Output Short	Shut off output voltage, restart to recover					
DC Input Reverse Polarity	By fuse					
ENVIRONMENT						
Working Temp.	0 ~ +40°C					
Working Humidity	20% ~ 90% RH non-condensing					
Storage Temp. & Humidity	-30C ~ +70°C, 10 ~ 95% RH					
SAFETY & EMC						
Safety Standards	Certified UL458 (only for "GFCI" receptacles)			****		
Isolation Resistance	IP - Q/P: 100M Ohms / 500VDC					
EMI Conduction & Radiation	****			****		
EMS Immunity	****			****		
GENERAL	S1500-112	S1500-124	S1500-148	S1500-212	S1500-224	S1500-248
Dimension	274 x 101 x 378.8mm (W x H x D)					
Packing	8.16kgs; 2pcs / 17.3kgs / 2.55CUFT					
Cooling	Load controlled fan					
Application	Home and Office appliances, Power tools and Portable equipments, Vehicle, Yacht and off-grid Solar power systems ...etc.					

APPENDIX L: Anemometer



Kestrel[®]
Kestrel Weather Meters
Model Numbers 1000-3500



**Certificate of
Conformity**

This instrument was produced under rigorous factory production control and documented standard procedures. It was individually inspected and leak tested and the functioning of the display, backlight, buttons and firmware was verified. The accuracy of each of its primary measurements was individually calibrated and/or validated against standards traceable to the National Institute of Standards and Technology ("NIST") or other calibrated standards in accordance with the documented standard test methods detailed below. This instrument is warranted to perform in compliance with the published specifications for the specific measurements and features of its model number including specified typical drift since its date of manufacture. (See *Kestrel Limited Warranty* for full warranty terms.)

<p>Standards Used in Testing</p> <p>Wind Speed: The Kestrel Weather & Environmental Meter impeller installed in this unit was individually tested in a subsonic wind tunnel operating at approximately 300 fpm (1.5 m/s) and 1200 fpm (6.1 m/s) monitored by a Gill Instruments Model 1350 ultrasonic time-of-flight anemometer. The Gill 1350 is calibrated regularly and is traceable to NIST with a maximum combined uncertainty of $\pm 1.04\%$ within the airspeed range 711.4 to 3930 fpm (3.61 to 19.96 m/s), and $\pm 1.66\%$ within the airspeed range 170 to 711.4 fpm (0.86 to 3.61 m/s).</p> <p>Temperature: Temperature response is verified in comparison with an Ametek DTI-050 Digital Temperature Indicator and STS Reference Sensor. The DTI-050 is calibrated annually and is traceable to NIST with a maximum relative expanded uncertainty of $\pm 0.04\text{C}$.</p>	<p>Relative Humidity: Relative humidity is verified in comparison with an Edgetech HT120 Humidity Transmitter. The HT120 is calibrated annually and is traceable to NIST with a maximum relative expanded uncertainty of $\pm 1.0\%RH$.</p> <p>Barometric Pressure: Pressure response is verified against a Vaisala PTB210A Digital Barometer. The Vaisala Barometer is calibrated annually and is traceable to NIST with a maximum relative expanded uncertainty of $\pm 0.3hPa$.</p>
--	--

Approved By:

Michael Naughton
Chief Product Officer, Nielsen-Kellerman

© 2020. The enclosed Kestrel Weather Meter was manufactured by Nielsen-Kellerman Co. at its facilities located at 21 Creek Circle, Boothwyn, PA 19061 USA.

Product Specifications for Kestrel Weather Meters, Model Numbers 1000-3500

SENSORS				
SENSOR	ACCURACY (+/-)	RESOLUTION	SPECIFICATION RANGE	NOTES
Wind Speed (Air Speed)	Larger of 3% of reading, least significant digit or 20 ft/min	0.1 m/s 1 ft/min 0.1 km/h 0.1 mph 0.1 knots 1 ft	0.6 to 40.0 m/s 118 to 7,874 ft/min 2.2 to 144.0 km/h 1.3 to 89.5 mph 1.2 to 77.8 knots 0 to 12 ft	1 inch (25 mm) diameter impeller with precision axle and low-friction Zytel® bearings. Startup speed stated as lower limit, readings may be taken down to 0.4 m/s (79 ft/min) (1.5 km/h) (9 mph) (0 ft) after impeller startup. Off-axis accuracy: -1% @ 5° off axis; -2% @ 10°; -3% @ 15°. Calibration drift < 1% after 100 hours use at 16 MPH (7 m/s). Replacement impeller (NK-PN-0801) field installable without tools (US Patent 5,783,793). Wind speed calibration and testing should be done with triangle on impeller located at the top front face of the Kestrel. Measuring wind speeds above 60 m/s / 134.2 mph can damage the impeller.
Ambient Temperature	0.9 °F 0.5 °C	0.1 °F 0.1 °C	-20.0 to 158.0 °F -29.0 to 70.0 °C	Airflow of 2.2 mph (1 m/s) or greater provides fastest response and reduction of insulation effect. For greatest accuracy, avoid direct sunlight on the temperature sensor and prolonged sunlight exposure to the unit in low airflow conditions. Calibration drift is negligible for the life of the product. For further details, see Display & Battery Operational Temperature Limits.
Relative Humidity	3%/RH	0.1 %RH	5 to 95% 25°C non-condensing	To achieve stated accuracy, unit must be permitted to equilibrate to external temperature when exposed to large, rapid temperature changes and be kept out of direct sunlight. Calibration drift is typically less than ±0.25% per year.
Pressure	1.5 hPa/mbar 0.044 inHg 0.022 PSI	0.1 hPa/mbar 0.01 inHg 0.01 PSI	25°C/77°F 750-1100 hPa/mbar 22.15-32.49 inHg 10.86-15.95 PSI	Monolithic silicon piezo-resistive pressure sensor with second-order temperature correction. Between 1100-1600 mbar, unit will operate with reduced accuracy. Sensor may not operate above 1600 mbar and can be damaged above 6,000 mbar or below 10 mbar. Calibration drift is negligible for the life of the product.

CALCULATED MEASUREMENTS			
MEASUREMENT	ACCURACY (+/-)	RESOLUTION	SENSORS EMPLOYED
Altitude	Typical: ±0.8 ft/2 m from 750 to 1100 mBar max: ±6.2 ft/14.7 m from 300 to 750 mBar	1 ft 1 m	Pressure, User Input (Reference Pressure)
Barometric Pressure	0.07 inHg 2.4 hPa/mbar 0.03 PSI	0.01 inHg 0.1 hPa/mbar 0.01 PSI	Pressure, User Input (Reference Altitude)
Delta T	3.2 °F 1.8 °C	0.1 °F 0.1 °C	Temperature, Relative Humidity, Pressure
Dew Point	3.4 °F 1.9 °C 15-25% RH. Refer to Range for Temperature Sensor	0.1 °F 0.1 °C	Temperature, Relative Humidity
Heat Index	7.1°F 4.0°C	0.1 °F 0.1 °C	Temperature, Relative Humidity
Wet Bulb Temperature - Psychrometric	3.2 °F 1.8 °C	0.1 °F 0.1 °C	Temperature, Relative Humidity, Pressure
Wind Chill	1.6 °F 0.9 °C	0.1 °F 0.1 °C	Wind Speed, Temperature

ADDITIONAL PRODUCT INFO	
Display	Reflective LCD
Backlight	Standard or dim red (NV models only) backlight. Manual activation with auto-off.
Response Time & Display Update	Display updates every 1 second. After exposure to large environmental changes, all sensors require an equilibration period to reach stated accuracy. Measurements employing RH may require longer periods particularly after prolonged exposure to very high or very low humidity.
Auto Shutdown	After 45 minutes with no key presses.
Clock	Real Time Hour-Minute Display
Certifications	CE certified, RoHS and WEEE compliant. Individually tested to NIST-traceable standards.
Origin	Designed and manufactured in the USA from US and imported components. Complies with Regional Value Content and Tariff Code Transformation requirements for NAFTA Preference Criterion B.
Bluetooth Data Connect	Wireless range up to 100ft. Employs Kestrel Link protocol for data transmission with Kestrel Link BetaLite App. (iOS/Android)
Battery	Requires one CR2032 battery, included. Up to 300 hours of use, reduced by backlight or Bluetooth use.
Shock Resistance	MIL-STD-883C, Thrust Shock, Method 516.7 Procedure IV, unit only; impact may damage replaceable impeller.
Sealing	Waterproof (IP67 and NEMA-6)
Display & Battery Operational Temperature Limits	14° F to 131° F -10 °C to 55 °C Measurements may be taken beyond the limits of the operational temperature range of the display and batteries by maintaining the unit within the operational range and then exposing it to the more extreme environment for the minimum time necessary to take reading.
Storage Temperature	-22.0 °F to 140.0 °F -30.0 °C to 60.0 °C
Size & Weight	4.8 x 1.9 x 1.1 in 12.2 x 4.8 x 2.8 cm, 3.6 oz 102 g (including slip-on cover).

*Note: Accuracy calculated as uncertainty of the measurement derived from statistical analysis considering the combined effects from primary sensor specifications, circuit conversions, and all other sources of error using a coverage factor of k=2, or two standard deviations (2σ)

**Note: For Kestrel 1000, 2000, 2500, 3000, 3500 series these specifications are valid for units with a serial number higher than 2262687. If your product has a lower serial number, please reference the K4000 specifications 329011.

329001_3_02.10.2020

APPENDIX M: Community report

 Cape Peninsula University of Technology

 TU Delft Delft University of Technology

Department Of Mechanical Engineering

Community Engagement

Belhar Early Childhood Development Centre (BECDC) Progress Report



BELEAF
GROWERS
aquaponic farm

Compiled by:
Matthew Schouw, Fareed Ismail and Christian Hartzenberg (CPUT & BECDC)

Compiled for:
Douwe Schoemaker, Nina van Savooijen and Stijn Burmanje (NGO Beleaf)

Date: May 2019

1

Contents

Contents	2
1. Introduction	3
Section One: Financial Progress:	4
2.1 Sales	4
2.1.2 Selling Price Comparison	5
2.2 Expenses:	6
2.3 Income:	7
Section Two: Aquaponics System Progress:	8
3.1 Vegetation	8
3.2 Aquaculture	10
Section Three: Educational progress	11
Section Four: Additional Progress:	12
4.1 Solar Water Heating	12
4.2 Trials and Tribulations	12
5. Conclusion	13
6. Appendices	14

1 • Introduction

The Cape Peninsula University of Technology.(CPUT)is a university located in Cape Town South Africa and runs a project called The Modular Solar Powered Aquaponic System (MSPAS) which was incepted in 2011 by Fareed Ismail from the Mechanical Engineering Department . He currently supervises the two systems: a prototype at the university and a system at the Belhar Early Childhood Development Centre (BECDC). The prototype is used for experimenting and research purposes such as integrating renewable energy solutions to the systems. The system at the BECDC provides financial and educational value to the centre which is managed by Christiaan and Maria Hartzenberg.

Scope :

The main aim of this report is to indicate the current situation and progress of the MSPAS system is located at Belhar Early Childhood Development Centre (BECDC) to update NGO Beleaf

This report is divided into the following sections:

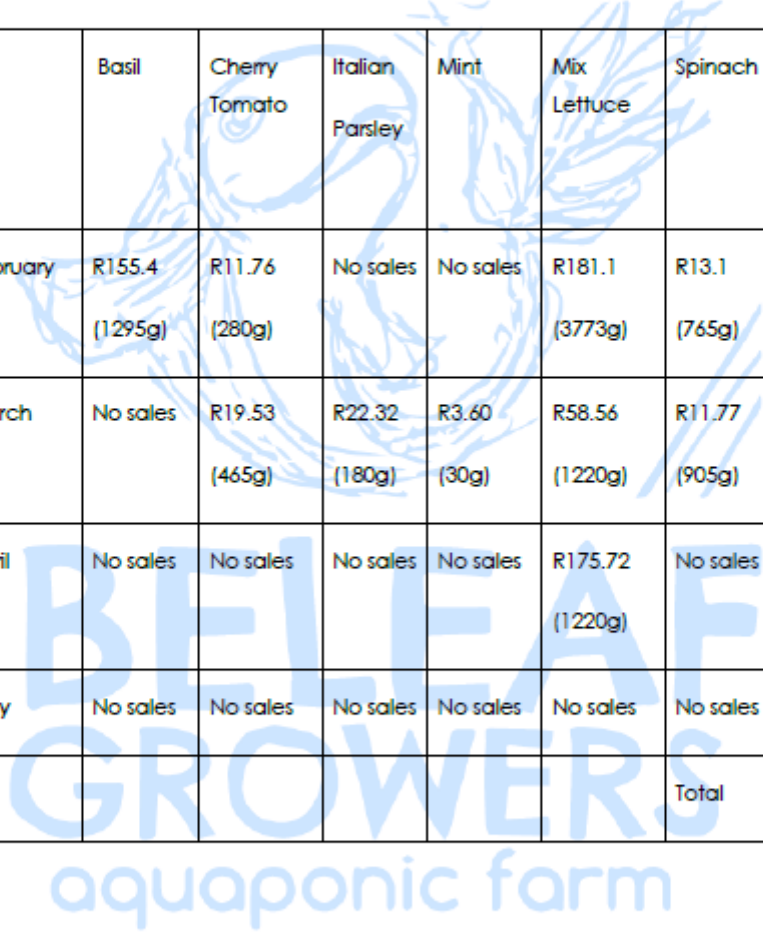
- Section One :Financial Progress
- Section Two:Aquaponic System Progress
- Section Three :Educational progress
- Section Four :Additional progress

Section One: Financial Progress:

2.1 Sales

Mr .Hartzenberg uses a excel spreadsheet to track any sales to any clients. See Appendix A. The current sales for the months of January – May 2019 is summarised below:

	Basil	Cherry Tomato	Italian Parsley	Mint	Mix Lettuce	Spinach	Total Sales for the Month
February	R155.4 (1295g)	R11.76 (280g)	No sales	No sales	R181.1 (3773g)	R13.1 (765g)	R193.52
March	No sales	R19.53 (465g)	R22.32 (180g)	R3.60 (30g)	R58.56 (1220g)	R11.77 (905g)	R115.78
April	No sales	No sales	No sales	No sales	R175.72 (1220g)	No sales	R175.72
May	No sales	No sales	No sales	No sales	No sales	No sales	
						Total	R485.08



2.1.2 Selling Price Comparison

The total sales for the 5 months is R485.08 .however, if you look at prices from retailers there is a major disparity. For instance, if you compare the price of the average mint basil and parsley per gram in Table 1 i.e ; R 0.375/gram from your standard retailers to the sale price of the community sat R 0.12/gram. This a percentage difference of 68%.However, lettuce is sold at a higher at price at 56% more than retail price.

Retailer Prices are Appendix C

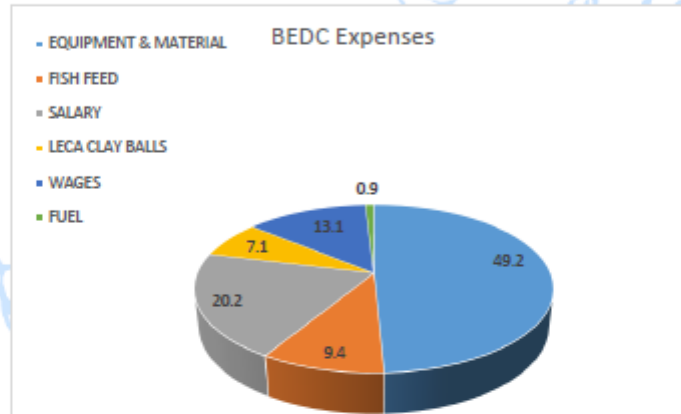
Vegetable	Community Price R /gram	Retailer Price R /gram	% Difference
Mint	0.12	0.375	68
Basil	0.12	0.375	68
Parsley	0.12	0.39	69
Lettuce	0.048	0.021	56

BELEAF
GROWERS
aquaponic farm

2.2 Expenses:

Similarly, the community expenses are tracked by a excel spreadsheet. See Appendix B.

- Expenses from the December to April 2019.



Based on the graph, it can be seen that majority of the expenses (50%) are used for operational, maintenance and upgrade of costs of the aquaponics system. Labour costs i.e. Wages and Salary which is (33%) is the second highest. Fish feed followed with 9.4%, the remaining expenses were for LECA clay balls and fuel. The individual cost for each expense is in Table 1 below.

Table 1: Expense Cost Breakdown

ITEM	AMOUNT
EQUIPMENT & MATERIAL	R 38559.4
FUEL	R700
WAGES	R 10300
SALARY	15800
FISH FEED	7379.22
LECA CLAY BALLS 8 - 16MM	R 5600
TOTAL	R 77638.62

2.3 Income:

The income for this expenditure was contributed from the NETHERLANDS CONSULATE (R15 000) & STUDENTS4SUSTAINABILITY by the TU Delft students (R8650) during December 2018 and again in January from the STUDENTS4SUSTAINABILITY (R31350).

DATE	INCOME SOURCE	AMOUNT (Rands)
DEC 2018	NETHERLANDS CONSULATE	15 000
DEC 2018	STUDENTS4SUSTAINABILITY	8650
JAN 2019	STUDENTS4SUSTAINABILITY	31350
FEB-APRIL 2019	AQUAPONICS SALES	485
	Total	R55485

2.4 Profit:

INCOME	EXPENSES
R55485	R77638.62
Profit :	- R 22153

- Currently, the community is running at loss of R22153 based on this analysis

BELEAF
GROWERS
aquaponic farm

Section Two: Aquaponics System Progress:

3.1 Vegetation

The community has 10 grow beds in total with sizes 300mm in height , base 1200 X 1000mm filled 16mm LECA clay balls. Currently in the grow beds 1,2,3,4,5 ,6,(Figure 1, 2 & 3) and 10 are filled with soup and table celery as per PURE GOOD requirements and was planted in March whereas in grow bed 7 and 9 is filled with mixed lettuce(Figure 3) which was also planted in March. The celery is expected to be harvested early June and the lettuce at the end of May. Thereafter, more lettuce will be planted as per PURE GOOD requirements.

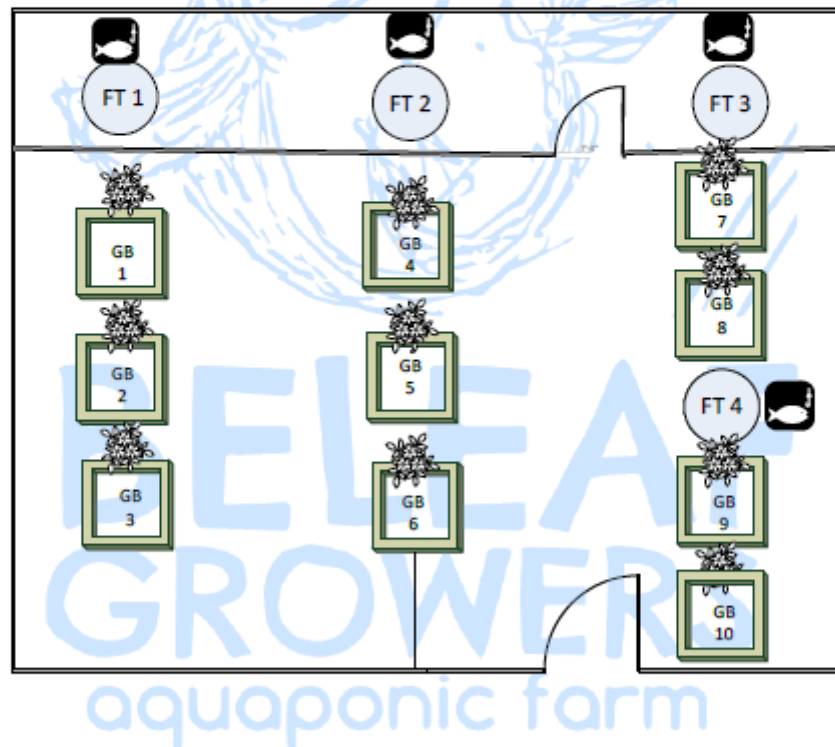


Figure 1: Schematic of Aquaponics (April 2019)



Figure 2 : Overview of Grow Beds (April 2019)



Figure 3: Celery in Growbeds(April 2019)

BEEF
GROWERS
aquaponic farm



Figure 4 : Lettuce Grow Beds (April 2019)

3.2 Aquaculture

There are four fish tanks at the community, with sizes 1100mm in height, base 1200 X 1000mm. The fish tanks house ,predominately Nile Tilapia (approximately 80%) and Mozambican Tilapia . In Fish tank 2 and 3 Nile Tilapia and in Fish tank 1 Mozambican Tilapia are present .The exact quantity of fish is not known and further plans are being developed to determine the amount and weight of the fish .



Figure 5 : Nile Tilapia in Fish tanks(April 2019)

Section Three: Educational progress

The aquaponics system is also used for educational purposes at the BEDC. There is no set curriculum for the children, however, a specified routine is conducted. For instance , when it's time for planting and harvesting of vegetation and every consecutive morning the children are allowed to feed the fish.



Figure 6: Children planting seeds at the Aquaponic system(May 2019)



Figure 7: Children feeding the Tiplia fish in Aquaponic system(May 2019)

Section Four: Additional Progress:

4.1 Solar Water Heating

A evacuated tube solar water heater was commissioned by CPUT to the community during May ,however , the systems still requires piping , pumps and timers to be incorporated so that the system can be fully operational. Moreover, after the installation about 8 fish died. Currently, an investigation is being held to determine the cause of this situation



Figure 8: Evacuated Tube solar water heating system (May 2019)

4.2 Trials and Tribulations

- Initiated the system with old basil plants but was not edible due to hardy taste
- Basil results in excess yield which results wastage and profit loss
- Tomatoes and Cucumber were planted but was not successful and thus requires more expertise/control to grow properly
- Peppers, Rocket and Italian Parsley are grown in the soil as there is lack of grow beds.
- Water Temperature was not adequate which resulted in longer fish and plant growth, this is due to inefficient water heating system. Moreover, celery stems were taller not thicker as expected.

5. Summary

During the period of Jan-May, the system only produced R485.08 for vegetation sales and received income from the NETHERLANDS CONSULATE and STUDENTS4SUSTAINABILITY . Majority of the expenses/overheads are for operational, maintenance and upgrade of costs of the aquaponics system. Moreover, the current system is still not profitable with the community is running at loss of R22153.

In terms of selling price, there is a percentage difference of 68% between the community and retailer price for vegetation sales.

In terms of vegetation, Mostly Celery is currently in the grow beds and expected to sold in June. Peppers, Rocket and Italian Parsley are currently grown in the soil as there is lack of grow beds.

An evacuated tube solar water heater was commissioned to the community, which will heat water for the fish and reduce electricity consumption. However, further research is being undertaken to ensure the correct implementation.

Recommendations:

- The community needs to increase their sale price to increase profits
- More grow beds need to be installed to ensure more probability and to grow Peppers, Rocket and Italian Parsley
- An alternative energy system needs to be designed and commissioned for the aquaponics system
- A crop management plan will need to be developed
- A more accurate method to determine the quantity and weight of fish
- The Tilapia fish is not currently sold ,this could further increase profits
- Development of more educational materials for children at the BEDC

aquaponic farm

6. Appendices

Appendix A: Sales Spreadsheet

Beleaf Aquaponics Sales Report Feb - Mar 2019										
Sale #	2	3	4	5	6	7	8	9	Total	
date	05-Feb	13-Feb	27-Feb	05-Mar	13-Mar	10-Apr	16-Apr	25-Apr	weight (R)	
lettuce (R)	1500	1100	573	1045	95	2600	1070	1225	9888	474.62
lettuce (R)	72	816	27.5	50.19	8.4			58.0		
basil (g)	206	860	245						1295	
basil (R)	24	102	23.4						155.4	
cherry tomat (R)	90		30	140	325				745	
cherry tomat (R)	3.78		7.19	5.68	11.55				31.23	
spinach (g)		450	315	680	225				1670	
spinach (R)		3	4.1	8.64	2.33				24.07	
mint (g)										
mint (R)					30				30	
mint (R)					3.6				3.6	
italian parsley (g)										
italian parsley (R)				85	85				170	
italian parsley (R)				11.38	11.54				22.92	
grand tot.									16808	712.1

Appendix B: Income and Expense Spreadsheet

BELEAF AQUAPONICS GROWERS							
INCOME			EXPENSE				
DATE	RECEIVED FROM	AMOUNT	DATE	SUPPLIER	REF	ITEM	AMOUNT
10	NETHERLANDS CONSUL	15000	10	SASOL HINDLE ROAD	1208484	FUEL	200
21	STUDENTS4SUSTAINAB	8850	11	EFFAST	INV484079	EQUIPMENT & MATER	316.9
			11	MY AQUAPONICS		EQUIPMENT & MATER	6350 (oleg)
			12	BUILT IT BEL-HAR	#335235	EQUIPMENT & MATER	498
			12	BUILDERS	CS375574	EQUIPMENT & MATER	35.8
			12	CFRUMS & CONTAINERS		EQUIPMENT & MATER	1703 (light tanks)
			12	RV SERVICE STATION	12890	FUEL	300.07
			13	EFFAST	INV484208	EQUIPMENT & MATER	85.37
			13	EFFAST	INV484208	EQUIPMENT & MATER	88.97
			14	EFFAST	INV484260	EQUIPMENT & MATER	36.87
			14	EFFAST	INV484289	EQUIPMENT & MATER	238.88
			14	EFFAST	INV484679	EQUIPMENT & MATER	2090.8
			14	SPILHAUS	IN194891	EQUIPMENT & MATER	391.92
			14	BRIGHTS HARDWARE	CS-180027983	EQUIPMENT & MATER	2000.7
			14	BRIGHTS HARDWARE	CS-180027983	EQUIPMENT & MATER	5708.2
			17	BRIGHTS HARDWARE	CS-180028298	EQUIPMENT & MATER	647.87
			18	BUILT IT BEL-HAR	#100803	EQUIPMENT & MATER	4.2
			18	BUILT IT BEL-HAR	#100807	EQUIPMENT & MATER	7
			18	TROPICUM PETS SHOP BOSTON		EQUIPMENT & MATER	888 (air pump)
			20	SPILHAUS	IN192040	EQUIPMENT & MATER	104.83
			20	BUILT IT BEL-HAR	#100800	EQUIPMENT & MATER	631
			20	BUILT IT BEL-HAR	#10073	EQUIPMENT & MATER	210
			20	EFFAST	INV484700	EQUIPMENT & MATER	36.57
			20	EFFAST	INV484898	EQUIPMENT & MATER	185.4
			20	ESKAY TRADERS	#118019	EQUIPMENT & MATER	900
			21	EFFAST	INV484758	EQUIPMENT & MATER	120.04
			21	CLARENCE	PAYSLIP	WAGES	1000
			21	INDONES	PAYSLIP	WAGES	400
			24	PAVORAMA PET SHOP	#7240	ANIMAL FEED	283.3
			24	SMILA	1287	EQUIPMENT & MATER	11
			27	BELSTAR SERVICE STATI	4524	FUEL	203
			27	BUILT IT BEL-HAR	#102462	EQUIPMENT & MATER	4.9
			27	SPILHAUS	IN192244	EQUIPMENT & MATER	888.8
			27	BRIGHTS HARDWARE	CS-180027983	EQUIPMENT & MATER	888.8

BELEAF
GROWERS
aquaponic farm

Appendix C: Retailer Price

	Pick n Pay	Spar luxe	Balmoral	average
Rosemary (20g)	9,99R	7,99R	6,25R	8,08R
Mint (20g)	9,99R	7,99R	4,5R	7,49R
Thyme (20g)	9,99R	//	6,25R	8,12R
Basil (20g)	9,99R	11,99R	6,25R	9,41R
Parsley (20g)	9,99R	7,99R	5,5R	7,82R
Rucola (80g)	17R	//	16R	16,5R
Lettuce (1 crop)	9,99R	10R	13,99R	11,33R
Cucumber	11,99R	6,99R	5R	7,96R
Tomato (kilo)	20,99R	20R	15R	18,67R
Cabbage	24,99R	30R	18R	24,33R



BELEAF
GROWERS
 aquaponic farm